

Role of cell-to-cell communication in guiding breast cancer cell physiology

submitted in partial fulfilment of the requirements for the degree,

MSc in Human Physiology at the Faculty of Health Sciences,

University of Pretoria

Date: March 2022

Candidate

Leslie Pedzisayi

U14218594

Human Physiology

Faculty of Health Sciences

University of Pretoria

Supervisor

Dr Iman van den Bout

Principal Investigator, Centre for
Neuroendocrinology

Senior Lecturer, Department of
Physiology

Faculty of Health Sciences

University of Pretoria

Co-supervisor

Dr Claire Newton

Deputy Director, Centre for
Neuroendocrinology

Senior Lecturer, Department of
Immunology

Faculty of Health Sciences

University of Pretoria

Head of Department

Professor Annie Joubert

Department of Physiology

Faculty of Health Sciences

University of Pretoria

DECLARATION OF ORIGINALITY

I, Leslie Blessing Pedzisayi, declare that I understand the University's policy on plagiarism and the following thesis titled, "The role of cell-to-cell communication in guiding breast cancer cell physiology" is my own original work, has not been submitted by me or another party to another institution and where other people's work was utilised, it was acknowledged according to the University guidelines. I hereby submit to the University of Pretoria for the degree, Master of Science in Human Physiology.

Signature:



ACKNOWLEDGEMENTS

First and foremost, I dedicate this to my parents, Beatrice and Lewis Pedzisayi, immigrants who sacrificed so much to afford their children opportunities to reach heights they never could. I love you so much!

To my sisters, thank you for supporting me and always holding me accountable. To my friends and family, thank you for your love and support throughout this journey.

To my supervisor, Dr Iman van den Bout, this project would have not been possible without your excellent supervision, patience and contagious love for the sciences. Thank you.

To my co-supervisor, Dr Claire Newton and the Centre for Neuroendocrinology, thank you for always being there to assist, your support is very much appreciated.

Lastly, I would like to thank the NRF for funding this project.

EXECUTIVE SUMMARY

The ability of cells to communicate constitutes an important characteristic of all multi-cellular organisms. Cells participate in a continuous relay of information between their environment and other cells. These connections and the relayed information (exchange of biomolecules) influence how cells grow and function, with some literature suggesting that cell-to-cell communication may play a role in tumour progression. For instance, cancer cells interacting with stromal cells are believed to lead to the remodelling of the extracellular matrix to promote invasion and metastasis.

The development of metastasis has been implicated as a major cause of the worsening of prognosis for the majority of cancer patients. Breast cancer is only lethal when primary tumours travel to secondary sites or organs and impede their normal function, for example, when metastatic breast cancer invades the lungs or brain and results in death. Bearing in mind that breast cancer is the most prevalent form of cancer affecting women, preventing this complex process could impact many lives.

These interactions are not limited to neoplastic cells communicating with normal cells, and vice versa, but also between different neoplastic cells as well. The methods and mechanisms of action have not yet been characterized. This presents an opportunity in cancer studies/therapeutic development, in that targeting a non-metastatic cell capable of influencing a metastatic cancer cells' behaviour (or vice versa) would not only present a single target to impact metastasis, but also the opportunity to impact two neoplastic cell populations with one therapeutic target.

In this study, we investigated intercellular crosstalk between breast cancer cell lines and the possible resulting effects. The data generated shows that communication does take place between the different breast cancer cell lines. We observed that the biomolecules communicated from the metastatic MDA-MB-231 cell line triggered cell cycle exit and eventual apoptosis within the non-metastatic BT20 cell line. Additionally, we confirmed that biomolecule transfer occurs between donor and recipient cell within a two- and three-dimensional culture setting via the inducible colour switch system.

Keywords: Breast cancer, metastasis, cell-to-cell communication, biomolecules, colour switch

TABLE OF CONTENTS

Declaration of originality	ii
Acknowledgements	iii
Executive summary	iv
Table of Contents	v
List of Symbols and Abbreviations	viii
List of Figures	xii
List of Tables	xiv
1. Introduction	1
1.1 Cancer	2
1.2 Cancer biology	3
1.3 Hallmarks of cancer	4
1.3.1 Sustaining proliferative signaling	4
1.3.2 Evading growth suppressors	5
1.3.3 Evading apoptosis	6
1.3.4 Deregulating cellular energetics	6
1.3.5 Genome instability and mutation	7
1.3.6 Avoiding immune destruction.....	7
1.3.7 Enabling replicative mortality.....	8
1.3.8 Inducing angiogenesis.....	8
1.3.9 Tumor promoting inflammation	9
1.3.10 Activating invasion and metastasis	10
1.4 The metastatic cascade	11
1.4.1 Epithelial mesenchymal transition.....	11
1.4.2 Mechanisms of cell invasion following EMT	13
1.4.3 Survival detachment and circulation	14
1.4.4 Extravasation, colonization and proliferation	15
1.5 Cell-to-cell communication	17
1.5.1 Mechanisms of cell-to-cell communication	17
1.5.2 Direct vs Indirect communication.....	18
1.5.2.1 Direct communication	18
1.5.2.2 Indirect communication.....	21

1.5.2.3 Extracellular vesicles	22
1.6 Research problem	24
2. Aim and Objectives	25
2.1 Aim	26
2.2 Objectives.....	26
3. Materials and Methods	27
3.1 Cell lines	28
3.2 Cell maintenance, counting and storage.....	30
3.3 Investigating cellular attachment utilising crystal violet assay.....	32
3.4 Investigating cellular migration utilising the scratch assay.....	33
3.5 Investigating the effect of conditioned media treatment on the cell cycle utilising flow cytometry.....	34
3.6 Immunohistochemistry.....	36
3.7 Investigating cell adhesion architecture post treatment with conditioned media using confocal microscopy.....	37
3.8 Investigating the effect of MDA-CM on BT20 cells using real-time confocal microscopy	38
3.9 Investigating the Colour switch system using confocal microscopy	38
3.10 Generation of stable cell lines.....	40
3.11 Resazurin assay	44
3.12 Statistical analysis	46
4. Results	47
4.1: Treatment with conditioned media from the MDA-MB-231 cells inhibit BT20 cell proliferation	48
4.2: MDA-MB-231 cell conditioned media does not decrease cellular metabolism of BT20 cells.....	61
4.3 The biomolecules communicated between the metastatic MDA-MB-231 cell line and the non-metastatic BT20 cell line promote cellular rounding and apoptosis over time	73
4.4: MDA-MB-231 conditioned media treatment does not affect the actin cytoskeleton or cell adhesion structures.....	78
4.5: Treatment of BT20 cells with MDA-MB-231 conditioned media induces cell cycle exit.....	79
4.6: Conditioned media treatment of MDA-MB-231 breast cancer cell line does not impact migration rate	87
4.7: Biomolecules are transferred from MDA-MB-231 cells to BT20 cells	89
5. Discussion.....	102

5.1 A metastatic breast cancer cell line secretes biomolecules that decrease the proliferation of the BT20 cell line.....	103
5.2 MDA-CM induces cellular rounding and the appearance of apoptotic bodies	106
5.3 MDA-MB-231 conditioned medium induces BT20 cells to exit the cell cycle	106
5.4 Extracellular vesicles transfer biomolecules from MDA-MB-231 to BT20 cells	108
6. Conclusion	111
7. References	114
8. Appendix	123
Appendix A: Serum interferes with fluorescence during measurement.....	124
Appendix B: Serum-free media does not affect fluorescence during measurement.....	125
Appendix C: Plasmid map; CreERT2.....	126
Appendix D: Plasmid map; LV-CFP	127
Appendix E: Plasmid map; The switch module	128
Appendix F: Three dimensional co-cultures.....	129
Appendix G: Title change approval within intent to submit	130
Appendix H: MSc committee approval.....	131
Appendix I: Letter of statistical clearance	132
Appendix J: Ethics approval 2019	133
Appendix K: Ethics approval 2020	134
Appendix L: Ethics approval 2021	135

LIST OF SYMBOLS AND ABBREVIATIONS

+	Positive
-	Negative
°C	degrees Celsius
µl	microlitre
µm	micrometer
2D	Two-dimensional
3D	Three-dimensional
ADSCs	Adipose derived stem cells
APCs	Antigen presenting cells
ATP	Adenosine triphosphate
BT20	Breast tumour-20 breast cancer cell line
BT20-CM	Breast tumour-20 conditioned media
Bcl-2	B cell leukaemia/lymphoma 2
C8	EE-15-one
CAT	Collective to ameboid transition
CDKs	Cyclin-dependent kinases
cDNA	Complimentary DNA
CO ₂	Carbon dioxide
CIN	Chromosomal instability
CLSM	Confocal laser scanning microscopy
CFP	Cyan fluorescent protein
CM	Conditioned medium
CS	Colour switch
Cyt c	Cytochrome c
DAPI	4',6-diamidino-2-phenylindole
dH ₂ O	Distilled water
DMEM	Eagle's Minimal Essential Medium
DMSO	Dimethyl sulfoxide
EGF	Epidermal growth factor

<i>E. coli</i>	Escherichia coli
ER	Estrogen receptor
ER- α	Estrogen receptor alpha
ER- β	Estrogen receptor beta
EVs	Extracellular vesicles
EMT	Epithelial-mesenchymal transition
EMT-TFs	EMT transcription factors
FAK	Focal adhesion kinase
FACS	Fluorescence assisted cell sorting
GLUT1	Glucose transporter 1
HEK293	Human embryonic kidney cell line 293
HER2	Human epidermal growth receptor 2
hMSC	Human bone marrow derived mesenchymal stem
cellHrs	Hours
HIV-1	Human immunodeficiency virus type 1
IL-1 α	Interleukin-1 alpha
IL-6	Interleukin-6
IL-10	Interleukin-10
kDa	Kilodalton
LB broth	Luria-Bertani broth
MET	Mesenchymal-epithelial transition
MEM	Minimum Essential Media
MAT	Mesenchymal to ameboid transition
MCF7	Michigan Cancer Foundation 7 cell line
Mc1-1	Myeloid cell leukaemia 1
MDA-MB-231	M.D. Anderson metastatic breast 231 breast cancer cell line
MDA-CM	M.D. Anderson metastatic breast 231 conditioned media
MDCK	Madin-Darby canine kidney
MHC	Major histocompatibility complex
miRNA	microRNA
ml	millilitre

MMPs	Matrix metalloproteinases
MSC	Mesenchymal stem cells
MSI	Microsatellite instability
MVs	Microvesicles
Myo10	Myosin10
NCS	Non-colour switch
NIN	Nucleotide instability
nm	Nanometer
ng	Nanogram
PDGF	Platelet-derived growth factor
PM	Plasma membrane
PR	Progesterone receptor
proBDNF	Pro-brain derived neurotrophic factor
RFU	Relative fluorescent units
RNS	Reactive nitrogen species.
ROS	Reactive oxygen species
RNA	Ribonucleic acid
SEM	Standard error of the means
TAA	Tumour-associated antigen
TGF- β	Transforming growth factor β
TNBC	Triple-negative breast cancer
TNFR1	Tumour necrosis factor receptor 1
TWIST1	Twist-related protein 1
VEGF	Vascular epidermal growth factor
USA	United States of America
UV	Ultraviolet
VSV-G	Vesicular stomatitis virus-G
v/v	Volume to volume
w/v	Weight to volume
WHO	World Health Organisation

ZEB1 Zinc finger E-Box binding homeobox 1
ZEB2 Zinc finger E-Box binding homeobox 2

LIST OF FIGURES

Figure 1.1: The hallmarks of cancer

Figure 1.2: The metastatic cascade

Figure 1.3: Epithelial-mesenchymal-transition

Figure 1.4: Forms of chemical signalling

Figure 1.5: Intercellular communication between two cells can occur via direct or non-direct mechanisms

Figure 1.6: The different forms of extracellular vesicles produced

Figure 4.1: MDA-CM has an anti-proliferative effect on BT20 cell growth

Figure 4.2: MDA-CM has an anti-proliferative effect on BT20 cell growth

Figure 4.3: Conditioned media from the non-metastatic MCF7 breast cancer cell line has no effect on BT20 cell proliferation

Figure 4.4: Conditioned media from the non-metastatic MCF7 breast cancer cell line has no effect on BT20 cell proliferation

Figure 4.5: BT20-CM has no effect on MDA-MB-231 cell proliferation

Figure 4.6: BT20-CM has no effect on MDA-MB-231 cell proliferation

Figure 4.7: MDA-CM does not have anti-proliferative effects on MCF7 cells

Figure 4.8: MDA-CM does not have anti-proliferative effects on MCF7 cells

Figure 4.9: Conditioned media from the MDA-MB-231 cell line does not decrease BT20 cell metabolism.

Figure 4.10: Conditioned media from the MDA-MB-231 cell line does not decrease BT20 cell metabolism

Figure 4.11: Conditioned media from the BT20 cell line does not decrease cell metabolism in MDA-MB-231 cells

Figure 4.12: BT20 CM does not decrease cell metabolism in MDA-MB-231 cells

Figure 4.14: Neither pellet nor supernatant from fractionated MDA-MB-231

conditioned media has an adverse effect on BT20 cell metabolism

Figure 4.15: Neither pellet nor supernatant from fractionated MDA-MB-231 conditioned media has an effect on BT20 cell metabolism

Figure 4.16: Neither pellet nor supernatant from fractionated BT20 conditioned media has an effect on MDA-MB-231 cell metabolism

Figure 4.17: Neither pellet nor supernatant from fractionated BT20 conditioned media has an effect on MDA-MB-231 cell metabolism

Figure 4.18: MDA-CM increases cell rounding and apoptosis in BT20 cells over time

Figure 4.19: MDA-CM decreases cellular protrusions while inducing an increase in cell rounding and apoptosis in BT20 cells

Figure 4.20: MDA-CM significantly increases cellular apoptosis

Figure 4.21: MDA-CM does not alter cell adhesion structure architecture in BT20 cells

Figure 4.22: MDA-CM results in more cells in G0 phase of cell cycle

Figure 4.23: Conditioned media from the metastatic MDA-MB-231 cell lines results in more quiescent cells in the BT20 cell cycle

Figure 4.24: MDA-231 cell cycle relatively unaffected by treatment

Figure 4.25: Treatment of the metastatic MDA-MB-231 cell line with any of the conditions does not significantly alter the cell lines' progression through the cell cycle

Figure 4.26: Treatment of MDA-MB-231 cells with BT20-CM and MDA-CM does not influence migration

Figure 4.27: The colour switch system is inducible

Figure 4.28: The stable (donor) but not parental MDA-MB-231 cells displayed CFP fluorescence

Figure 4.29: The stable (recipient) but not parental BT20 cells displayed dsREd fluorescence

Figure 4.30: Tamoxifen induces the production of Cre recombinase leading to a colour switch in recipient cells

Figure 4.31: There is no colour switching in the absence of tamoxifen for donor and reporter cell co-cultures

Figure 4.32: The normal MDA-MB-231 variant does not produce Cre recombinase when treated with tamoxifen

Figure 4.33: The MDA-CRE-CFP variant produces Cre recombinase when treated with tamoxifen resulting in the induction of colour switching

Figure 4.34: Biomolecule transfer occurs in 3D co-culture spheroids after tamoxifen exposure

LIST OF TABLES

Table 3.1: Cell lines utilised in the study

Table 3.2: Cell culture reagents and materials

Table 3.3: Crystal violet reagents and materials

Table 3.4: Scratch assay materials

Table 3.5: Flow cytometry reagents and materials

Table 3.6: Immunohistochemistry reagents and materials

Table 3.7: Characteristics of the plasmids utilised in making the stable cell lines

Table 3.8: Transformation and transfection reagents and materials

Table 3.9: Resazurin assay reagents and materials

Table 4.1: One-way ANOVA with Bonferroni's multiple comparison test for BT20 cells treated with MDA-CM

Table 4.2: One-way ANOVA with Bonferroni's multiple comparison test for BT20 cells treated with MCF7-CM

Table 4.3: One-way ANOVA with Bonferroni's multiple comparison test for MDA-MB-231 cells treated with BT20-CM

Table 4.4: One-way ANOVA with Bonferroni's multiple comparison test for MCF7 cells treated with MDA-CM

Table 4.5: One-way ANOVA with Bonferroni's multiple comparison test for BT20 cells treated with MDA-CM

Table 4.6: One-way ANOVA with Bonferroni's multiple comparison test for MDA-MB-231 cells treated with BT20-CM

Table 4.7: One-way ANOVA with Bonferroni's multiple comparison test for BT20 cells treated with fractionated MDA-CM

Table 4.8: One-way ANOVA with Bonferroni's multiple comparison test for MDA-MB-231 cells treated with fractionated BT20-CM

Table 4.9: Dunnett's multiple comparison test results for the three parameters of BT20 cells post MDA-CM treatment

Table 4.10: One-way ANOVA with Dunnett's multiple comparison test for BT20 cells comparing all treatments to the control – serum-free media (SFM)

Table 4.11: One-way ANOVA with Dunnett's multiple comparison test for MDA-MB-231 cells comparing all treatments to the control – serum-free media (SFM)

CHAPTER 1 INTRODUCTION

1. INTRODUCTION

1.1) Cancer

Cancer is a family of diseases that occur when there is unregulated cell proliferation. It was documented as early as 3,500 years ago on Egyptian scrolls. Mentioned were the palpable lumps characteristic of the late stages of the pathology in tissues such as the breasts.¹ There are numerous forms of cancer, named according to the tissue where they originate, such as breast cancer or prostate cancer. Furthermore, cancers can be characterised by the tissue types they arise from. For example, sarcomas are cancers of connective, non-epithelial tissue whilst carcinomas are cancers of epithelial tissue.² Physicians in ancient Greece known as Hippocratic physicians (named after the man considered to be the father of modern medicine, Hippocrates [460-370 BC]) are credited with the origins of the term *karkinoma*, which evolved to carcinoma.^{1,3}

Cancer develops as a result of DNA damage leading to uncontrolled proliferation. As cells age, the integrity of nucleic acid sequences making up the genome are compromised.³ The body is usually able to repair this DNA damage but where it fails to do so, genetic instability (mutations) may give rise to cancer.^{1,4} These mutations allow unregulated cell proliferation and additional mutations to occur. Such mutations can occur in a number of genes to initiate cancer. Indeed, cancer is mostly the result of mutations in multiple genes.⁵ This feature explains the heterogeneity of cancer as a disease.^{4,6} A small proportion of cancer occurs through genetic inheritance, which results from the inheritance of mutated genes. However, the majority are a result of DNA damage due to exposure to external chemical substances known as carcinogens or lifestyle choices such as smoking.⁵⁻⁶

In the seventies, two important gene families were identified as being intimately linked to tumorigenesis: oncogenes and tumour suppressor genes.^{3,7} Oncogenes are genes formed by the mutation of normal genes (proto-oncogenes) which, when present, activate uncontrolled cell growth leading to the formation of cancerous cells. Conversely, tumour suppressor genes are genes that inhibit uncontrolled cellular division in normal cells, play a role in DNA repair and programmed cell death and are silenced through mutation in cancers.^{3,5}

There were an estimated 18 million new cancer cases diagnosed globally in 2018. This was increased from an estimated 14 million new cases in 2012,^{2,8} and is projected to grow to approximately 24 million by the year 2035.⁸ Second only to cardiovascular disease, cancer has a significant negative impact on global life expectancy.² Developed countries exhibit the highest incidence of cancer, with urban and economic development having been implicated as role players in the increased frequency of cancer. For instance, well known lifestyle diseases such as obesity and diabetes, as well as the consumption of processed foods, are important contributing factors.¹ However, although incidence is lower, cancer-related mortality is higher in developing countries due to a lack of adequate health care.⁷

1.2) Cancer biology

There are over a hundred distinct types of cancers, with each having many subtypes.⁴ In contrast to most of the diseases that have plagued humanity over the years, cancer does not have a single causative agent.⁹ Not only is the cause of cancer not isolated to a single causative agent, it is a group of diseases that has developed mechanisms or acquired capabilities that constitute an organizing principle to not only survive but thrive within a competent immune system.^{4,6} The hallmarks of cancer are the key alterations in a cell's physiology and biochemistry that underlie the initiation and progression of all cancers. They include sustaining proliferative signalling, evading growth suppressors, avoiding immune destruction, enabling replicative immortality, tumour promoting inflammation, activating invasion and metastasis, inducing angiogenesis, genome instability and mutation, resisting cell death and deregulating cellular energetics.⁴ Put forward in an influential review in the year 2000 by Douglas Hanahan and Robert Weinberg, these hallmarks of cancer cumulatively dictate the development of malignant growth.^{4,6} Hanahan and Weinberg suggest that the large catalogue of cancers is a manifestation of these ten "acquired capabilities" (Figure 1.1).⁴

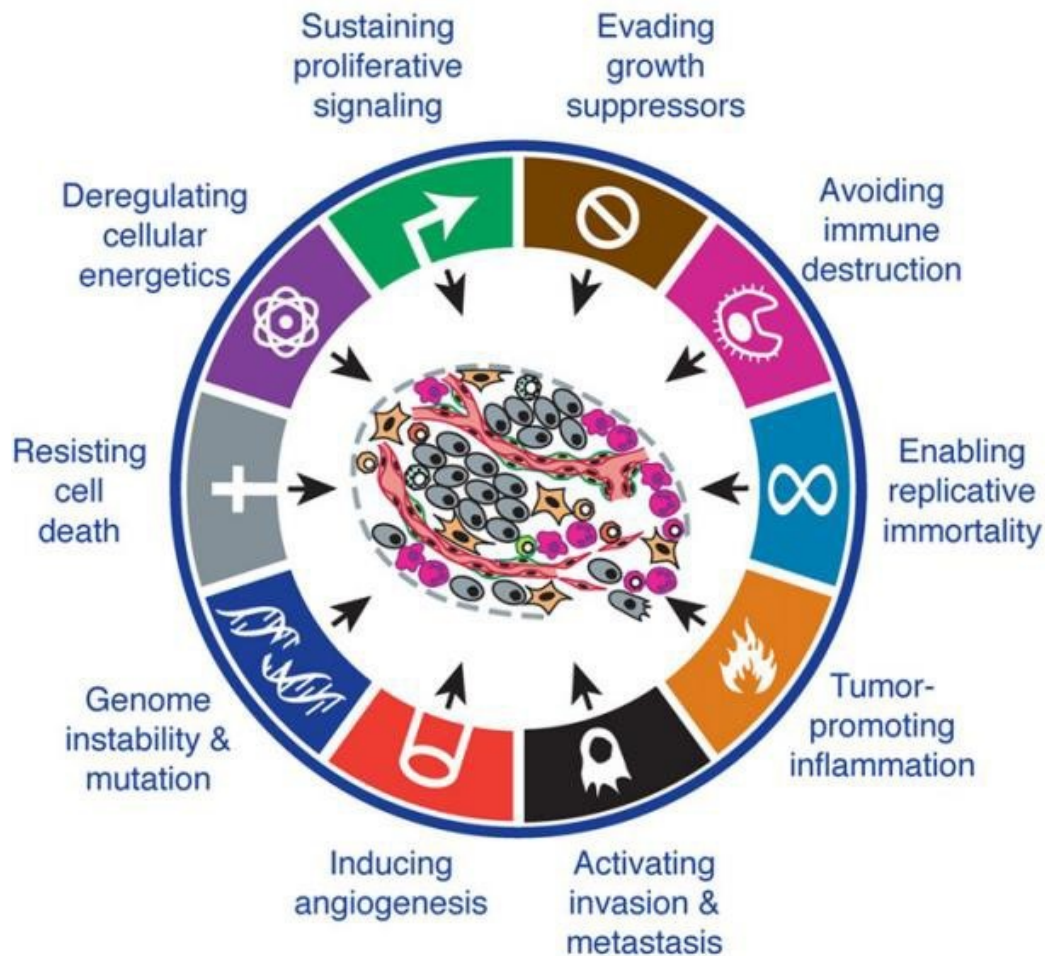


Figure 1.1: The hallmarks of cancer. *The pro-neoplastic mechanisms of survival employed by cancer cells put forward by Hanahan and Weinberg. These hallmarks allow the cancer cell to circumvent many checkpoints and resist many immune regulated counter measures resulting in the spread, attachment and growth of cancer. Reproduced from Hanahan and Weinberg with permission.⁴*

1.3) The hallmarks of cancer

1.3.1) Sustaining proliferative signalling

Normal cellular growth is dependent on mitogenic growth signals, necessary for the progression of a cell from a quiescent to a proliferative state.¹⁰ Normal cells cannot

undergo this progression into an active state in the absence of these signals.¹⁰⁻¹¹ This is not the case with neoplastic cells (those with uncontrolled cell growth). Neoplastic cells have been shown to generate their own signals and, through this, be independent of exogenous signalling.¹¹⁻¹² Acquiring autonomy in signalling (sustaining proliferative signalling) was the first hallmark clearly described.⁴ The autonomy is achieved through the modification of extracellular growth signals, modification of the transcellular transducers of these signals or the modification of internal circuits meant to translate the said signals.¹¹ Through these alterations, the cancer cells acquire the ability to produce growth factors they are responsive to, resulting in a positive feedback loop known as autocrine stimulation.¹² The synthesis of platelet-derived growth factor (PDGF) by glioblastomas and tumour growth factor- α (TGF α) by sarcomas are examples of self-sufficiency in growth signalling.^{4,10}

1.3.2) Evading growth suppressors

In addition to developing self-sufficiency in proliferative signalling, neoplastic cells have to circumvent suppressive signals.⁴ Within normal tissue, homeostasis and cellular quiescence are maintained through a balance between multiple proliferative signals such as soluble growth factors and different antiproliferative signals such as extracellular matrix (ECM) bound (immobilized) inhibitors.⁴ Similar to the proliferative signals, anti-proliferative signals utilize transmembrane cell surface receptors that convey the signals to intracellular circuits.⁶ Both proliferative and anti-proliferative signals have been shown to affect different phases of the cell cycle, namely G₀, a phase where the cell has exited the replicative cell cycle and is in a quiescent state, which is a viable and metabolically-active state (regardless of lack of proliferation), where the cell is also capable of re-entry into cell cycle; G₁ phase (Gap 1) characterized by cell growth and synthesis of molecules crucial to the replicative cell cycle such as mRNA and proteins; S phase, characterized by DNA synthesis; G₂ phase (Gap 2) characterized by rapid cell growth and protein synthesis in preparation for mitosis; M (Mitotic) phase where the cell divides copied DNA content and cytoplasm to produce two daughter cells.¹²⁰ Anti-proliferative signals suppress cellular growth through two mechanisms, either through forcing a cell out of active proliferation into quiescence (G₀), from which they can exit if acted upon by specific proliferative signals, or a permanent loss of proliferative potential by entering a post-mitotic state.^{4,13}

1.3.3) Evading apoptosis

Maintaining homeostasis is a largely important theme throughout biology with various processes contributing to the balance.¹⁴ Apoptosis (programmed cell death) is a highly conserved process crucial to normal tissue development, tissue homeostasis and the maintenance of integrity in multi-cellular organisms.¹⁵ In addition to regulating aging or damaged cells, apoptosis plays crucial roles in the cell cycles of organisms, for example, separation of digits of the human embryo.¹⁶ This highly conserved process occurs via a series of sequential and precise steps; nuclear DNA fragmentation, cell shrinkage, chromosome condensation, membrane blebbing then the formation of apoptotic bodies which are engulfed by cells, such as lysosomes, for degradation.^{4,16} Programmed cell death serving as a barrier to tumorigenesis has been established through compelling studies over the last couple of decades. Literature has shown that evading apoptosis is a cancer hallmark of many, if not, all cancer types.^{4,6,13-17}

1.3.4) Deregulating cellular energetics

The unregulated proliferation profile or limitless replicative potential associated with cancer is coupled to, if not dependent on, adjustments to cellular energy requirements.¹⁸ In the presence of free oxygen (aerobic respiration), healthy cells initially process a single glucose molecule into pyruvate (glycolysis within the cytosol) then, through oxidative phosphorylation within the mitochondria, process this pyruvate to produce 36 molecules of adenosine triphosphate (ATP) with carbon dioxide (CO₂) and water as by-products.⁴ This is a very efficient process. The absence of free oxygen (anaerobic respiration) favours glycolysis unrelated to oxidative phosphorylation, small amounts of pyruvate are transported to the oxygen dependent mitochondria and an ATP yield of only 2 molecules is generated.⁴ Cancer cells exhibit a metabolic switch where, even with an abundance in oxygen, they seem to counterintuitively favour anaerobic respiration-linked glycolysis, yielding 2 ATP molecules, and producing lactate as a by-product.¹⁸ This phenomenon is known as the “Warburg effect”.¹⁸⁻¹⁹ This reprogrammed energy metabolism can favour, for example, hypoxic phenotypic switching, which in turn promotes tumoral plasticity and heterogeneity.^{4,18}

1.3.5) Genome instability and mutation

The p53 gene is hailed the “guardian of the genome” due to its crucial role in controlling cell death and division.²⁰ The aim of somatic cellular division is the production of daughter cells with genetic content identical to that of the parent cell, maintaining the integrity of the genome.²⁰ Failure to accomplish this, possibly as a result of inactivation of the p53 gene, for example, leads to genomic instability and genetic mutations, increased sensitivity to mutagens by cells and/or gain/loss of entire chromosomes (Aneuploidy).²⁰⁻²¹ Genomic instability and mutation are driving forces for the acquisition of more genetic alterations, clonal evolution and a major factor behind tumour heterogeneity.²¹ The body utilises different strategies to prevent premature DNA replication outside the normal division cycle, or it responds to varying extracellular and intracellular cues regarding damage to the genome.²² There are four biological mechanisms or strategies the body implements to try and safeguard the integrity of the genome, namely a well-coordinated cell cycle with checkpoints, meticulous chromosome segregation during mitosis, high-fidelity DNA replication and error-free DNA damage repair.^{20,23}

1.3.6) Avoiding immune destruction

There are two widely accepted theories within the field of cancer, first, that it arises from a series of genetic alterations that transform healthy cells into malignant ones, and secondly, that specific biological machinery or programming must be disrupted or deregulated to allow and sustain the development of cancer.²⁴ Cancer is an illness characterised by an abnormal accumulation of defective cells.²⁵ Hallmarks such as genomic instability allow for the transformation of normal cells to malignant ones whilst hallmarks such as deregulating cellular energetics and resisting cell death (avoiding apoptosis) allow for the disruption of normal regulatory processes.^{16,26} After the development of malignancies, avoiding immune destruction sustains the development and spread of cancer. The concept of ‘immune surveillance’ suggests the presence of an ever-alert defence system that actively monitors, identifies, and destroys any threats to the human body.^{18,27} That evasion of this immune surveillance is an important factor in cancer development is supported by literature showing that chronic immunosuppression following organ transplants, for example, is associated with an

increased prevalence in particular cancer types, specifically those of viral origins.¹⁸ Therefore, the emergence of solid tumours in otherwise healthy individuals suggests cancer manages to circumvent the surveillance system or limit the effectiveness of said system.²⁷ In addition to the indirect contribution of the tumour microenvironment (hypoxic and immunosuppressive), cancer utilises different strategies to avoid immune destruction.²⁸ The strategies employed range from the creation of low immunogenicity, creation of immune tolerance, the suppression of immune cell checkpoints/chemotaxis to downright resistance of immune cell mediated lysis.^{18,28}

1.3.7) Enabling replicative immortality

Normal cell populations undergo a finite number of divisions until they stop growing, this cellular characteristic is associated with two barriers to proliferation, namely senescence and crisis.⁶ Senescence is a permanent state of cyto arrest that can be induced by intrinsic or exogenous factors.^{11,29} Intrinsic triggers of senescence can be telomere dysfunction or the initiation of oncogene expression whilst exogenous triggers can include oxidative stress or a range of DNA damaging compounds such as ultraviolet (UV) radiation.²⁹ When the process of senescence is circumvented, for example, the disabling of the retinoblastoma tumour suppressor protein in cultured human fibroblasts, the cell enters a state of crisis, characterised by substantial cell death.⁶ The processes of senescence and crisis protect the genome from possibly defective or aged cells.¹¹ The disruption of autonomous internal circuits responsible for inducing cell senescence or crisis disrupt cellular limits on multiplication and there can be an emergence of cells from the crisis phase. These cells display an unlimited replicative potential, in a change termed immortalization. The enabling of replicative immortality by neoplastic cells, a hallmark, is necessary to produce macroscopic tumours.⁴

1.3.8) Inducing angiogenesis

The supply of oxygen and nutrients, coupled to removal of waste products, is crucial to normal cellular function, this is facilitated by the blood vessels.³⁰⁻³¹ These important functions are why almost all cells within tissue are limited to residing in close proximity

to vasculature (within 100 μm).^{6,30} The ability to induce the formation of new blood vessels (initiation of angiogenesis) is initially absent within neoplastic cellular populations but its development is necessary to produce clinically relevant tumours.^{6,31} The realization that rapidly proliferating tumours were massively vascularised whilst dormant ones were not, was the first indication of the crucial role angiogenesis plays in tumour progression.³² Angiogenic homeostasis is regulated by both pro-angiogenic (activator) and anti-angiogenic (inhibitor) molecules.^{30,32} Tumour cell aggression is reflected in the relative levels of expression of pro-angiogenic or anti-angiogenic factors.³⁰ When these factors are in balance, there is vasculature quiescence and endothelial cells do not proliferate.³² The initiation of angiogenesis occurs when there is dominant expression of pro-angiogenic factors such as vascular endothelial growth factor (VEGF).^{6,30} The induction of this process in tumour cells is termed the “angiogenic switch”.³¹⁻³²

1.3.9) Tumour promoting inflammation

The immune system functions to protect the body from infection.³³ Short-term defence against infection is carried out by acute inflammation whilst chronic inflammation protects the body against prolonged exposure to infection related to numerous diseases including carcinogenesis.³⁴ The link between cancer and inflammation was first recorded in the nineteenth century by Jean-Nicolas Marjolin, a French surgeon who, through observation, noted the development of carcinomas in burn victims years after incidence.^{33,35} The presence of leukocytes in tumours and the tumour microenvironment provided a clue on the relationship between inflammation and cancer.³³ Historically, the presence of cells from the innate and/or adaptive branches of the immune system, either as subtle infiltrations or major inflammation, were considered an attempt to combat tumour progression.^{4,33} However, the past couple of decades have produced research centred on the link between the immune system and cancer progression.³³ Current literature reports a direct link between said immune responses and neoplastic progression (tumour promoting inflammation), a cancer hallmark.³³ It is estimated that approximately a fifth of all cancer-related chronic or acute inflammatory responses are due to tumour-promoting effects.⁹ This direct causal link is further established through evidence of chronic inflammatory diseases such as

colitis and pancreatitis resulting in an increased risk of developing colon and pancreatic cancers.^{33,35}

1.3.10) Activating invasion and metastasis

The movement of cells is a highly dynamic process crucial to numerous physiological processes such as collective movement during early embryogenesis.³⁶ It describes the directed or random movement of cells from one region, site or tissue to another.³⁷ Cell migration plays a role in all life phases, from the 'initiation' of life (starting with the flagella-dependent movement of sperm and then the process of embryonic development), the 'maintenance' of life (for example, in epithelial wound healing and immune responses) and the 'ending' of life (for example, tumour progression and cancer metastasis).³⁷ Activation of invasion and metastasis, the final cancer hallmark, is a major contribution to the lethality of cancer. It is defined as the process by which tumour cells disseminate from the primary tumour, travel through the circulatory system to colonise and proliferate at a secondary site (Figure 1.2).^{4,38}

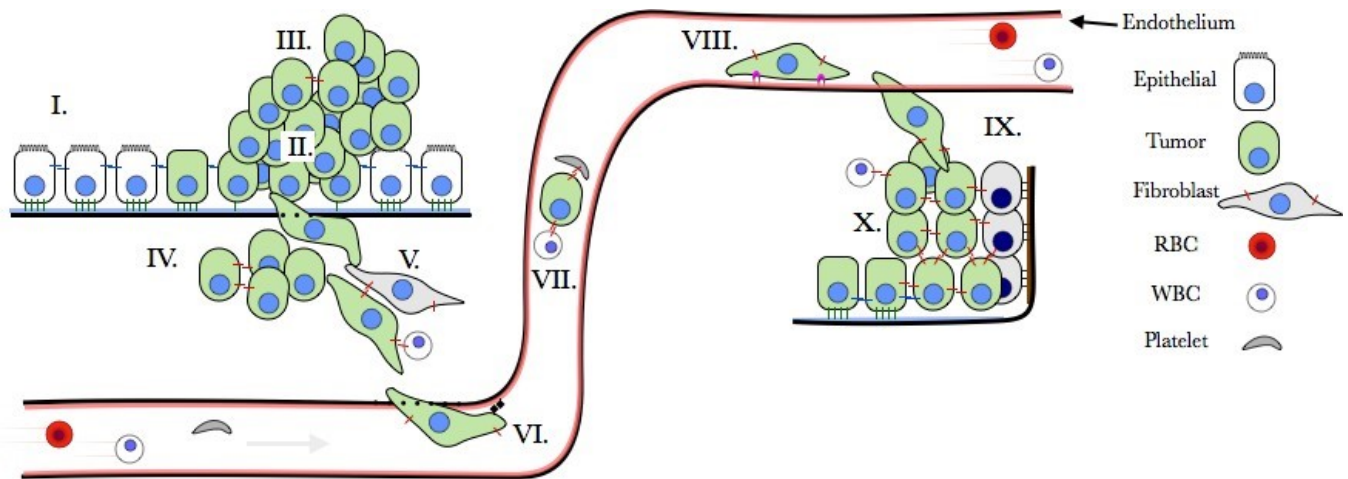


Figure 1.2: The metastatic cascade. (I-V) Tumour cells disseminate from the primary tumour and break through the basement membrane. (V-IX) The cells enter the circulatory system, survive and colonise a secondary site. (X) The cells start to proliferate at the secondary site. RBC – red blood cell; WBC – white blood cell. Obtained from Eslami-S and Cortés-Hernández (Open access).³⁸

1.4) The metastatic cascade

1.4.1) Epithelial-mesenchymal transition

Metastasis requires cells to change their phenotypic characteristics. The term epithelial-mesenchymal transition (EMT) describes a process by which epithelial cells, with strong apical-basal polarity, transition to an invasive mesenchymal state (Figure 1.3).³⁹⁻⁴¹ This transition entails a decrease in expression of genes coding for proteins that favour a cellular epithelial state such as E-cadherin and occludin, coupled to a subsequent increase in the expression of genes encoding proteins for a cellular mesenchymal state such as N-cadherin and fibronectin (Figure 1.3).⁴⁰ E-cadherin promotes adherence junction health. Cell surface E-cadherin domains of neighbouring cells interact (adhere) to one another to strengthen cell-to-cell interactions whilst intracellular domains bind to β - and α -catenins connecting junctions to the cytoskeleton.⁴²⁻⁴³ The phenotypic or morphological shifts associated with EMT confers

upon the neoplastic cell properties that aid and promote cellular invasion, with increased metastatic potential being characteristic of mesenchymal cells.⁴⁴ Such changes include tight junction dissociation, loss of microvilli, a cytoskeleton reorganisation and an up-regulation of matrix metalloproteinases (MMPs), all of which aid cell invasion and motility.^{39,45} EMT has been implicated as a major role player in the development of cancer drug resistance and the initiation and progression of metastasis.⁴⁰

EMT is induced by numerous extracellular cues, most originating from the cells' microenvironment.⁴⁶ EMT, whether as a normal physiological process (embryonic development) or pathology (cancer metastasis), is dependent on the activation of signalling pathways, including the Wnt, Notch and transforming growth factor β (TGF- β) pathways.⁴⁶⁻⁴⁷ These signalling pathways alter the expression profile of adhesion receptors and extracellular matrix (ECM) proteins.⁴⁸ The coordinated action of these proteins then causes a remodelling of the microenvironment around the cells undergoing EMT. Cell-to-cell adhesion is disrupted, and cell morphology changes allowing the detachment of cells from one another.⁴⁷⁻⁴⁸ This detachment promotes migration.

The TGF- β pathway has proved to be unique, in that a single growth factor promotes the release of numerous growth factors, which, in turn, enhance the transition/differentiation process.⁴⁶⁻⁴⁸ EMT initiated by TGF- β is largely mediated by specific transcription factors including Snail, Twist, Zip, Slug, ZEB1 and ZEB2.⁴⁹ For example, Snail directly represses the transcription of E-cadherin which is an epithelial cell marker.⁴⁹ Overexpressing Snail in Madin-Darby Canine Kidney (MDCK) cells resulted in loss of cell-to-cell adhesion due to decreased E-cadherin expression.^{48,50} Silencing EMT transcription factors (EMT-TFs) such as Snail and Twist-related protein 1 (TWIST1) has been shown to significantly abrogate the occurrence of lung metastases, however, this did not entirely eliminate them.^{49,51} This has led researchers to believe that EMT-TFs act more as catalysts and not drivers of EMT.⁴⁹⁻⁵⁰ Jolly *et al* showed that the level of EMT-TFs and/or mesenchymal markers present affect the mode of migration cells adopt during EMT i.e. single cell or collective migration.⁴⁹

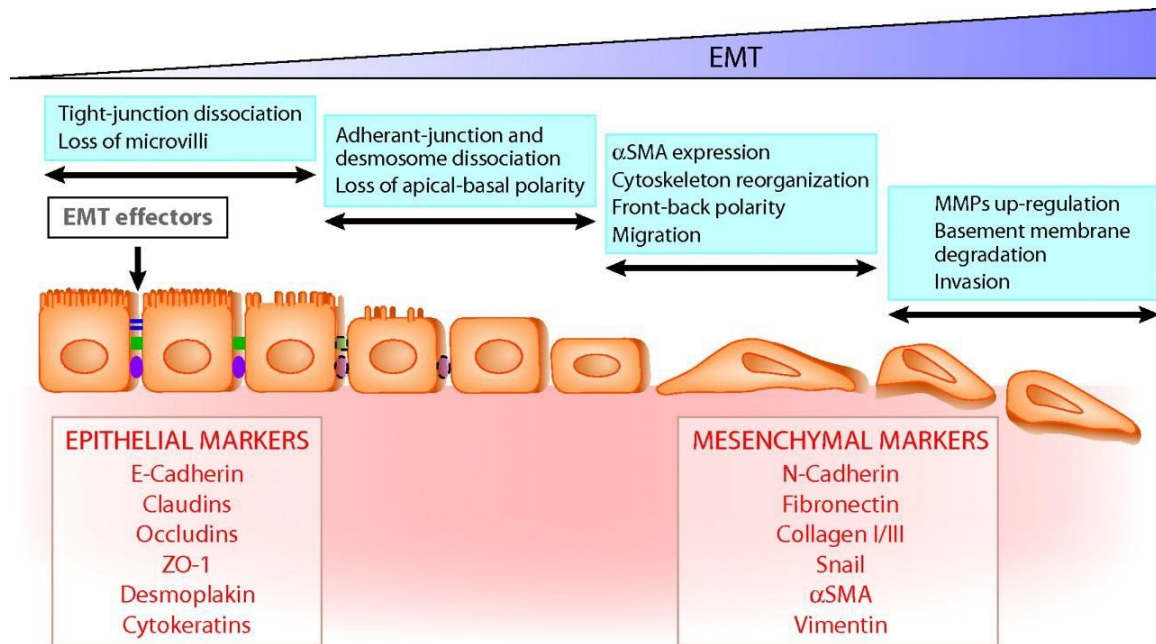


Figure 1.3: Epithelial-mesenchymal-transition. *EMT effectors such as Prrx1 and signalling pathways such as the TGF- β pathway initiate the EMT process. Cells of an epithelial nature undergo tight junction dissociation and loss of microvilli; this leads to loss of apical-basal polarity followed by cytoskeleton reorganisation. The cells then exhibit a mesenchymal state. This promotes the cells' ability to migrate to and invade into a secondary site or circulation. α SMA – alpha smooth muscle actin. ZO-1 – Zonula occludens-1. Reproduced from Angadi and Kale with permission.⁴⁵*

1.4.2) Mechanisms of cellular invasion and migration following EMT

Within cancer, invasion is defined as the infiltration by neoplastic cells of tissue substrate, i.e. basement membrane (Figure 1.2).⁵² Metastatic cells need to pass through their surrounding environment to reach distant organs. This requires the employment of invasion promoting molecules such as MMPs, upregulated upon initiation of EMT.⁵³⁻⁵⁴ MMPs promote cellular invasion through enzyme driven remodelling of substrate. This enzymatic promotion of invasion favours cellular migration in numerous ways, most notably the removal of physical barriers within the stromal tissue and activation of chemotactic molecules.⁵⁴ Following EMT, as mentioned above, an increase in the expression of mesenchymal markers such as N-

cadherin result in cytoskeletal rearrangement.⁴⁸ The rearrangement affects focal adhesion kinase (FAK), which binds actin fibres to attach cells to the substrate.⁴² Subsequently, pro-migratory molecules such as Rho, Rac1 and Cdc42 are activated, leading to the formation of lamellipodia (Rac1) or the formation of filopodia (Cdc42) whilst Rho modulates cellular contractility.⁴² Filopodia trigger cellular migration in numerous cell types, and an increased filopodia prevalence and density has been reported within cancer.^{52,54-56} Migrating cells project lamellipodia that bind the ECM, disrupting existing ECM bonds at their 'back-end', following contraction, this continuous process allows migratory cells to pull forward.^{52,55}

During collective cellular migration, the front invasive cell is known as the 'tip cell', it has front-back polarity and leads the way while the rest of the cells follow.^{42,57} The engagement of integrins and polymerization of actin within the 'tip cell' propels the cell forward.⁵⁷ Important to note, is that the trailing cells can conserve their epithelial nature.⁴² Single cell migration can either be mesenchymal or ameboid.⁵⁷ Cells can detach from migrating clusters into either one of the migration forms through, for example, 'collective to ameboid transition' (CAT) or further transition into an ameboid form of migration from mesenchymal, via a process known as 'mesenchymal to ameboid transition' (MAT).⁵⁸ Each single cell migration form utilizes specific movement mechanisms. Mesenchymal single cell migration utilizes focal adhesions and traction, whilst ameboid single cell migration is dependent on propulsion from cells contracting.⁵⁷ The fastest form of single cell migration is ameboid cellular migration, it presents with a complete loss of cellular polarity.⁵⁷⁻⁵⁸

1.4.3) Surviving detachment and circulation

A prerequisite for successful metastasis is the ability of cells to withstand apoptosis induced by the loss of cell adhesion, also called anoikis.⁵⁹⁻⁶⁰ Anoikis is a crucial physiological defense mechanism that prevents cells that have detached from reattaching to new matrices incorrectly, preventing dysplastic growth.⁶⁰ The extracellular matrix provides a substrate to which epithelial cells attach inducing survival and growth.⁶¹ Once detached, these pro-survival cues are lost and cells will usually enter anoikis.⁶¹⁻⁶² Neoplastic cells develop the ability to proliferate independently of cell adhesion, and are termed anoikis-resistant cells.⁶¹⁻⁶²

Once detached, the metastatic cells must disseminate to a secondary site via the circulation (Figure 1.2). The metastatic cascade is very inefficient, with less than 0.1% of disseminated cancer cells surviving to form a metastatic tumour.^{42,63} There is an extensive elimination of metastasising cells at multiple steps. For example, cells have to survive primary tumour cell dissemination, sheer force and changes in pH in the circulatory system, immune system attack and lack of compatibility at the secondary site.^{42,63-65} Due to these selection pressures, metastasising tumour cells have been shown to sometimes become dormant. Undetectable tumour cell populations known as micrometastases can survive in circulation for decades.⁶⁶⁻⁶⁷ These micrometastases are a result of either cell cycle arrest or the tumour cell population effectively balancing proliferation and apoptosis.⁴² Some of these micrometastases are capable of eventually growing to clinically relevant lesions/neoplasms (macrometastases), causing patient relapse.^{63,66}

1.4.4) Extravasation, colonization and proliferation

Upon surviving circulation and its associated pressures, metastatic cells extravasate and colonize a secondary site or organ (Figure 1.2). Certain cancer types have a propensity to metastasize to specific organs. For example, breast cancer commonly metastasizes to the bone, brain, lungs and liver.⁶⁸⁻⁷¹ This shows that, to a degree, the metastatic process occurs in a predictable (non-random) manner or pattern, with multiple factors in play.⁷⁰ Such a conclusion is not a novel one, in 1889 Dr Steven Paget interrogated the relationship between the organ distribution of metastases that developed from various human neoplasms by analysing over a thousand autopsy records of female breast cancer patients.⁷² His work documented a methodical pattern for the development of metastasis suggesting that it was not by chance. He theorised that specific tumour cells – “the seed”, had a certain affinity for the setting provided by certain organs – “the soil”. He summarised that metastases would occur only when/if the “seed and soil” were compatible.⁷³⁻⁷⁵ The present day definition of the theory comprises of three principles.^{72,75} First, a tumour is of a heterogeneous biological nature and it contains multiple subpopulations of cells with varying properties^{68,75} Second, the metastatic process is selective for cells that carry out all of the steps as

shown by the fact that metastases can be of clonal origin and that different forms of it can originate from the propagation of a single cell.⁷³⁻⁷⁵ Lastly, the results of metastasis are dependent on numerous interactions (“cross-talks”) between the metastatic tumour cells and homeostatic mechanisms which the tumour cells can employ.⁷⁵ The original Paget theory is now widely accepted,^{68-69,73-75} with the “seed” being retitled the progenitor, stem or metastatic cell and the “soil” the niche, host factor or organ/tissue microenvironment. Irrespective of terminology, the progression and success of the metastatic process is highly dependent on the on-going interaction between the tumour cell and its microenvironment.^{71,73,75} In addition to these physiological factors, mechanical factors can also play a role in determining the sites of metastases. For example, the lung is a common organ for metastasis but this is, in part, due to circulating tumour cells getting stuck in the narrow passageways of the bronchioles.⁷¹

As mentioned above, the epithelial phenotype is characterised by apical-basal polarity, attachment to substrate and expression of markers such as E-cadherin, occludins and collagen.⁷⁶⁻⁷⁷ In contrast, the mesenchymal phenotype is characterised by front-back polarity, a lack of attachment to substrate and expression of markers such as n-cadherin, fibronectin and vimentin.^{76,78} Cells in the mesenchymal state are multipolar, have no junctions and are spindle shaped with strong migratory potential, whilst cells in an epithelial state have a polygonal shape, have strong cellular adhesion with the presence of adherens, tight and gap junctions.⁷⁶ To colonize the secondary site, cells have to trade in the mesenchymal phenotype (gained via EMT), and its associated markers and advantages towards metastasis, and return to an epithelial phenotype in a process called mesenchymal-epithelial transition (MET).⁷⁶ It has been shown that the re-expression of markers such as E-cadherin and occludins brought about by MET increases tumour cell survival and drug resistance at the secondary site.⁷⁷⁻⁷⁸

1.5) Cell-to-cell communication

1.5.1) Mechanisms of cell-to-cell communication

No cell is an island. One of the central features of a multi-cellular organism is the development of diverse tissues as collaborative communities of cells. With this, each cell possesses an individual identity, but is dependent on a continuous interaction and communication with other cells (Figure 1.4).⁷⁹ Intercellular cross-talk is a crucial physiological occurrence necessary for the spreading of chemical signals between cells, either at close proximity or at a distance.⁸⁰ This cross-talk enables the proper regulation of cellular growth, metabolism, homeostasis and motility.⁸⁰⁻⁸¹ Cell signalling consists of three stages that convey an external message to an internal cellular response. It is initiated when there is reception of the signalling molecule (the first stage), which results in intracellular signal transduction (the second stage) and concludes with an intracellular response (the third stage).⁸²⁻⁸³ As mentioned above, cell-to-cell communication can either be at close proximity (direct) or at a distance (indirect).⁸⁰ Direct forms of intercellular communication occur between cells physically in contact with one another, where the chemical signal passes through the cytoplasmic fluid. Indirect intercellular communication occurs via chemical diffusion where the chemical signal passes through interstitial fluid or blood.⁸²

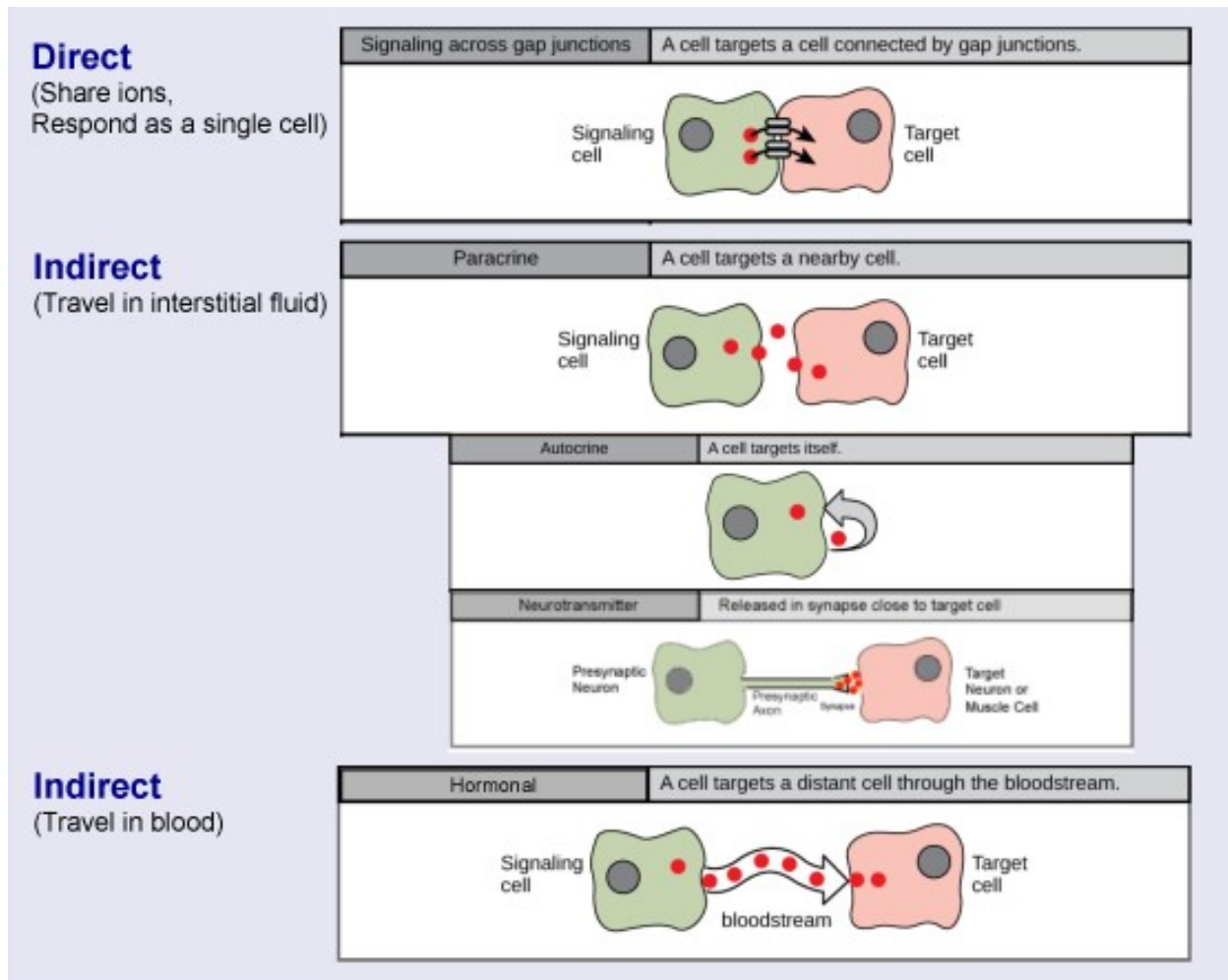


Figure 1.4: Forms of chemical signalling. Cell signalling can either be direct or indirect. Direct forms of communication consist of signalling across gap junctions. Indirect forms consist of paracrine, autocrine and neurotransmitter-based communication that travels in interstitial fluid or hormonal communication that travels in blood. Reproduced from Dong and Liu (Open access).⁸²

1.5.2) Direct versus indirect intercellular communication

1.5.2.1) Direct cell-to-cell communication

Surface proteins give cells their identity.⁷⁹ Cells in contact communicate by ‘reading’ each other’s tissue-specific surface-residing cell markers.⁸¹ The majority of these cell-surface markers are comprised of carbohydrate containing lipids known as

glycolipids.⁸⁴ The makeup and arrangement of the physical connections between adjacent cells determine what is communicated between the cells. These connections determine the nature of the tissue, which in turn determines its function.⁷⁹ There are different forms of these physical cell connections, namely adhesive junctions, tight/septate junctions and gap junctions.^{79,84}

With primitive forms being identified in sponges, adhesive junctions appear to be the first to have evolved.⁷⁹ Adhesive junctions function to mechanically attach the cytoskeletons of adjacent cells to each other or to attach cells to the ECM.^{79,85-86} There are four types of adhesive junctions, namely desmosomes, adherens junctions, hemidesmosomes and focal adhesions.⁷⁹ Adherens junctions exert their function through one cell's cadherin binding the extracellular domain of an adjacent cell's cadherin. They are primarily found in tissues that endure high stress, such as the skin.⁷⁹ Unique to vertebrates, desmosomes provide strong and flexible cellular connections.^{79,85} They contain desmocollin and desmoglein, forms of cadherins that bind the intermediate filaments of the cytoskeleton.⁸⁵ They are most common in epithelium.⁷⁹ Hemidesmosomes and focal adhesions connect cells to substrate through the use of integrins. These connections to the substrate are important during development and cell movement.⁷⁹

Septate or tight junctions are present in both vertebrates and invertebrates.⁸⁶ They form a barrier that seals off cells, forcing material to pass through, but not between, cells.^{79,86} Septate junctions are widespread and their distribution suggests that they evolved with, or directly after, adhesive junctions.⁷⁹ Tight junctions, which are unique to vertebrates block (occlude) the passage of material between cells. They exert their function through the protein occludin.⁷⁹

Gap junctions are physical cell connections that allow communication between cells of multicellular organisms.^{79,84-86} This relay of information occurs through the 'sharing' of small molecules using channels between the cells. These channels are known as gap junctions in animals and plasmodesmata in plants.⁷⁹ Gap junctions are defined as collections of intercellular channels spanning the plasma membrane of neighbouring cells that facilitate direct intercellular communication.^{83,87} Gap junctions prevent dilution of the chemical signal by preventing its entry into an extracellular space, and rather allow hydrophilic molecules, secondary messengers and ions of a mass smaller

than 2 kilodalton (kDa) to easily diffuse through aqueous channels between the cytoplasm of adjacent cells.^{82-83,87}

Nanotubules are open-ended, actin-based cytoplasmic extensions that physically connect cells to facilitate direct intercellular communication (Figure 1.5).⁸⁸ First described by Rustom *et al*, these nanotubules, also known as tunnelling nanotubules (TNTs), can range from 50 to 200 nanometers (nm) long.⁸⁹ TNTs are part of the family of actin based projections which also includes filopodia and invadopodia.⁹⁰ However, unlike the adhesive projections, TNTs lack adherence to the substratum *in vitro* and have small diameters.^{89,91-92} These cytoplasmic bridges function to transport cargo between cells and are capable of transporting cargo ranging from full length RNA (mRNA) to whole organelles and pathogens.⁹²⁻⁹³ The biosynthesis of TNTs is largely actinomyosin dependent.^{88,91} Firstly, TNT inducer proteins such as the small GTPase RalA and M-Sec direct the development of filopodia-like protrusions in a process called 'actin driven protrusion mechanism'. Alternatively, TNT formation occurs as a result of previously linked cells detaching, known as the 'cell dislodgement mechanism'.^{92,94} The elevated expression of motor proteins such as myosin10 and actin regulatory proteins such as Eps8 have also been shown to significantly increase the formation of TNTs.^{92,94}

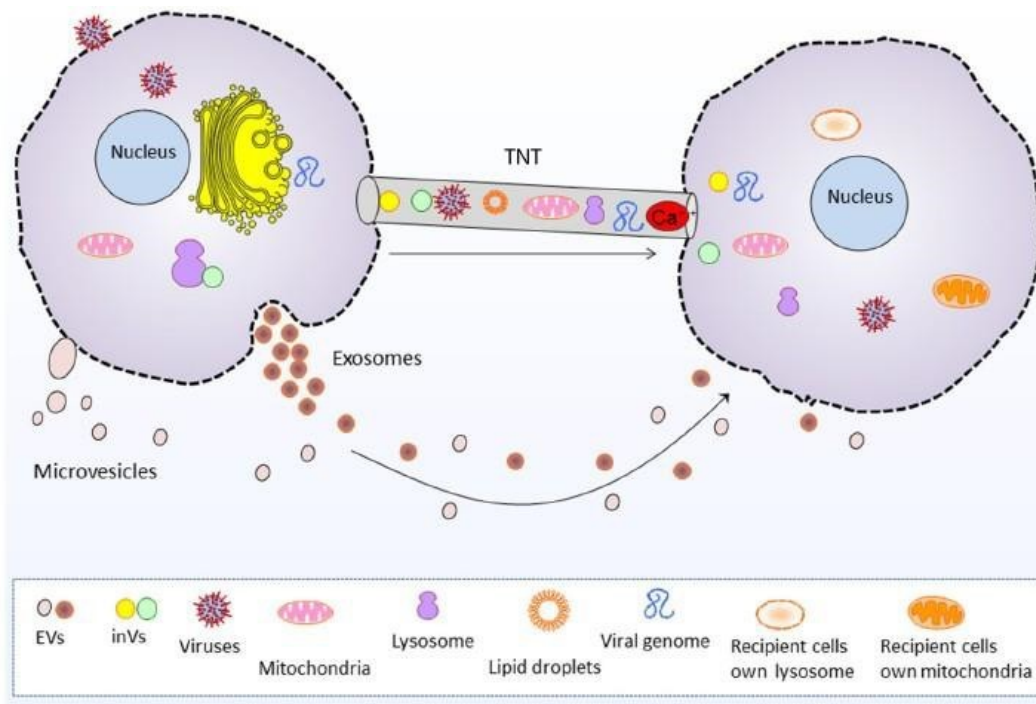


Figure 1.5: Intercellular communication between two cells can occur via direct or non-direct mechanisms. *Intercellular communication between two cells can occur via direct or non-direct mechanisms, with the form of communication dictating the biomolecules communicated. Extracellular vesicles (EVs) require packaging of relatively small cargo as opposed to tunnelling nanotubes (TNTs). The nanotubes can transport whole organelles and pathogens. Obtained from Nawaz and Fatima (Open access).⁸⁸*

1.5.2.2) Indirect cell-to-cell communication

Chemical signalling can occur over varying distances, the indirect signalling processes are primarily characterised by where the signal acts.⁹⁵⁻⁹⁷ These chemical signals play important roles in the regulation of the immune system, tissue function and other numerous crucial physiological functions.⁹⁷ Indirect cell-to-cell communication can be classified as paracrine, autocrine or endocrine.^{95,98} Paracrine cell signalling occurs when a cell produces a chemical signal that acts on neighbouring cells that are not in direct contact to the donor cell, inducing a change in behaviour in these nearby cells.⁹⁵ Autocrine cell signalling occurs when a cell produces chemical signals that act on the

very cell that produced them.⁹⁵ For both paracrine and autocrine cell signalling, the biomolecules secreted are present at a high concentration in close proximity to the cells that secreted them and the signals travel via the interstitial fluid.^{95,99} In contrast, endocrine cell signalling is a form of indirect cell signalling that involves the trafficking of the chemical signal to a distant site via the bloodstream - these signals are known as hormones.⁹⁹

1.5.2.3) Extracellular vesicles

One of the most commonly researched mediators of indirect non-endocrine communication is extracellular vesicles (EV).⁸¹ However, this has not always been the case and in the 1980's and 90's extracellular vesicles were believed to merely be a cells waste disposal mechanism, or were widely considered just to be artifacts of dying or dead cells due to their similarities (mainly in size) to apoptotic bodies.¹⁰⁰ It was not until the late 1990's that there was renewed interest in this form of indirect cell signalling, after Raposo *et al* described them as an intercellular communication tool.¹⁰¹ The first clue that they were important for communication was the observation that communicated cargo could elicit a response.¹⁰¹ It was discovered that EVs house numerous biomolecules ranging from antigens, lipids and nucleic acids, such as microRNA (miRNA), which when taken up (endocytosed) repress the host RNA and machinery resulting in the modification, regulation and initiation of a wide range of cellular functions.¹⁰²⁻¹⁰⁴ For example, they're released by antigen-presenting cells (APCs) to elicit a response in immune response cells, and are also involved in establishing immune memory in B cells.^{100,105} Additionally, oncogenes have been isolated from EVs.¹⁰⁰ This suggests that their transfer could play a role in the development or progression of cancer related phenotypes. Their known ability to modulate cellular behaviour could mean the promotion or furthering of pro-neoplastic conditions such as angiogenesis or metastasis.^{100,103,106} The effect of secreted EVs in physiological processes is dependent on their interaction with the target cells.^{103,107}

EVs are small membrane-derived, cytosol-containing, secreted biomolecule transportation tools packaged within a lipid bilayer (Figure 1.6).^{101-102,108} There are four types of EVs, namely oncosomes, microvesicles (MVs), apoptotic bodies and

exosomes (Figure 1.6).^{100,102,108} The largest form of EVs, oncosomes (1 – 10 micrometers (μm) diameter), are produced by tumour cells as a result of the scission of cellular membrane protrusions.^{101-102,108} The second largest form of EVs are known as microvesicles. They are formed inside cells through the fusion of multiple endocytic vesicles and lysosomes.^{101-102,108} The third largest form of EVs are released from cells undergoing programmed cell death. These vesicular apoptotic bodies have a diameter range of 50 nm – 2 (μm). Exosomes are the smallest, with a diameter range of 40-120 nm.¹⁰² They are formed when internalised multivesicular bodies fuse with the plasma membrane (PM) and release their content externally.¹⁰² They have a diameter range of 100 nm – 1000 nm.¹⁰²

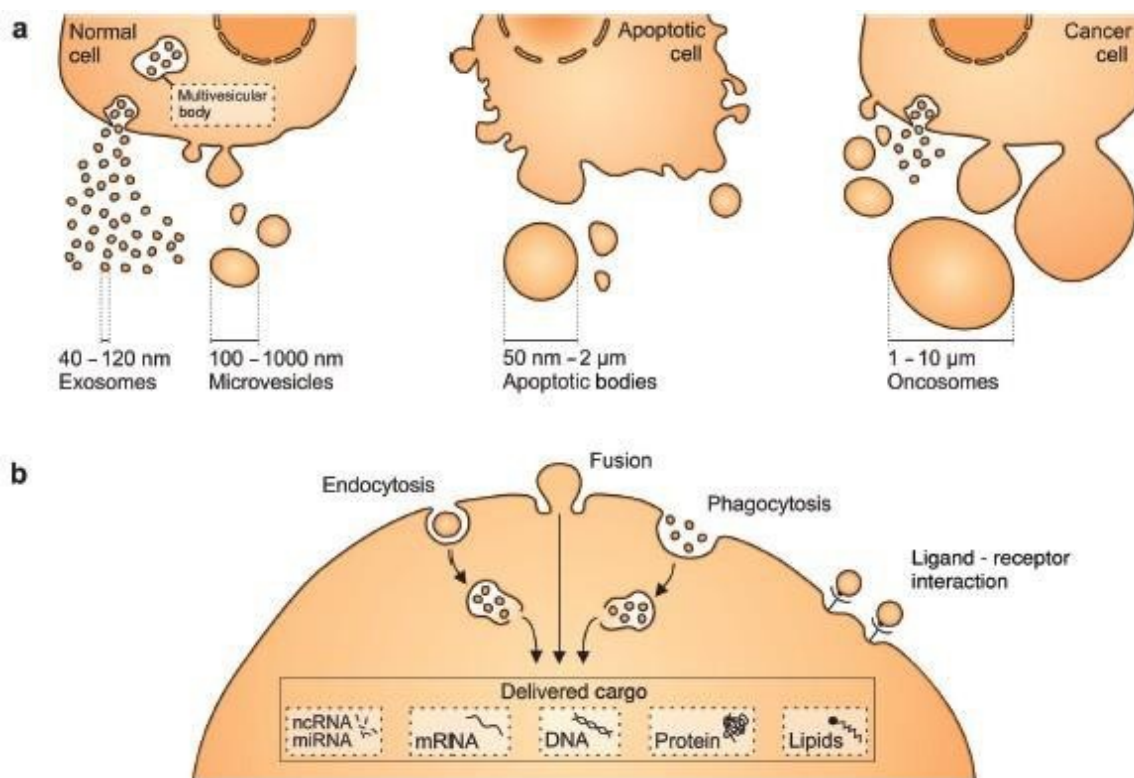


Figure 1.6: The different forms of extracellular vesicles produced. a) The varying forms and sizes of extracellular vesicles. *Exosomes and microvesicles (MVs) can be produced by both normal and pathological states. Apoptosis produces apoptotic bodies and neoplastic cells produce the large oncosomes.* b) *EVs can utilise different mechanisms to deliver their cargo. Obtained from Zaborowski and Balaj with permission.*¹⁰²

1.6) Research problem

Recent literature has emphasized the importance of the complex interplay between the matrix, immune and neoplastic cells within the tumour microenvironment, but little is known about how neoplastic cells interact and influence other neoplastic cells.¹⁰⁹⁻¹¹⁰ This overlooked intercellular communication, which can be direct or indirect via communication tools such as EVs, could be a driver of processes with greater implications.¹⁰⁹ For example, the metastatic spread of tumour cells remains an underlying cause of breast cancer-related deaths.¹¹¹ Metastatic progression could be promoted through miRNAs such as the ones isolated from EVs within the tumour microenvironment, that diffuse through it, reaching immune and neoplastic cells alike, influencing phenotypes and regulating protein expression.⁹⁵

Biomarkers are quantifiable 'characteristics' that represent normal or pathogenic conditions.¹¹² There are a wide range of biomarkers associated with breast cancer but there are three that are most extensively used to characterise the pathology within clinical practice like estrogen receptor (ER), progesterone receptor (PR), and human epidermal growth receptor 2 (HER2).¹¹²⁻¹¹³ Estrogen is a known carcinogen and approximately eighty percent of all breast cancers are ER-positive.¹¹² The PR gene is modulated by estrogen therefore PR expression correlates to a faultless or thriving ER pathway.¹¹² Tumours that are ER-positive and PR-negative have been shown to be less responsive to common treatments such as tamoxifen in comparison to tumours expressing both receptors.¹¹²⁻¹¹³ Thirteen to twenty percent of all invasive breast cancer has been shown to be HER2-positive with more than half of the cases lacking hormone receptors (ER- and PR-).¹¹² HER2 overexpression is a clinical prognostic tool used to predict patient responsiveness to treatments such as trastuzumab.¹¹² There is a subset of tumours that that are negative for all three receptors, known as triple-negative breast cancer (TNBC).¹¹² It is generally faster growing and more aggressive with a higher chance of recurrence.¹¹²⁻¹¹³ Therefore, the aim of this study was to investigate cell-to-cell communication between different types of breast cancer cells as a step towards unravelling its potential role in cancer cell physiology and metastasis.

CHAPTER 2 AIM AND OBJECTIVES

2. AIM AND OBJECTIVES

2.1) Aim

The aim of this study was to determine if cell-to-cell communication between different types of breast cancer cells can alter their cellular physiology.

2.2) Objectives

- To evaluate if cell-to-cell communication between non-metastatic and metastatic breast cancer cells, affects recipient cellular physiology by:
 - I. Determining the effect of conditioned medium from a metastatic cell line on the cell attachment of a non-metastatic cell line.
 - II. Determining the effect of conditioned medium from a metastatic cell line on the cellular metabolism of a non-metastatic cell line.
 - III. Determining the effect of conditioned medium from a metastatic cell line on cellular migration of breast cancer cell lines
- To show that biomolecule transfer does occur between different breast cancer cells by establishing a transfer model through:
 - I. Creation of stable recombinant donor and recipient cell lines
 - II. Confirmation of cell-to-cell communication via the successful colour switching of the recipient cell line
 - III. Establishing whether biomolecule transfer occurs in a 3D spheroid model

CHAPTER 3 MATERIALS AND METHODS

3. MATERIALS AND METHODS

Table 3.1: Cell lines utilised in the study

Cell line	Associated disease	Biomarker expression	Supplier	City & Country	Catalogue number
MCF7 (metastatic)	Adenocarcinoma	Estrogen receptor	ATCC	Virginia, USA	HTB-22
MDA-MB-231 (metastatic)	Adenocarcinoma	Triple-negative	ATCC	Virginia, USA	CRM-HTB-26
BT20 (non-metastatic)	Carcinoma	Triple-negative	ATCC	Virginia, USA	HTB-19
HEK293 (non-metastatic)	None but tumorigenic, can form tumours in nude mice	N/A	ATCC	Virginia, USA	CRL-1573

3.1) Cell lines

This study utilised three breast cancer cell lines and a human embryonic kidney cell line (Table 3.1). These were the Breast Tumour-20 (BT20), Michigan Cancer Foundation-7 (MCF7), M.D. Anderson metastatic breast-231 (MDA-MB-231) and the human embryonic kidney-293 (HEK293-T) cell lines.¹¹⁴⁻¹¹⁶ The BT20 human breast cancer cell line is an adherent and tumorigenic but non-metastatic cell line isolated from the primary tumour in the mammary glands of a 74-year-old Caucasian female.¹¹⁷ The MDA-MB-231 human breast cancer cell line is an adherent, tumorigenic and metastatic cell line isolated from the pleural effusion of a 51-year-old Caucasian female with TNBC.¹¹⁵ The MCF7 cell line is an adherent and

tumorigenic, non-metastatic cell line isolated from the pleural effusion of an estrogen receptor positive 69-year-old Caucasian female.¹¹⁷ Previously known as 293tsA1609neo, the HEK293 cell line is an adherent cell line derived from embryonic kidney cells. HEK293 cells are widely used in experiments because they are relatively easy to transfect and stably express SV40 large T-antigen which allows them to replicate vectors housing the SV40 origin of replication.¹¹⁵ They yield high titres when utilised for retrovirus production and are primarily used for the production of retroviruses, exogenous gene expression and protein production.^{114,116-117}

3.2) Cell maintenance, counting and storage

Table 3.2: Cell culture reagents and materials

Cell culture	Supplier	City & Country	Catalogue number
<u>Reagents</u>			
DMEM	Invitrogen	California, USA	10566016
MEM	Invitrogen	California, USA	21090022
Ham's F-12	Invitrogen	California, USA	21765029
FCS	Invitrogen	California, USA	10499044
GlutaMax™	Invitrogen	California, USA	35050061
Trypsin-EDTA	Invitrogen	California, USA	25200056
Trypan blue solution	Gibco	California, USA	15250061
DSMO	Invitrogen	California, USA	D12345
<u>Materials</u>			
T75 culture flask (75 cm ²)	Greiner Bio-One	Kremsmunster, Austria	658940
15 ml falcon tube	Lasec	Cape Town, South Africa	*
Serological pipettes	Lasec	Cape town, South Africa	*
Eppendorf® tubes	Lasec	Cape town, South Africa	*
Freezing tubes	Greiner Bio-One	Kremsmunster, Austria	E21083EP
Mr. Frosty™ freezing containers	ThermoFisher scientific	Massachusetts, USA	5100-0001
Countess™ cell counting chamber slides	ThermoFisher scientific	Massachusetts, USA	C10228

* Consumables obtained from Lasec; link:

<https://www.lasec.com/catalogue/consumables/bioscience-plastics.html>

Method

All cell culture was performed using aseptic techniques in a laminar flow cabinet. Cell culture media was incubated in a warming oven at 37°C for an hour before undertaking of experiments, whilst trypsin-EDTA was warmed at room temperature. The MDA-MB-231, MCF7 and HEK293 cell lines were cultured in Dulbecco's modified eagle medium (DMEM) supplemented with 10% foetal calf serum (FCS) (v/v) whilst the BT20 cell line was cultured in phenol red-free Minimum essential media (MEM) supplemented with 10% FCS and 1% GlutaMax™ (v/v). Each cell line was cultured in a T75 flask. When the cell monolayer reached 80% confluence in the T75 culture flask, cells were passaged. The media was aspirated and the cells washed with 10 ml of phosphate buffered saline (PBS; 1.37 M NaCl; 27 Mm KCl; 18 mM KH₂PO₄; 100 mM Na₂HPO₄, at pH 7.4) then incubated in 1 ml of 1 x trypsin-EDTA for 5-10 min at 37°C. A volume of 9 ml fresh culture media was then added to the cell suspension, the total volume of 10ml cell suspension was pipetted into a 15 ml Falcon tube and centrifuged for 3 min at 300 xg to pellet the cells. The trypsin-EDTA-containing media was carefully aspirated leaving an undisturbed cell pellet. Cells were resuspended in 10 ml fresh growth media. For the MDA-MB-231, MCF7 and HEK293 cell lines, 1 ml of the cell suspension was returned to a T75 culture flask then 9 ml fresh media was added to sustain the cells until the next passage. For the BT20 cell line, 3 ml of the cell suspension was returned to a T75 culture flask then 7 ml fresh media added to sustain the cells until the next passage.

For use in assays, cell density of the post-passage cell suspension was measured using a Countess™ II automated cell counter (ThermoFisher Scientific, Massachusetts, USA). A volume of 10 µl of the cell suspension was mixed with a volume of 10 µl of Trypan blue within a 500 µl volume Eppendorf® tube, then 10 µl of this mixture was carefully pipetted onto a Countess™ cell counting chamber slide and was loaded into the counting chamber to obtain the ratio and number of live to dead cells within the suspension. Live cell values were utilised for calculation of experimental seeding densities. To maintain low-passage cell stocks, samples of each cell line were stored in liquid nitrogen. To generate these, 0.75 ml of the post-passage cell suspension was added to 0.75 ml of 2 x freeze media (80% FCS; 20% dimethyl sulfoxide (DMSO) (v/v)) and was transferred to 2 ml cryovials. The cryovials were transferred to Mr. Frosty™ freezing containers and were incubated at -80°C

overnight to allow for a gradual decrease in temperature before storage in liquid nitrogen (vapour phase). To produce conditioned media, serum-free media (Serum-) was added onto cell monolayers grown to fifty percent confluence and was incubated for 48 hrs. Confluence was calculated using cell number at seeding and cellular doubling time. The resultant conditioned media was centrifuged at 1500 xg for 12 min to remove large cellular debris.¹¹⁸ Both BT20 and MDA-MB-231 cells were used to generate conditioned media (BT20-CM and MDA-CM, respectively).

For EV isolation, we utilised a protocol from Li *et al.*¹⁰⁷ A volume of 50 ml of conditioned media was initially spun down at 300 xg for 10 min using a Beckman Coulter Optima XL-90 swinging rotor ultracentrifuge (355896, California, USA) to get rid of any cells. Following which the supernatant was spun down at 2,000 xg for 10 min to get rid of dead cells, then 10 000 xg for 30 min to get rid of cell debris.¹⁰⁷ Finally, the supernatant was spun at 100 000 xg for 70 min to pellet all EV types. The EVs were resuspended in serum-free media equal to the remaining volume of supernatant, which contained the soluble factors.¹⁰⁷

3.3) Investigating cellular attachment utilising a crystal violet assay

Table 3.3: Crystal violet reagents and materials

Crystal violet	Supplier	City & Country	Catalogue number
<u>Reagents</u>			
Glutaraldehyde	Sigma Aldrich	St Louis, Missouri, USA	G6257
Crystal violet	Sigma Aldrich	St Louis, Missouri, USA	C6158
Triton™ X-100	Sigma Aldrich	St Louis, Missouri, USA	X100
<u>Materials</u>			
96-well plate	Greiner Bio-One	Kremsmunster, Austria	655201

Method

The MDA-MB-231, MCF7 and BT20 cell lines were seeded at a density of 5×10^4

cells/ml in sterile 96-well culture plates at a volume of 200 μ l/well and incubated overnight at 37°C. The next day, media was aspirated and 200 μ l/well of Serum+ media, Serum- media, EE-15-one (C8) a methoxy-estradiol derivative, BT20-CM or MDA-CM and were incubated for 24 hrs, 48 hrs or 72 hrs. Background control samples were included, in which empty wells were incubated with the crystal violet dye. The absorbance measurements from the control samples were subtracted from the absorbance values obtained from the experimental samples for normalisation. At the end of each incubation timepoint, media was aspirated from each well and 100 μ l of 1% (v/v) glutaraldehyde was added and incubated for 15 min at room temperature. The glutaraldehyde was discarded, cells stained with 100 μ l of 1% (w/v) crystal violet dye and incubated at room temperature for 30 min. After incubation, the dye was discarded, and plates submerged in tap water to wash off any unbound dye. The plates were left to air dry overnight. To solubilize the dye from the cells, 200 μ l of 0.2% Triton™ X-100 (v/v) was added to each well and incubated at room temperature for 30 min. The absorbance of the solubilised dye was measured using a Biorad iMark microplate spectrophotometer at a wavelength of 570 nm. The experiment was repeated for a minimum of three independent biological repeats, in which each data point was performed with three technical repeats.

3.4) Investigating cell migration utilising a scratch assay

Table 3.4: Scratch assay materials

Scratch assay	Supplier	City & Country	Catalogue number
<u>Materials</u>			
12-well plate	Greiner Bio-One	Kremsmunster, Austria	665180
200 μ l volume yellow pipette tip	Lasec	Cape town, South Africa	732008

Method

The MDA-MB-231 and BT20 cell lines were seeded into sterile 12-well culture plates at densities of 2.5×10^4 cells/ml and 4×10^4 cells/ml, respectively, at a volume of 1000 μ l/well. These cell densities were optimised prior to commencement of the assay

using densities ranging from 1×10^4 cells/ml to 5×10^4 cells/ml. Cell density selected following the formation of a monolayer where confluence is approximately 90%. The cells were left to grow overnight 37°C then a sterile 200 μl volume yellow pipette tip was used to scratch the cell monolayer from one end of the well to the other, creating a cell free zone. Detached cells were gently washed away using 1 ml PBS. The cells were then treated with conditioned media (MDA-CM or BT20-CM) or control media (Serum+ media or Serum- media). Images of the cell free zones at '0-hr' (before) were taken with a Zeiss Axiovert inverted microscope (Zeiss, Germany) immediately after treatment. Cells were then incubated at 37°C for an 18-hr period. After which, an '18-hr' (after) image was taken for each treatment condition. Cells along the edge of the cell free zone are expected to migrate into the zone at different rates as a result of the effects of the different treatments. The crossing point of the scratches was used as a reference point for images to be taken. The change in width of the cell free zone was calculated using Image J analysis software and the percentage difference in surface area was used as a proxy for cell migration. The experiment was repeated for a minimum of three independent biological repeats, in which each data point was performed with a minimum of three technical repeats.

3.5) Investigating the effect of conditioned media treatment on the cell cycle utilising flow cytometry

Table 3.5: Flow cytometry reagents and materials

Flow cytometry	Supplier	City & Country	Catalogue number
<u>Reagents</u>			
Trypsin-EDTA	Invitrogen	California, USA	25200056
DMEM	Invitrogen	California, USA	10566016
FCS	Invitrogen	California, USA	10499044
Ethanol	Sigma Aldrich	St Louis, Missouri, USA	24194
Propidium iodide	Sigma Aldrich	St Louis, Missouri, USA	81845

Ribonuclease A	Sigma Aldrich	St Louis, Missouri, USA	R4875
<u>Materials</u>			
6-well plate	Greiner Bio-One	Kremsmunster, Austria	657960
Polypropylene sample tubes	Beckman Coulter	California, USA	2523749
15 ml Falcon tubes	Lasec	Cape town, South Africa	*

* Consumables obtained from Lasec; link:

<https://www.lasec.com/catalogue/consumables/bioscience-plastics.html>

Method

The MDA-MB-231 and BT20 cell lines were seeded in sterile 6-well culture plates at a density of 2.5×10^5 cells/ml at a volume of 2ml/well. The cells were incubated overnight at 37°C then treated with conditioned media (MDA-CM or BT20-CM) or control media (Serum+ media or Serum- media), following which, the cells were incubated for a 72-hr period. The cells then underwent a 3 x 5 minutes PBS wash, following which the cells were incubated with 1 ml per well of 1 x trypsin-EDTA for 8 mins and then were resuspended in 1 ml of growth media. The resultant cell suspensions were transferred to 15 ml Falcon tubes then centrifuged for 5 min at 300 xg and the supernatants were carefully aspirated. The pellets were resuspended in ice cold PBS containing 0.1% FCS. Subsequently, 4 ml of 70% ethanol (v/v) was added in a drop-wise manner whilst vortex mixing the suspensions at very slow speeds to ensure fixation of all cells and minimize cell clumping. Samples were kept at 4°C, undergoing fixation for at least 30 min. (Note: Samples can be kept at these conditions for several weeks). After fixation, cells were washed with PBS via centrifugation at 300 xg for 5 min and careful aspiration of the supernatant. Cells were then resuspended in 750 µl PBS added to 200 µl propidium iodide (PI) (40 µg/ml) and 50 µl ribonuclease A (100 µg/ml) and were incubated at room temperature for 5 to 10 min. The cell suspensions were then slowly mixed before transfer of 1 ml volumes to polypropylene sample tubes. Fluorescence intensity of the samples was then measured using a CytoFLEX® flow cytometer (Beckman

Coulter, California, USA). Cell cycle distributions were calculated using Kaluza and Kaluza C analysis software from Beckman Coulter which assigned relative DNA content per cell to the phases of the cell cycle. The experiment was repeated for a minimum of three independent biological repeats, in which each data point was performed with a minimum of three technical repeats.

3.6) Immunohistochemistry

Table 3.6: Immunohistochemistry reagents and materials

Immunohistochemistry	Supplier	City & Country	Catalogue number
<u>Reagents</u>			
DMEM	Invitrogen	California, USA	10566016
DMEM (phenol red-free)	Invitrogen	California, USA	31053044
Ham's F12	Invitrogen	California, USA	21765029
PFA	Sigma Aldrich	St Louis, Missouri, USA	P6148
Triton™ X-100	Sigma Aldrich	St Louis, Missouri, USA	X100
BSA	Sigma Aldrich	St Louis, Missouri, USA	A7030
DAPI	Invitrogen	California, USA	C6158
Phalloidin (Actin)	Abcam	Cambridge, UK	Ab176753
Anti-FAK (EP695Y)	Abcam	Cambridge, UK	Ab40794
Alexa Fluor 350® (DaM)	Abcam	Cambridge, UK	Ab150105
4HT	Sigma Aldrich	St Louis, Missouri, USA	T5648
Agarose	Bio-Rad	California, USA	1613102
Urea	Sigma Aldrich	St Louis, Missouri, USA	U5378
D-sorbitol	Sigma Aldrich	St Louis, Missouri, USA	S1876
Glycerol	Sigma Aldrich	St Louis, Missouri, USA	G5516
DSMO	Invitrogen	California, USA	D12345
<u>Materials</u>			
24-well plate	Greiner Bio-One	Kremsmunster, Austria	657960

96-well plate	Greiner Bio-One	Kremsmunster, Austria	655201
8-well microplate	Zeiss	Oberkochen, Germany	*
12 mm coverslips	Lasec	Cape town, South Africa	1000F-02-1009
Glass microscopy slides	Lasec	Cape town, South Africa	03052020
Eppendorf tubes	Sigma Aldrich	St Louis, Missouri, USA	EP0030124707
50 ml Falcon tube	Greiner Bio-One	Kremsmunster, Austria	210270

* Consumables obtained from Lasec; link:

<https://www.lasec.com/catalogue/consumables/bioscience-plastics.html>

3.7) Investigating cell adhesion architecture post treatment with conditioned media using confocal microscopy

Method

BT20 cells were seeded at a density of 7×10^4 cells/ml onto 12 mm glass microscopy cover slips, in 24-well culture plates at a volume of 1 ml/well and were incubated at 37°C overnight to allow attachment. Cells were treated with conditioned media (MDA-CM or BT20-CM) and control media (Serum+ media or Serum- media) for 48 hrs at 37°C. After incubation, media was aspirated and 1 ml of 2% paraformaldehyde (PFA) (v/v) was added to the wells and incubated at room temperature for 15 min making sure to cover the samples with foil due to light sensitivity. The PFA was then aspirated and samples washed at least three times with PBS before addition of 1 ml of 0.2% Triton™ X-100 and further incubation for 5 min. Samples were then washed at least three times with PBS before addition of 0.5 ml of 2% bovine serum albumin (BSA) (w/v) in PBS and incubation for 1 hr at room temperature to block. The blocking solution was then removed, and the cover slips washed at least three times with PBS. To detect FAK, a rabbit monoclonal anti-FAK antibody was used (EP695Y;

Abcam; Cambridge; UK) and to detect actin, mouse phalloidin (Ab176753; Abcam; Cambridge; UK) dye was used. A volume of 20 µl of the primary antibody for focal adhesions – FAK (1:500) and actin fibres phalloidin (1:500) - was ‘spotted’ onto wrapping film in a drop-wise manner and slides were placed facing downwards onto the antibody. The slides were incubated for an hour then washed at least three times with PBS. The slides were then placed facing downwards onto the Alexa Fluor 350® DaM (150105; Abcam; Cambridge; UK) secondary antibody (1:200) and incubated for 30-60 min. Afterwards, the slides were washed at least three times with PBS and mounted onto glass slides using 4',6- diamidino-2-phenylindole (DAPI) mounting fluid. Confocal images were taken using the 63x oil objective of a LSM800 confocal microscope (Zeiss, Germany).

3.8) Investigating the effect of MDA-CM on BT20 cells using real-time confocal microscopy

BT20 cells were seeded at a density of 2×10^4 cells/well in 8-well confocal microplates and were and incubated at 37°C for 4 hrs in a humidified chamber of a Zeiss LSM800 confocal microscope (Zeiss, Germany). Cells were then treated with conditioned media (MDA-CM or BT20-CM) and control media (Serum+ media; C8). To allow for time for treatment to take effect, cells were incubated for a further 4 hrs before recording commenced, with the camera taking a frame-by-frame image every 20 min for a 24-hr period. Cell protrusions, cell rounding and apoptotic cells were quantified every 2 hrs using Image-J analysis software. The experiment was repeated for a minimum of three independent biological repeats, in which each data point was performed with a minimum of three technical repeats.

3.9) Investigating the colour switch system using confocal microscopy

The MDA-MB-231 cell line was grown in complete DMEM and the BT20 cell line in media comprising of 50% complete DMEM and 50% complete Ham's F-12 media (an alternative to MEM media). Therefore, for co-culture experiments, cells were grown in

50% complete DMEM and 50% complete F-12 media, to suit both cell types. To determine the cell density ratios to use for the co-cultures, a pilot study was conducted where a 12-well plate was seeded with MDA-MB-231 cells expressing Cre recombinase and Cyan fluorescent protein (CFP), (MDA-CRE-CFP), at concentrations of 5×10^2 cells/ml, 1×10^3 cells/ml and 2×10^3 cells/ml at a volume of 1 ml/well. Each cell density was co-cultured with 1×10^4 cells/ml of the BT20 cell line housing the switch module (BT20 Switch; See section 3.10) at a volume of 1 ml/well. The cells were seeded onto 12 mm glass microscopy coverslips. Based on the cell densities post-incubation, primarily looking at cellular overgrowth, the optimum cell ratio was determined to be a 1 to 10 'MDA-CRE-CFP' to 'BT20 Switch' cell. For 2-dimensional (2D) co-cultures, cells were seeded and allowed to attach overnight at 37°C. Each cell combination was treated with 3 μ M of 4-hydroxy tamoxifen (4HT) and incubated for at least 48 hrs at 37°C. The following day, the cells were washed with 1x PBS for 3 x 5 min washes, then mounted onto glass microscopy slides.

To generate 3-dimensional (3D) cultures (spheroids), cells were deprived of attachment to the bottom of the plate promoting attachment to one another. A PBS border was added to a 96-well plate at a volume of 150 μ l per well to prevent media evaporation. The plates were treated with 2% agarose media (w/v) made from agarose powder mixed into phenol red-free DMEM media at a volume of 100 μ l per well. Fluorescent cells in suspension were added at 100 μ l per well onto the agarose substrate at a ratio of 1 to 4 MDA-MB-231 (5×10^3) cells to BT20 cells (2×10^4). The plate was incubated for 72 hrs in a humidified incubator to allow formation of the spheroids. At least half of the spheroids were treated with 4HT and the spheroids grown for another week with media carefully changed every 72 hrs. Spheroid growth images were taken at magnifications of 10x and 20x using an Axiovert inverted microscope (Zeiss, Germany). Using a 1 ml filter tip with the end cut, the spheroids were gently aspirated and all 4HT-positive ones added to one Eppendorf tube and 4HT-negative ones in another. The spheroids were allowed to settle for 2 min then the media was carefully aspirated. A volume of 1 ml 4% PFA (v/v) was added to each tube to fix, and the tubes were wrapped in foil to protect from light. The tubes were put in a 50 ml falcon tube and left on a roller overnight at the lowest speed setting. The following day, the spheroids were washed with PBS for 3 x 5 min washes, carefully allowing

the spheroids to settle between each wash. Following this, the spheroids were then washed for an hour with PBS. The PBS was carefully aspirated, leaving the least amount possible without disrupting the spheroids. Prior to imaging, the spheroids were cleared from being opaque using a spheroid clearing solution (20% urea (w/v), 30% D-sorbitol (w/v) and 5% glycerol (w/v) in DMSO). A volume of 200 μ l of the clearing solution was added to each tube for 5 min and incubated at room temperature, then 1 ml dH₂O was added to dilute, before carefully aspirating the solution. The spheroids were mounted onto glass slides and left to set overnight before imaging. Confocal images were taken using the 63x oil objective of a LSM800 confocal microscope (Zeiss, Germany).

3.10) Generation of stable cell lines

Table 3.7: Characteristics of the plasmids utilised in making the stable cell lines

Plasmid	Vector backbone	Gene/Insert name	Selectable markers	Addgene catalog number
CFP	pLKO.1	H2B-CFP	Puromycin	25998
Switch	pLV	LoxP-DsRed-LoxP-eGFP	Ampicillin	65726
Cre	pLV	CMV.CreERT2	Puromycin	none

Table 3.8: Transformation and transfection reagents and materials

Transfection & transformation	Supplier	City & Country	Catalogue number
<u>Reagents</u>			
Qiagen® Plasmid midi kit	Whitehead Scientific	Modderfontein, South Africa	12143
Qiagen® tips	Whitehead Scientific	Modderfontein, South Africa	12145
Ribonuclease A	Sigma Aldrich	St Louis, Missouri, USA	R4875

XtremeGENE™	Sigma Aldrich	St Louis, Missouri, USA	XTGHP-RO
-------------	---------------	----------------------------	----------

Ampicillin	Sigma Aldrich	St Louis, Missouri, USA	A9393
Puromycin	Sigma Aldrich	St Louis, Missouri, USA	P9620
LB Broth	Sigma Aldrich	St Louis, Missouri, USA	L3522
<i>Escherichia coli</i>	Sigma Aldrich	St Louis, Missouri, USA	CMC0001
<u>Materials</u>			
6-well plate	Greiner Bio-One	Kremsmunster, Austria	657960
Petri dishes	Greiner Bio-One	Kremsmunster, Austria	627860
0.45µm filter	Sartorius stedim	Gottingen, Germany	00044103
15ml Falcon tubes	Lasec	Cape town, South Africa	*

* Consumables obtained from Lasec; link:

<https://www.lasec.com/catalogue/consumables/bioscience-plastics.html>

Method

DNA transformation and transfection:

For transformation, on the first day, a volume of 1 µl of each plasmid was added into its own Eppendorf tube. After which, 30 µl of chemically competent XL 10-Gold® bacteria – *Escherichia coli* (*E. coli*) were added into each tube and mixed gently. The tubes were then left on ice for 10 min before being heat-shocked in a water bath at 42°C for 90 sec. After the water bath, the tubes were immediately put back on ice for 5 min. The increase in temperature triggers expansion and opening of pores to take up DNA, whilst the decrease in temperature shrinks cell pores to keep DNA in. 400 µl of Luria-Bertani broth (LB broth) was then added to each tube and bacteria were

incubated in a shaker oven at 37°C for an hr. A volume of 200 µl of solution from each tube was transferred onto agar plates, carefully spreading the solution over the agar with a glass spreading loop (stored in ethanol). To sterilise the loop, it was moved over a Bunsen burner then touched onto bare agar to cool it before spreading the culture. The plates were incubated upside down overnight in an oven at 37°C, covered by a glass beaker to prevent drying out.

On the next day, in the morning, multiple colonies were observed on the agar plates. A volume of 3 ml of LB broth containing 100 µg/ml ampicillin was aliquoted into 15 ml volume tubes. A clean 200 µl yellow pipette tip was used to pick up single colonies and deposited then into the tubes. The tubes were put into a shaking incubator with the caps fitted loosely and were incubated for approximately 8 hrs at 37°C. These 'day cultures' were then added to 100 ml LB broth containing 100 µg/ml ampicillin in 2 L conical flasks, and the flasks were incubated in a shaking incubator at 37°C overnight.

A Qiagen® Plasmid Midi kit was utilized to extract and purify the propagated plasmids from the bacterial cultures. The bacteria were harvested from the conical flasks by centrifuging at 6000 *xg* for 25 min at 4°C. The bacterial pellet was then resuspended in 6 ml Buffer P1 (RNase A solution added to Buffer P1 before use/storage). A volume of 6 ml of Buffer P2 was added to the solution, mixed thoroughly by vigorously inverting the tube then incubated at room temperature for 5 min (the solution turned blue). A volume of 6 ml of prechilled Buffer P3 was then added to the solution, mixed thoroughly by vigorously inverting the tube then incubated on ice for 15 min, the solution turned colourless. It was then centrifuged at 20 000 *xg* for 30 min at 4°C, proceeding to transfer supernatant into a new falcon tube. A Qiagen® tip was equilibrated by adding 4 ml of Buffer QBT and allowing the column to empty by gravity flow. Supernatant from the centrifuged solution was applied first to a micro-cloth and falcon tube to filter out the pellet then to the Qiagen® tip and allowed to enter the resin by gravity flow. The Qiagen® tip was washed twice with 10 ml Buffer QC allowing the buffer to move through the tip via gravity flow. DNA was eluted by adding 5 ml Buffer QF into the Qiagen® tip and collecting the DNA in a clean falcon tube. DNA was then precipitated by adding 3.5 ml of room temperature isopropanol to the eluted DNA, making sure to carefully mix. The solution was centrifuged at 15 000 *xg* for 30 min at 4°C then the supernatant carefully decanted. The DNA pellet was washed with 2 ml of 70% ethanol

(v/v), centrifuged the solution at 20 000 xg for 10 min then carefully decanted the supernatant. Afterwards the DNA pellet was air-dried for 5 to 10 min then redissolved in a 500 μ l distilled water.

For lentiviral production, HEK 293T cells were seeded at 1×10^5 cells/ml in 6-well plates at a volume of 1ml/well and were incubated at 37°C for 24 hrs. The next day, cells were washed with PBS and 1 ml fresh growth media was carefully added to the cells. Each construct was added to a separate 1.5 ml volume Eppendorf tube, CRE (2,300 ng), SWITCH (2,300 ng) and CFP (2,300 ng), with each tube also containing vesicular stomatitis virus-G (VSV-G; 570 ng) (a viral envelope glycoprotein) and gag-pol (a plasmid containing genes of the human immunodeficiency virus type 1 (HIV-1) comprising of gag, encoding for packaging structural precursor protein and pol, the reverse transcriptase; 1100 ng).¹¹⁹ Transfection complexes were prepared in each tube by mixing 100 μ l serum-free media, plasmid DNA and X-tremeGENE™ transfection reagent at a ratio of 2 to 1 X-tremeGENE™ to DNA, making sure to add the transfection reagent last and directly onto the media because it can stick to the plastic sides of the tube. The solution was immediately vortex mixing after addition of the transfection reagent and incubated at room temperature for 15 to 30 min before being added to the wells by directly pipetting it into the media. The cells were incubated at 37°C overnight. In the morning, transfection media was carefully replaced with 2 ml of growth media and the cells incubated overnight. The following day, virus-containing media was harvested and stored at 4°C, then 1 ml of growth media added to each well, and the plate was incubated overnight. The next day, virus-containing media was harvested and combined with the media previously harvested and stored at 4°C. Virus-containing media was filtered using a 0.45 μ m filter and stored at 4°C until use.

Virus-containing media was added to T75 flasks of cells a 50% confluence. For the BT20 cell line, switch virus-containing media was added then, after 48 hrs of incubation in fresh media, cells were fluorescently sorted for dsRed positive cells using FACS (BT20-Switch). For the MDA-MB-231 cell line, Cre virus-containing media was added, incubated overnight and the virus-containing media replaced with fresh media in the morning. To obtain a pure Cre-expressing population, cells were selected using puromycin antibiotic, puromycin was administered to the cells at a concentration previously determined via a death/kill curve (1 μ g/ml). The puromycin was also

administered to normal MDA-MB-231 cells as a control. Cells were grown under these selection conditions until all cells were dead in the control flask, this took just over a week. Afterwards, the Cre-expressing MDA-MB-231 cell line was administered CFP-virus-containing media overnight. The virus-containing media was replaced with fresh media in the morning and the cells were incubated for a further 48 hrs. The cell line was then fluorescently sorted for CFP-positive cells using FACS to obtain MDA-MB-231 cells expressing both Cre and CFP (MDA-CRE-CFP).

3.11) Resazurin assay

Table 3.9: Resazurin assay reagents and materials

Resazurin	Supplier	City & Country	Catalogue number
<u>Reagents</u>			
Resazurin powder	Sigma Aldrich	St Louis, Missouri, USA	R7017-5G
DPBS	ThermoFisher scientific	Massachusetts, USA	14287072
<u>Materials</u>			
96-well plate	Greiner Bio-One	Kremsmunster, Austria	655201
0.2 µm filter	Merck	Darmstadt, Germany	R9EA25830

To make resazurin solution, high purity resazurin powder was dissolved in DPBS at pH 7.4 at a concentration of 0.15 mg/ml to produce a 0.65 mM (w/v) resazurin solution. The solution was then filtered through a 0.2 µm filter into a sterile, light protected container. The resazurin was stored protected from light at 4°C for frequent use or at -20°C for long term storage.

Prior to analysing metabolism in cells, the assay was optimised for use with serum containing medium.¹²⁰ For optimisation, MDA-MB-231 cells were seeded at 2.5×10^3 cells/well, and after 24h were exposed to 0.65 mM (w/v) resazurin in serum-positive

media for 4 hrs before fluorescence was quantified (day zero reading). Next, cells were exposed to serum positive media or serum-free media and measured using resazurin at different time- points (24 hr, 48 hr and 72 hr). The results showed that samples grown and measured in the serum-free media had higher fluorescence levels than those in the serum positive medium. Further testing showed that including serum in the medium when adding resazurin for 4 hrs reduced fluorescence (Appendix A). Hence, we adapted our assay to only measure resazurin in serum-free medium (Appendix B).

Method

MDA and BT20 cells were seeded in 96-well plates at 2.5×10^3 cells/well and were allowed to attach by overnight incubation at 37°C. The next day, the plates were treated with conditioned media (MDA-CM or BT20-CM) and control media (Serum+ media or Serum- media). The day zero wells were then aspirated, treated with serum-free media containing resazurin at a total volume of 120 μ l (comprising of 20 μ l resazurin solution and 100 μ l serum-free media at a 1 to 5 ratio). Three empty wells were treated with resazurin at the same time to act as media only blanks. The plates were covered with foil and incubated for 4 hrs at 37°C. The fluorescence was read on a BMG Fluostar® (BMG Labtec, Ortenberg, Germany) at 595 nm using a constant gain. To obtain the gain, serial dilutions of the sample we expect to obtain the highest metabolism from (those treated with Serum+ media) were made and measured using the Fluostar's automatic gain function. The following day, media was aspirated from the 24 hr samples, and these wells and three empty wells were treated with resazurin, as described above. The fluorescence was read on the BMG Fluostar® at 595 nm using the previously determined gain. This was repeated for the 48 hr and 72 hr time points.

3.12) Statistical analysis

Quantitative data analysis was carried out using GraphPad Prism software (version 5, San Diego, California, USA) and image analysis was done using Image J software. Experiments consisted of at least three technical repeats and three independent biological repeats performed. The average of three independent experiments was

calculated with error bars representing the standard error of the means (SEM) and statistical significance considered at a $p < 0.05$ using ANOVA, student's *T*-test, Dunnett's or Bonferroni post-tests, as appropriate.

CHAPTER 4 RESULTS

4. RESULTS

4.1 : Treatment with conditioned media from the MDA-MB-231 cells inhibits BT20 cell proliferation

To determine if a breast cancer cell line can produce biomolecules that affect the proliferation of a recipient breast cancer cell line, conditioned media containing secreted factors of the donor cells were generated and used to treat recipient cells. In these experiments both MDA-MB-231 and BT20 cells acted as donors and recipients. Thus, conditioned media was prepared and cells were exposed to normal growth media (Serum+ media; positive control), serum-free media (Serum- media; baseline control), EE-15-one (C8, negative control), MDA-CM or BT20-CM. Cell proliferation was monitored for 24-, 48- and 72-hr and was quantified using crystal violet staining of cells.

In vitro cell culture studies require culture media as a source for nutrients to sustain the cell lines.¹¹⁸ The culture media is supplemented with FCS which contains proteins such as growth factors.¹²¹ Since conditioned media was made by collecting serum-free media from cells after 48-hr incubation, we used serum positive media as our positive control whilst serum-free media was our baseline. EE-15-one (C8) supplemented media was used as a negative control since this compound induces cell death. A negative control typically would not be expected to cause any notable change to your variable while the positive control would.¹¹⁸ With these controls we would be able to determine if conditioned media could promote or inhibit cellular proliferation. As expected, treatment with serum positive media yielded the highest cellular proliferation rate compared to the other treatments (with the area under the curve reaching 6.8 for BT20 cells and 25 for MDA-MB-231 cells) (Figures 4.1. – 4.4) and the lowest cellular proliferation was observed with the negative control C8 treatment. Serum-free medium supported growth to about half of serum positive medium, with the area under the curve being 12 for MDA-MB-231 cells and 3.5 for BT20 cells (Figures 4.1 – 4.4).

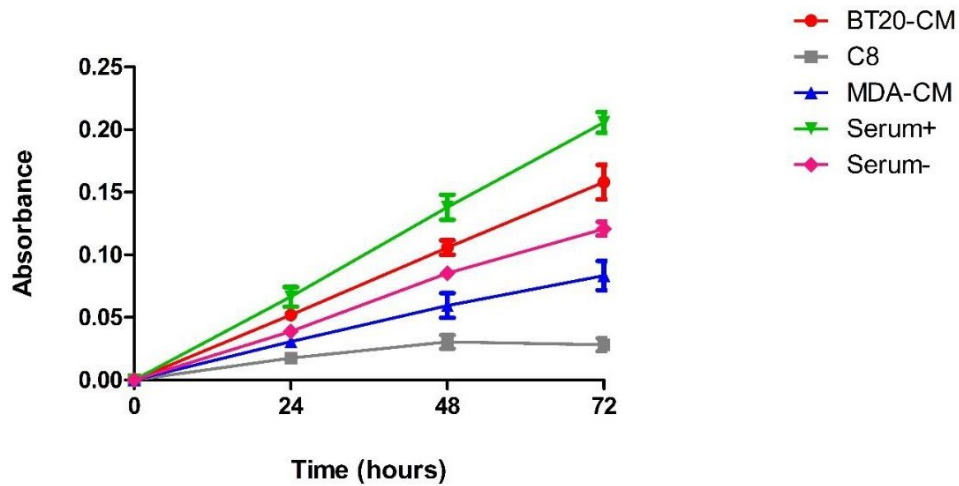


Figure 4.1: MDA-CM has an anti-proliferative effect on BT20 cell growth. Rate of cellular proliferation as influenced by different treatments over a 72-hr period. Line graph represents average cell density as determined by crystal violet absorbance. Treatment of BT20 cells with MDA-CM yielded a decreased rate of cellular proliferation in comparison to BT20-CM treatment lower than the baseline control Serum-treatment. (n=4)

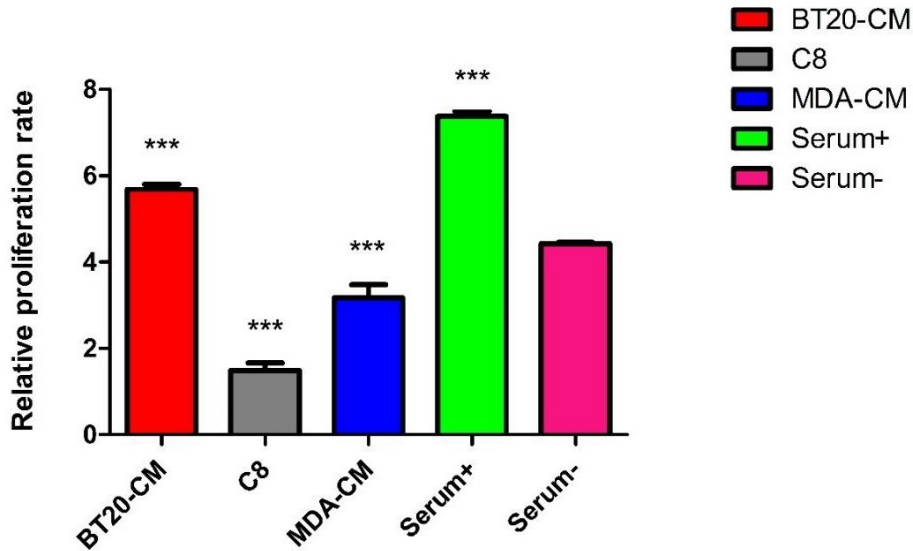


Figure 4.2: MDA-CM has an anti-proliferative effect on BT20 cell growth. Bar graph of the relative cellular proliferative rate as measured by calculating area under the curve for the crystal violet assay following treatment of BT20 cells with conditioned media. C8 yielded the lowest relative cellular proliferation whilst Serum+ treatment yielded the highest. There is an increase in proliferation with BT20-CM treatment and a decrease with MDA-CM. Statistical significance determined via a one-way ANOVA paired with a Bonferroni multiple comparison test against Serum-free media control ($P < 0.05$). ($n=4$)

Table 4.1: One-way ANOVA with Bonferroni's multiple comparison test for BT20 cells treated with MDA-CM

One-way analysis of variance				
P value			<0.0001	
P value summary			***	
Are means significantly Different? (P<0.05)			Yes	
Bonferroni's Multiple comparison test				
Groups	Mean Diff.	t	Significant? P<0.05?	Summary
BT20-CM vs MDA-CM	2.514	10.07	Yes	***
BT20-CM vs Serum-	1.257	5.033	Yes	***
C8 vs Serum-	-2.934	11.75	Yes	***
MDA-CM vs Serum-	-1.257	5.033	Yes	***
Serum- vs Serum+	2.952	11.82	Yes	***

Treatment of the BT20 cell line with conditioned media from the metastatic MDA-MB-231 cell line was investigated (Figure 4.1). As a control cells were also treated with conditioned media from BT20 cells. Exposure to BT20-CM increased proliferation significantly compared to serum-free medium (Figure 4.2). In contrast, MDA-MB-231 conditioned media reduced cellular proliferation of BT20 cells when compared to serum-free medium, although this reduction was not as large as the effect of C8 exposure. This data suggests that autologous conditioned media contains factors that can promote proliferation while heterologous conditioned medium from MDA-MB-231 cells inhibits BT20 proliferation. To investigate if the inhibitory action of the conditioned medium on BT20 cells was specific, conditioned medium from another breast cancer cell line, MCF7, was administered to BT20 cells along with all the controls (Figure 4.3). MCF7 conditioned medium did not significantly affect BT20 cell proliferation (Figure 4.4). As before, BT20 conditioned medium did result in a

significant increase in proliferation compared to serum-free medium. Thus, MDA-MB-231 cells produce factors in the medium that inhibit BT20 cell proliferation while MCF7 cells do not.

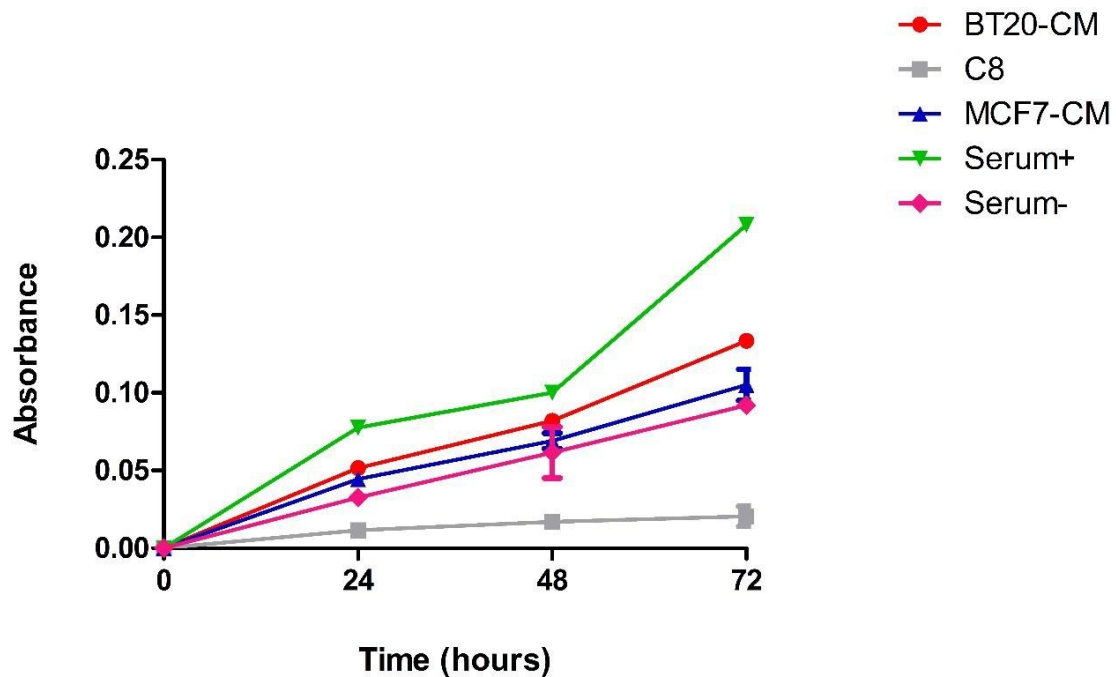


Figure 4.3: Conditioned media from the non-metastatic MCF7 breast cancer cell line has no effect on BT20 cell proliferation. Rate of cellular proliferation as influenced by different treatments over a 72-hr period. Line graph represents average cell density as determined by crystal violet absorbance. Treatment of BT20 cells with MCF7 conditioned media (MCF7-CM) results in a cellular proliferation lower than BT20 conditioned media (BT20-CM). (n=3)

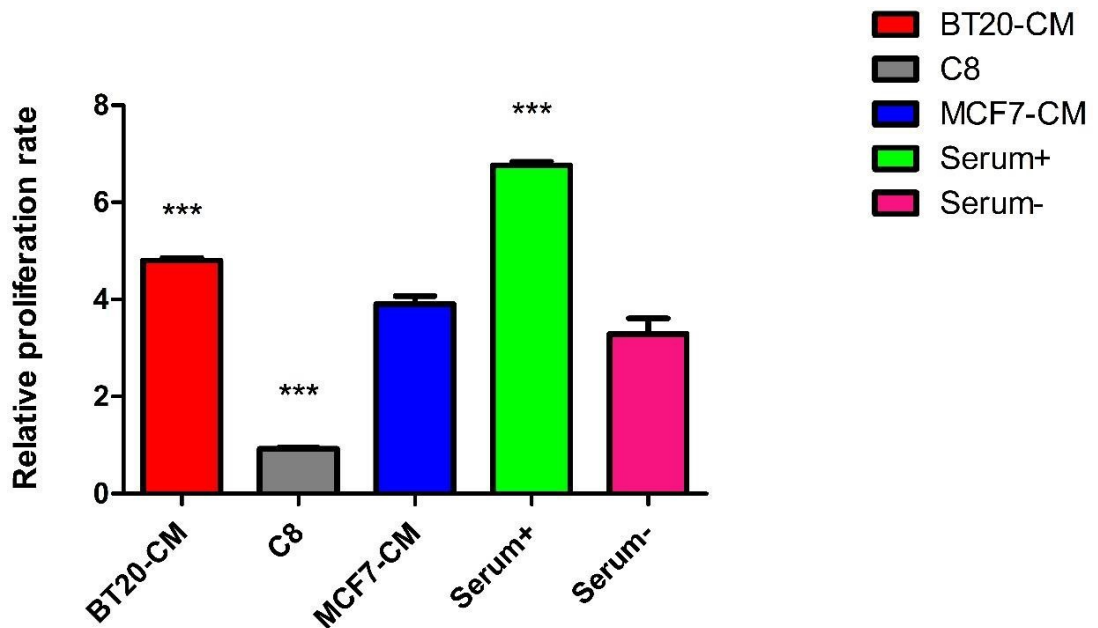


Figure 4.4: Conditioned media from the non-metastatic MCF7 breast cancer cell line has no effect on BT20 cell proliferation. Bar graph of the relative cellular proliferative rate as measured by calculating area under the curve for the crystal violet assay following treatment of BT20 cells with conditioned media. C8 yielded the lowest relative cellular proliferation whilst Serum+ treatment yielded the highest. There is an increase in proliferation with BT20-CM treatment and a slight increase with MCF7-CM. Statistical significance determined via a one-way ANOVA paired with a Bonferroni multiple comparison test against Serum-free media control ($P < 0.05$). ($n=4$)

Table 4.2: One-way ANOVA with Bonferroni's multiple comparison test for BT20 cells treated with MCF7-CM

One-way analysis of variance				
P value		<0.0001		
P value summary		***		
Are means significantly Different? (P<0.05)		Yes		
Bonferroni's Multiple comparison test				
Groups	Mean Diff.	t	Significant? P<0.05?	Summary
BT20-CM vs MCF7-CM	0.9040	3.817	Yes	*
BT20-CM vs Serum-	1.516	6.402	Yes	***
C8 vs Serum-	-2.368	9.999	Yes	***
MCF7-CM vs Serum-	0.6120	2.584	No	ns
Serum- vs Serum+	3.472	14.66	Yes	***

To test if the converse was the case and if BT20 cells can affect MDA-MB231 cell proliferation, BT20-CM was generated. MDA-MB-231 cells were exposed to BT20-CM, along with all normal controls (Figure 4.5). Treatment with conditioned medium from neither MDA-MB-231 nor BT20 cells affected cell proliferation compared to serum-free medium (Figure 4.6). The C8 control and serumpositive medium inhibited and enhanced proliferation, respectively, as expected. Thus, the proliferative effect is specific to MDA-CM.

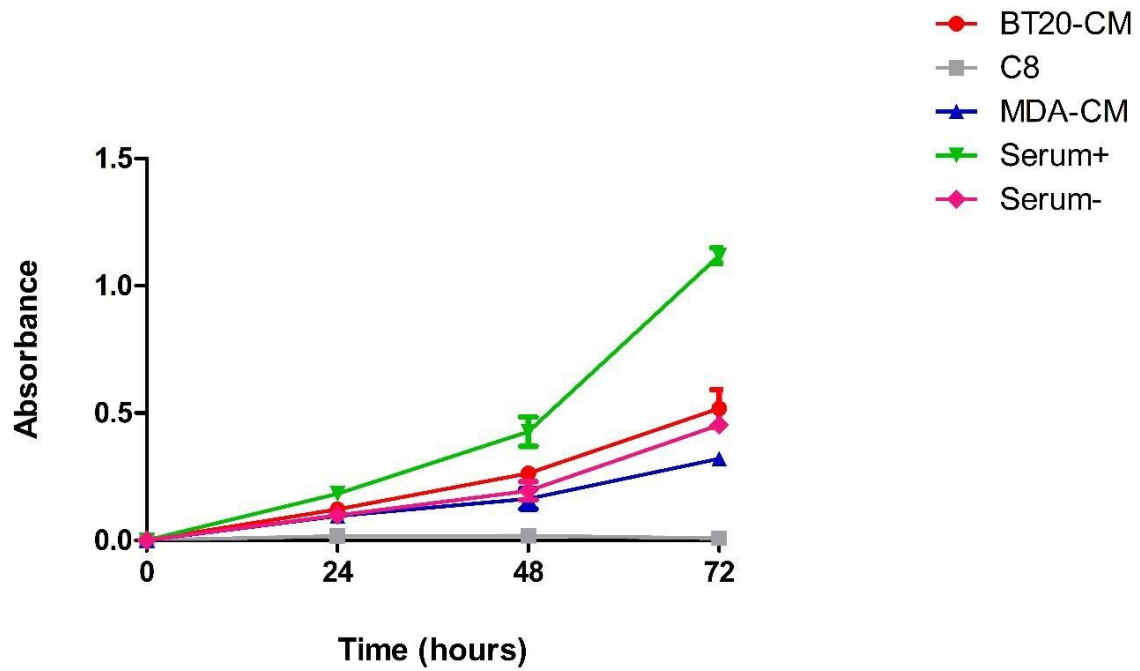


Figure 4.5: BT20-CM has no effect on MDA-MB-231 cell proliferation. *Rate of cellular proliferation as influenced by different treatments over a 72-hr period. Line graph represents average cell density as determined by crystal violet absorbance. Treatment of MDA-MB-231 cells with BT20 conditioned media (BT20-CM) yielded a rate of proliferation similar to that of serum-free media (Serum-). (n=3)*

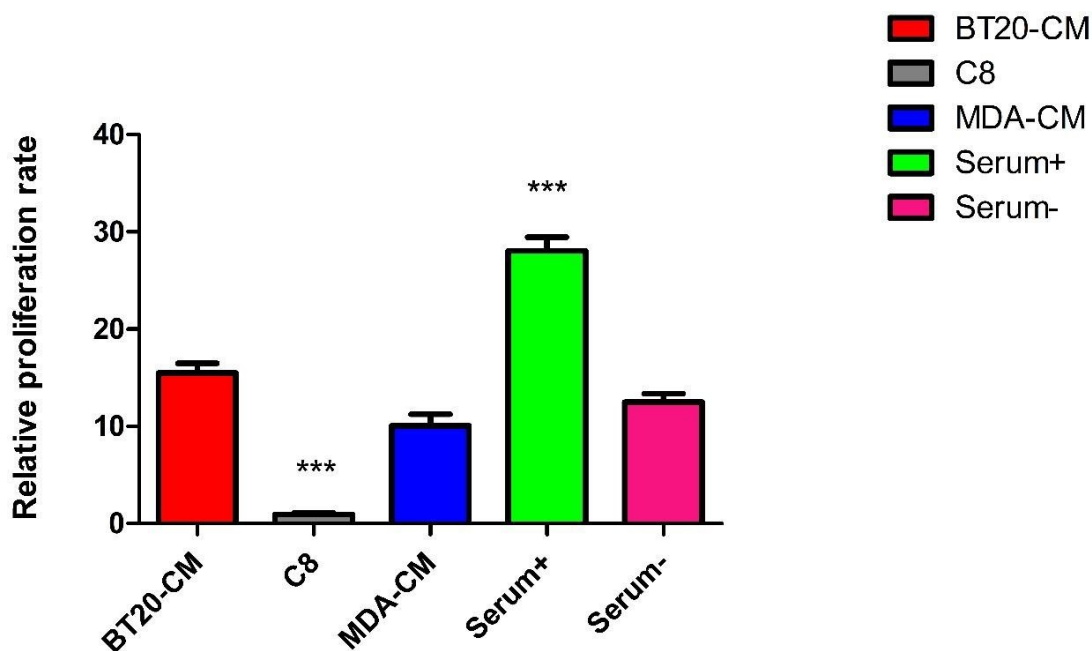


Figure 4.6: BT20-CM has no effect on MDA-MB-231 cell proliferation. *Bar graph of the relative cellular proliferative rate as measured by calculating area under the curve for the crystal violet assay following treatment of MDA-MB-231 cells with conditioned media. C8 yielded the lowest relative cellular proliferation whilst Serum+ treatment yielded the highest. There is a slight increase in proliferation with BT20-CM treatment and a slight decrease with MDA-CM. Statistical significance determined via a one-way ANOVA paired with a Bonferroni multiple comparison test against Serum-free media control ($P < 0.05$). ($n=3$)*

Table 4.3: One-way ANOVA with Bonferroni's multiple comparison test for MDA-MB-231 cells treated with BT20-CM

One-way analysis of variance				
P value				<0.0001
P value summary				***
Are means significantly Different? (P<0.05)				Yes
Bonferroni's Multiple comparison test				
Groups	Mean Diff.	t	Significant? P<0.05?	Summary
BT20-CM vs MDA-CM	5.419	3.812	Yes	*
BT20-CM vs Serum-	2.987	2.101	No	ns
C8 vs Serum-	-11.55	8.127	Yes	***
MDA-CM vs Serum-	-2.433	1.711	No	ns
Serum- vs Serum+	15.56	10.95	Yes	***

To test if MDA-CM specifically altered BT20 cell proliferation or more generally affects proliferation of many cell types, the effect of this conditioned medium on MCF7 cells was also examined (Figure 4.7). No significant changes in proliferation were observed when cells were treated with MDA conditioned medium when compared to serum-free medium-treated cells (Figure 4.8). As expected, significant changes in proliferation were observed in cells treated with C8 or with serum. This suggests that the inhibitory effect of MDA-CM is restricted to BT20 cells.

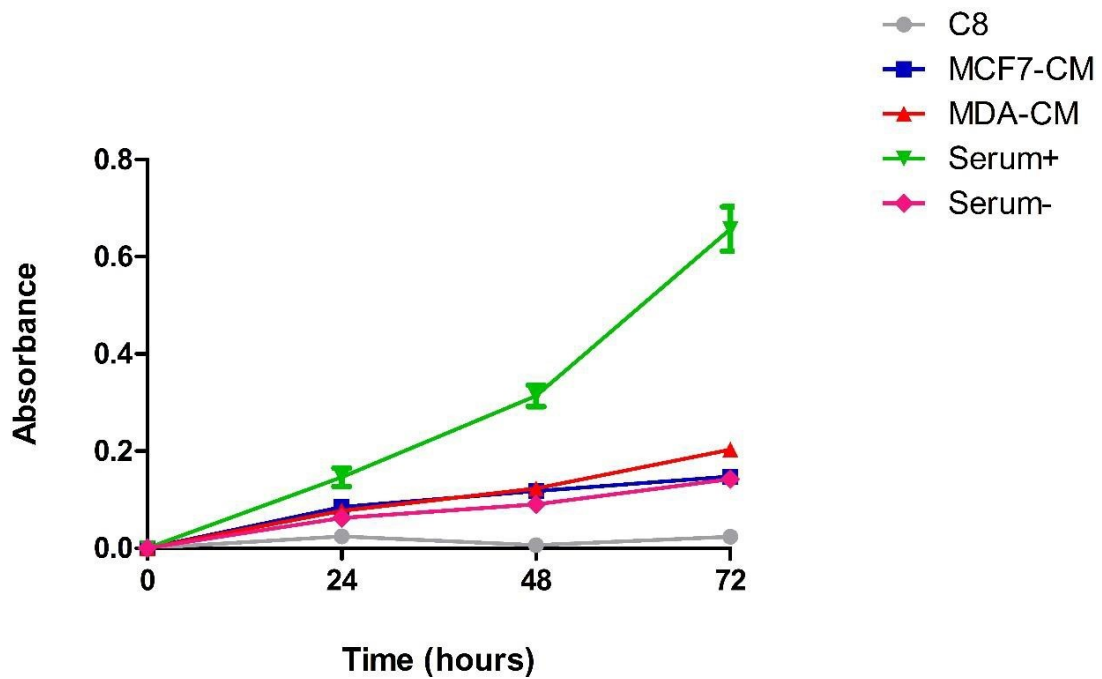


Figure 4.7: MDA-CM does not have anti-proliferative effects on MCF7 cells Rate of cellular proliferation as influenced by different treatments over a 72-hr period. Line graph represents average cell density as determined by crystal violet absorbance. Treatment of MCF7 cells with MDA-MB-231 conditioned media (MDA-CM) had no adverse effects on cell proliferation. (n=3)

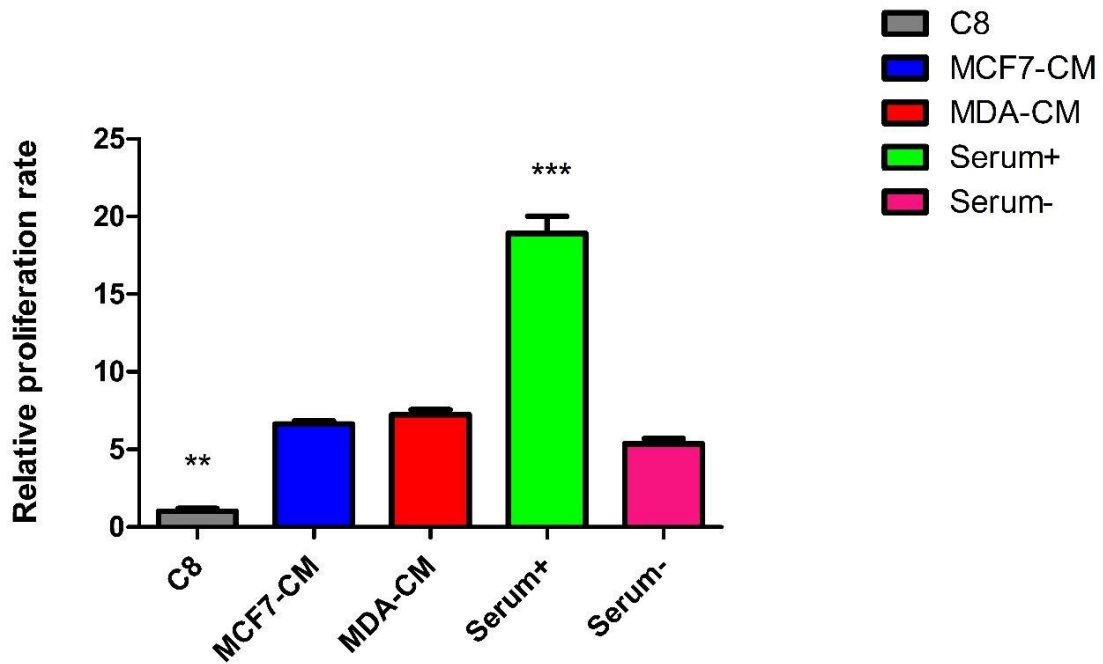


Figure 4.8: MDA-CM does not have anti-proliferative effects on MCF7 cells. Bar graph of the relative cellular proliferative rate as measured by calculating area under the curve for the Crystal violet assay following treatment of MCF7 cells with conditioned media. C8 yielded the lowest relative cellular proliferation whilst Serum+ treatment yielded the highest. There is a slight increase in proliferation with MCF7-CM and MDA-CM treatment. Statistical significance determined via a one-way ANOVA paired with a Bonferroni multiple comparison test against Serum-free media control ($P < 0.05$). ($n=3$)

Table 4.4: One-way ANOVA with Bonferroni's multiple comparison test for MCF7 cells treated with MDA-CM

One-way analysis of variance				
P value				<0.0001
P value summary				***
Are means significantly Different? (P<0.05)				Yes
Bonferroni's Multiple comparison test				
Groups	Mean Diff.	t	Significant? P<0.05?	Summary
MCF7-CM vs MDA-CM	-0.5960	0.7681	No	ns
MCF7-CM vs Serum-	1.268	1.634	No	ns
C8 vs Serum-	-4.348	5.603	Yes	**
MDA-CM vs Serum-	1.864	2.402	No	ns
Serum- vs Serum+	13.55	17.47	Yes	***

4.2: MDA-MB-231 cell conditioned media does not decrease cellular metabolism of BT20 cells

The crystal violet data suggested that MDA-MB-231 cells produce soluble factors that have an anti-proliferative effect on BT20 cells. To determine if the observed decrease in proliferation correlates with a decrease in cellular metabolism, a resazurin reduction assay was utilized. The resazurin assay measures the reductive potential of cells which is a proxy of cellular metabolism through the measurement of the fluorescence produced by conversion of resazurin to resorufin.¹²⁰

Similar to the crystal violet assays, cells were seeded in serum positive media, allowed to attach, before being treated with the respective conditioned media or control treatments for 24, 48, or 72 hrs before an endpoint reading was obtained using the resazurin assay. Although not significantly different from cells treated with serum-free media, BT20 cells exposed to MDA-CM had the lowest cellular metabolic rate (Figures 4.9 and 4.10). As expected, a significant increase in relative metabolism, compared to serum-free medium exposed cells, was measured in cells exposed to serum containing media. Thus, it appears that the anti-proliferative effect of MDA-CM on BT20 cells does not correlate with an inhibition of cellular metabolism. Treatment of MDA-MB-231 cells with BT20-CM, had no significant effect on metabolism similarly to the crystal violet data (Figures 4.11 and 4.12), although it is important to note that it was higher than that of MDA-CM and the serum -free media control.

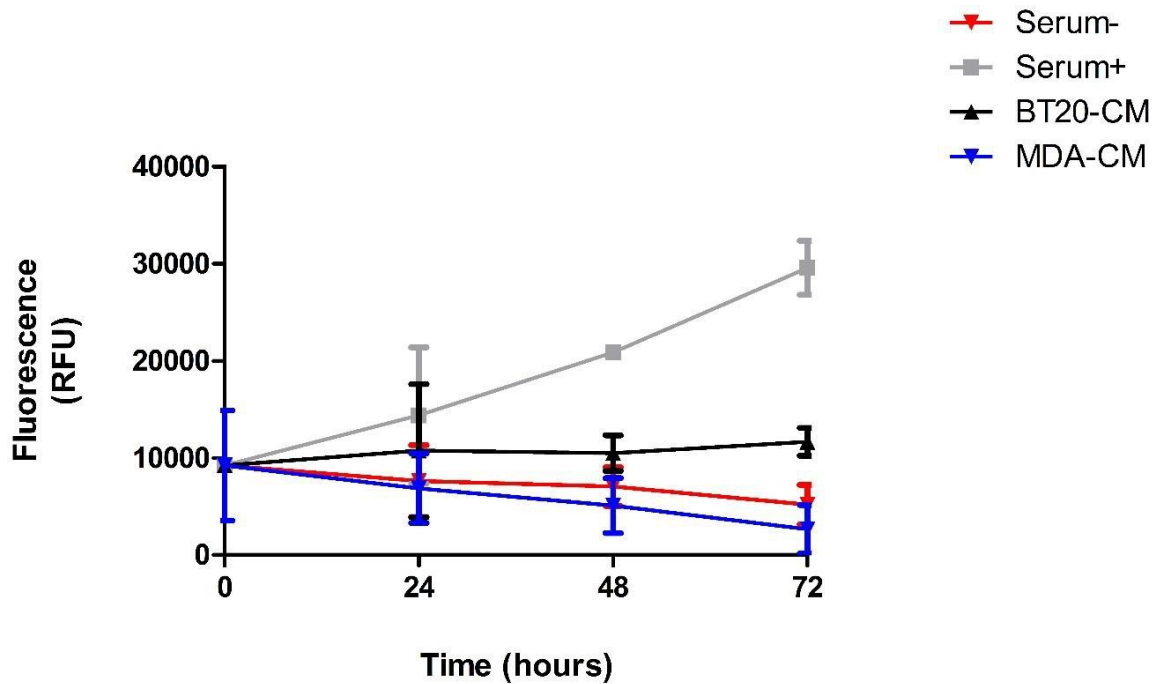


Figure 4.9: Conditioned media from the MDA-MB-231 cell line does not decrease BT20 cell metabolism. Resazurin assay showing fluorescence following treatment of BT20 cells with MDA-MB-231 conditioned media (MDA-CM). MDA-CM yielded the lowest cellular metabolism, lower than that of cells treated with serum-free media (Serum-). Line graph represents cell metabolism as determined by resazurin reduction. RFU – Relative fluorescent units. (n=3)

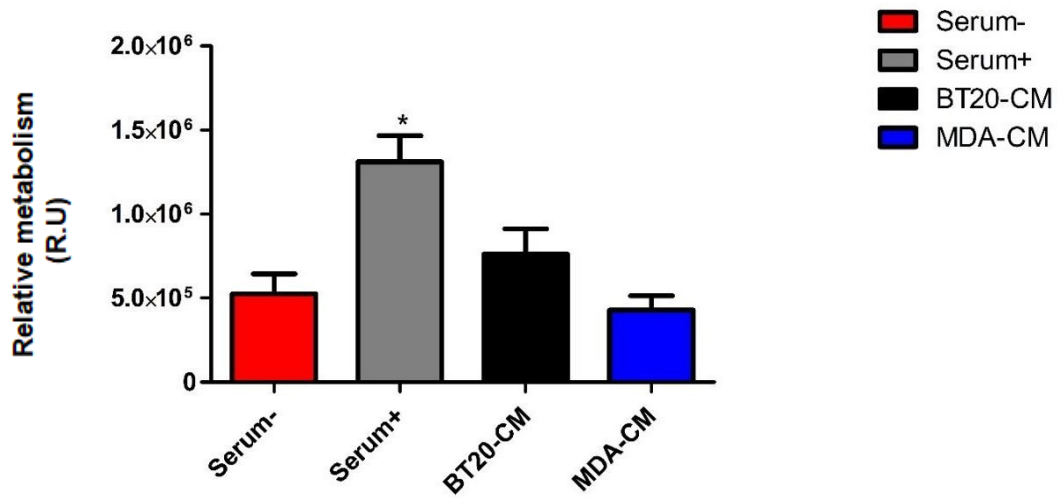


Figure 4.10: Conditioned media from the MDA-MB-231 cell line does not decrease BT20 cell metabolism. Bar graph of the relative cellular metabolic rate as measured by calculating relative area under the curve for the resazurin assay following treatment of BT20 cells with MDA-MB-231 conditioned media (MDA-CM). MDA-CM yielded the lowest cellular metabolism whilst Serum+ treatment yielded the highest. Statistical significance determined via a one-way ANOVA paired with a Bonferroni multiple comparison test against Serum-free media control ($P < 0.05$). RU – Relative metabolism units. ($n=3$)

Table 4.5: One-way ANOVA with Bonferroni's multiple comparison test for BT20 cells treated with MDA-CM

One-way analysis of variance				
P value				0.006
P value summary				**
Are means significantly Different? (P<0.05)				Yes
Bonferroni's Multiple comparison test				
Groups	Mean Diff.	T	Significant? P<0.05?	Summary
Serum- vs Serum+	-785600	4.234	Yes	*
Serum- vs BT20-CM	-235377	1.268	No	ns
Serum- vs MDA-CM	95758	0.5161	No	ns
Serum+ vs BT20-CM	550223	2.965	No	ns
Serum+ vs MDA-CM	881357	4.750	Yes	**
BT20-CM vs MDA-CM	331135	1.785	No	ns

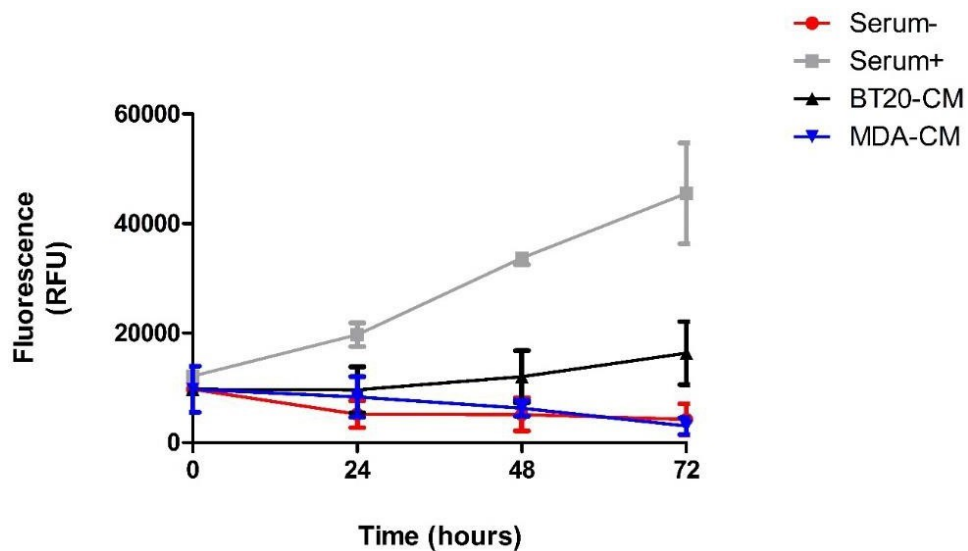


Figure 4.11: Conditioned media from the BT20 cell line does not decrease cell metabolism in MDA-MB-231 cells. *Resazurin assay showing cell fluorescence following treatment of MDA-MB-231 cells with BT20 conditioned media (BT20-CM). MDA-CM yielded a cellular metabolism profile similar to Serum- treatment. Line graph represents cell metabolism as determined by resazurin reduction. RFU – Relative fluorescent units. (n=3)*

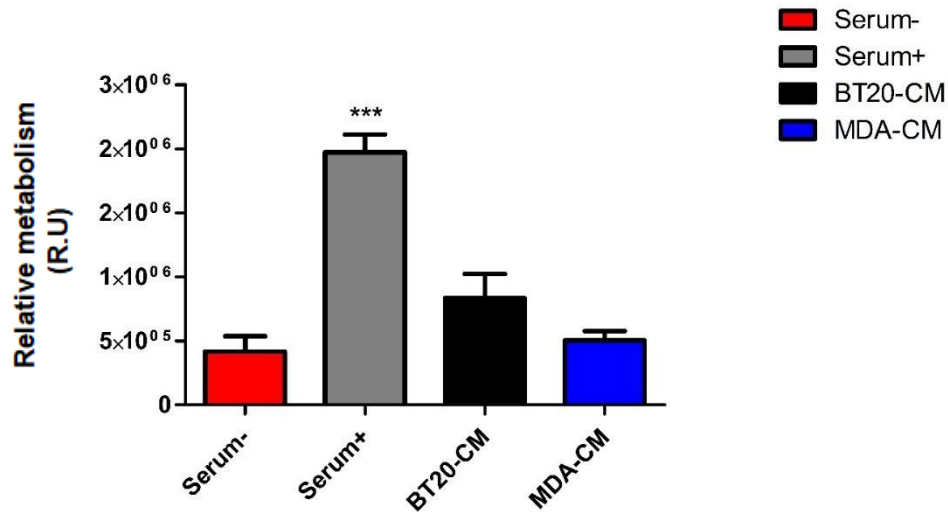


Figure 4.12: BT20 CM does not decrease cell metabolism in MDA-MB-231 cells. Bar graph of the relative cellular metabolic rate as measured by calculating relative area under the curve for the resazurin assay following treatment of MDA-MB-231 cells with BT20 conditioned media (BT20-CM). MDA-CM yielded a relative metabolic profile similar to Serum- whilst Serum+ treatment yielded the highest. Statistical significance determined via a one-way ANOVA paired with a Bonferroni multiple comparison test against Serum-free media control ($P < 0.05$). RU – Relative metabolism units. ($n=3$)

Table 4.5: One-way ANOVA with Bonferroni's multiple comparison test for MDA-MB-231 cells treated with BT20-CM

One-way analysis of variance				
P value				0.0007
P value summary				***
Are means significantly Different? (P<0.05)				Yes
Bonferroni's Multiple comparison test				
Groups	Mean Diff.	t	Significant? P<0.05?	Summary
Serum- vs Serum+	-1.556e+006	7.358	Yes	***
Serum- vs BT20-CM	-416683	2.203	No	ns
Serum- vs MDA-CM	-88480	0.4678	No	ns
Serum+ vs BT20-CM	1.139e+006	5.387	Yes	**
Serum+ vs MDA-CM	1.467e+006	6.939	Yes	**
BT20-CM vs MDA-CM	328203	1.735	No	ns

4.13: Medium fractionation of MDA-MB-231 conditioned medium does not alter the cellular metabolism of BT20 cells

Cells secrete soluble factors into the medium over time but can also deposit different membrane bound vesicles or exosomes through exocytosis. Several different types of extracellular vesicles can be generated by cells as discussed earlier (Section 1.5). Most of these can be isolated from the conditioned medium through differential centrifugation. To discriminate between soluble factors or insoluble vesicle-derived factors, conditioned medium from MDA-MB-231 cells was centrifuged and the pellet and supernatants used separately to treat BT20 cells. Resazurin reduction was then measured. As seen above, MDA-CM does not increase cellular metabolism within BT20 cells (Figure 4.10) and although BT20-CM results in metabolism higher than SFM and MDA-CM treatment, it was not a significant increase (Figure 4.12). Therefore, without surprise, upon fractionation of the conditioned media, we observed

that neither pellet nor supernatant had any significant effect on cellular metabolism (Figures 4.14 and 4.15). Similarly, as with the entire BT20-CM, treatment of MDA-MB-231 cells with fractionated BT20-CM caused no significant changes to metabolism when compared with serum-free medium treated cells (Figure 4.16 and 4.17)

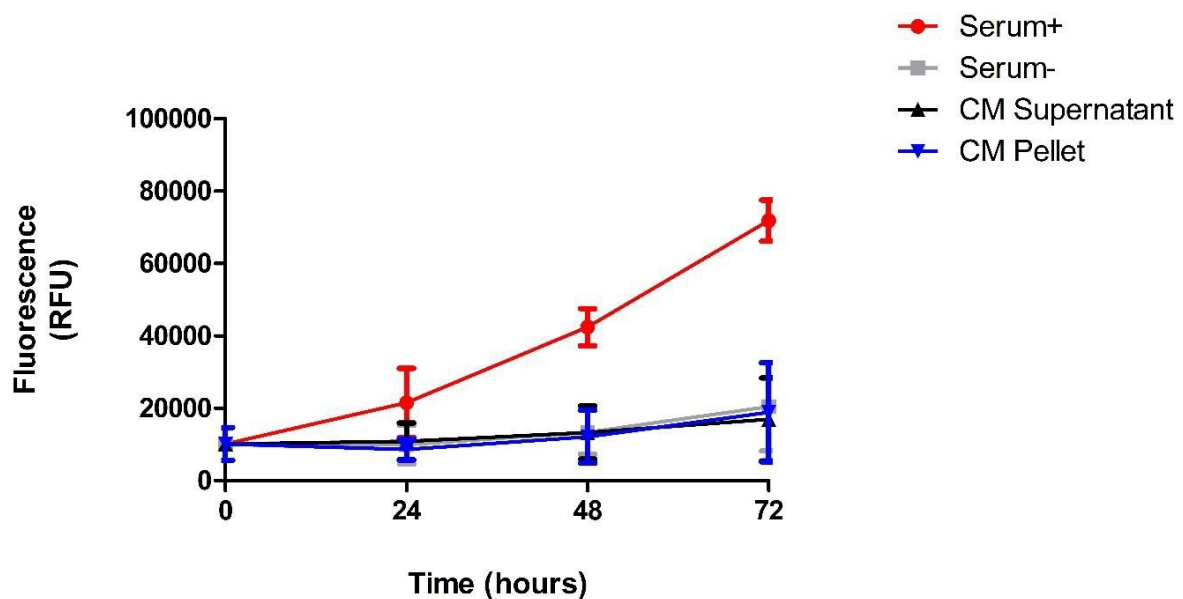


Figure 4.14: Neither pellet nor supernatant from fractionated MDA-MB-231 conditioned media has an adverse effect on BT20 cell metabolism. Supernatant (CM supernatant) and pellet (CM Pellet) media treatment yielded fluorescence similar to that of Serum- treatment. Line graph represents cell metabolism as determined by resazurin reduction. RFU – Relative fluorescent units. (n=3)

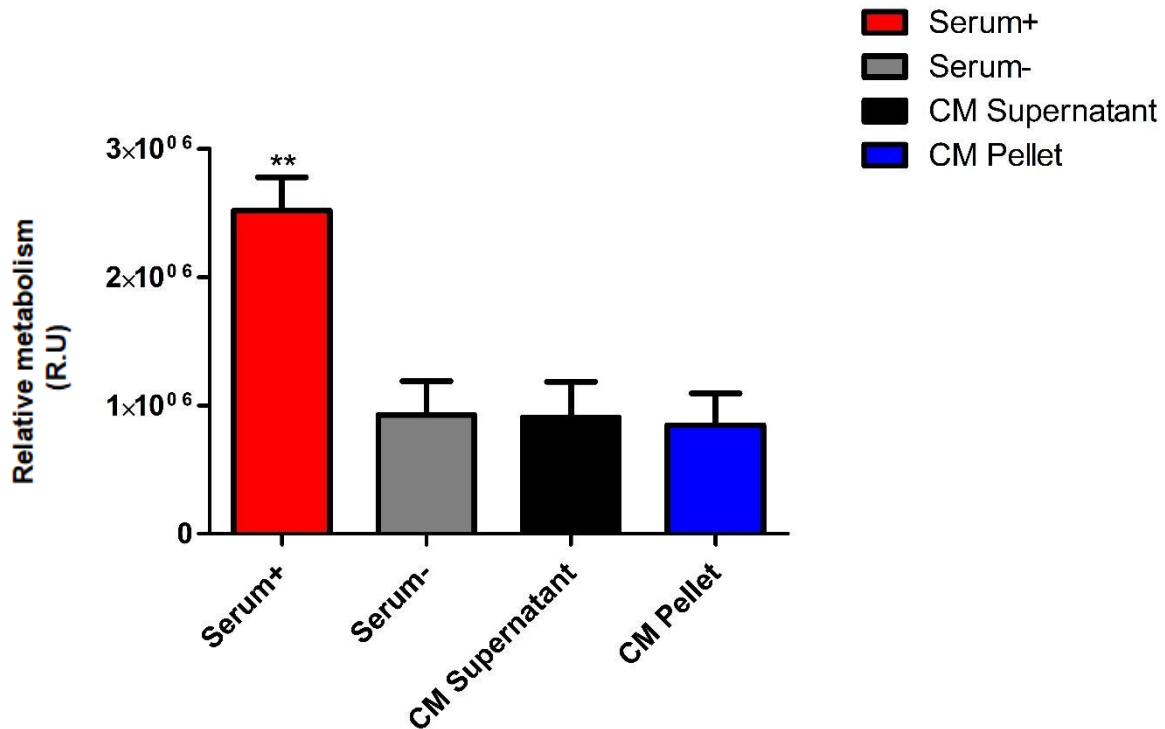


Figure 4.15: Neither pellet nor supernatant from fractionated MDA-MB-231 conditioned media has an effect on BT20 cell metabolism. *Bar graph of the relative cellular metabolic rate as measured by calculating relative area under the curve for the resazurin assay following treatment of BT20 cells with fractionated MDA-MB-231 conditioned media (MDA-CM). Supernatant (CM supernatant) and pellet (CM Pellet) media treatment yielded a metabolic profile relatively similar to that of serum-free media (Serum-). Statistical significance determined via a one-way ANOVA paired with a Bonferroni multiple comparison test against Serum-free media control ($P < 0.05$). RU – Relative metabolism units ($n=3$)*

Table 4.6: One-way ANOVA with Bonferroni's multiple comparison test for BT20 cells treated with fractionated MDA-CM

One-way analysis of variance				
P value				0.0062
P value summary				**
Are means significantly Different? (P<0.05)				Yes
Bonferroni's Multiple comparison test				
Groups	Mean Diff.	t	Significant? P<0.05?	Summary
Serum+ vs Serum-	1.592e+006	4.198	Yes	**
Serum+ vs CM Supernatant	1.614e+006	4.255	Yes	*
Serum+ vs CM Pellet	1.672e+006	4.408	Yes	*
Serum- vs CM Supernatant	21468	0.05661	No	ns
Serum- vs CM Pellet	79480	0.2096	No	ns
CM Supernatant vs Pellet	58012	0.1530	No	ns

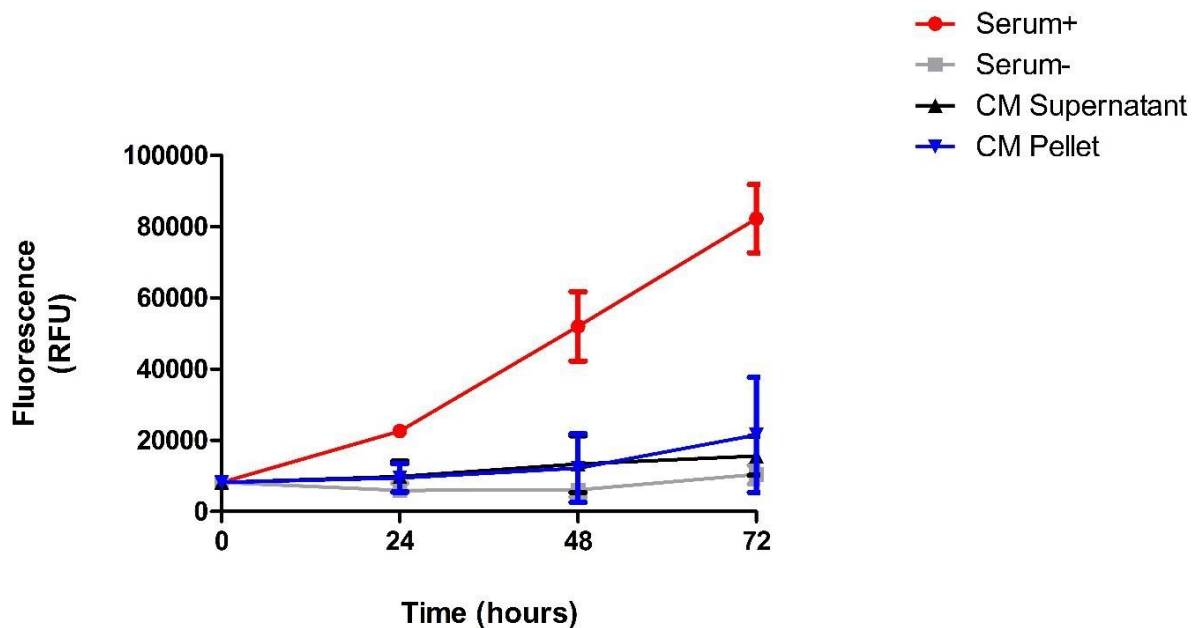


Figure 4.16: Neither pellet nor supernatant from fractionated BT20 conditioned media has an effect on MDA-MB-231 cell metabolism. Supernatant (CM supernatant) and pellet (CM Pellet) media treatment yielded fluorescence similar to that of Serum- treatment. Line graph represents cell metabolism as determined by resazurin reduction. RFU – Relative fluorescent units. (n=3)

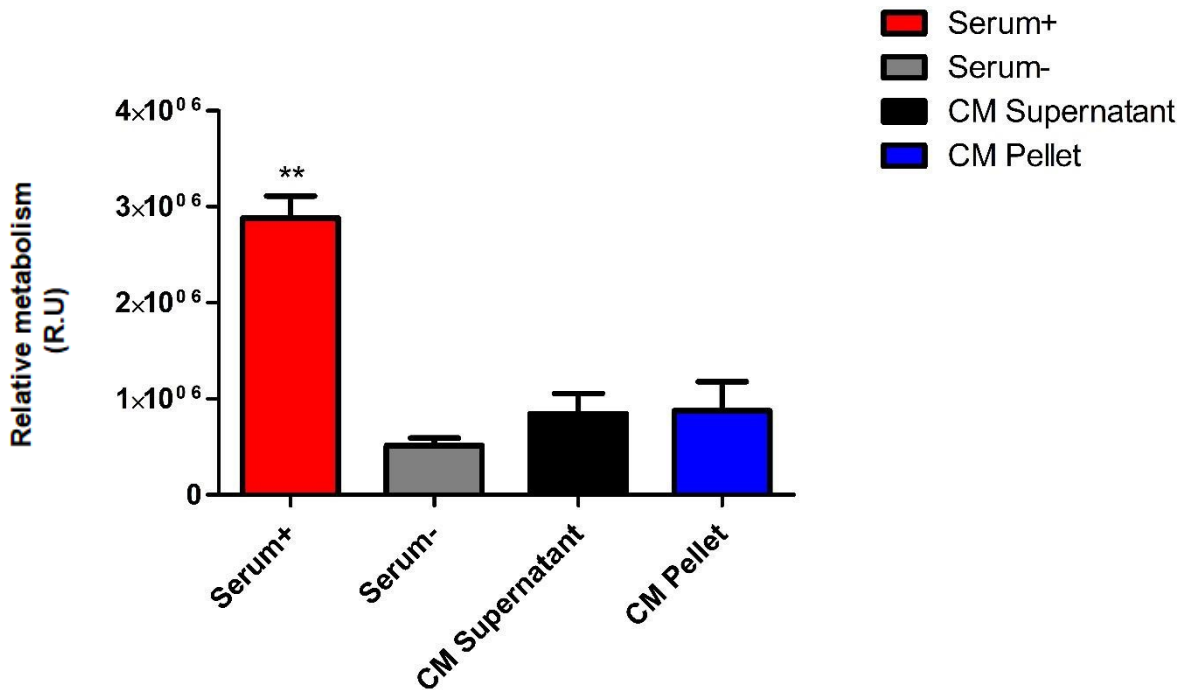


Figure 4.17: Neither pellet nor supernatant from fractionated BT20 conditioned media has an effect on MDA-MB-231 cell metabolism. Bar graph of the relative cellular metabolic rate as measured by calculating relative area under the curve for the resazurin assay following treatment of MDA-MB-231 cells with BT20 conditioned media (BT20-CM). BT20-CM yielded a relative metabolic profile slightly higher than Serum- treatment. Statistical significance determined via a one-way ANOVA paired with a Bonferroni multiple comparison test against Serum-free media control ($P < 0.05$). RU – Relative metabolism units ($n=3$)

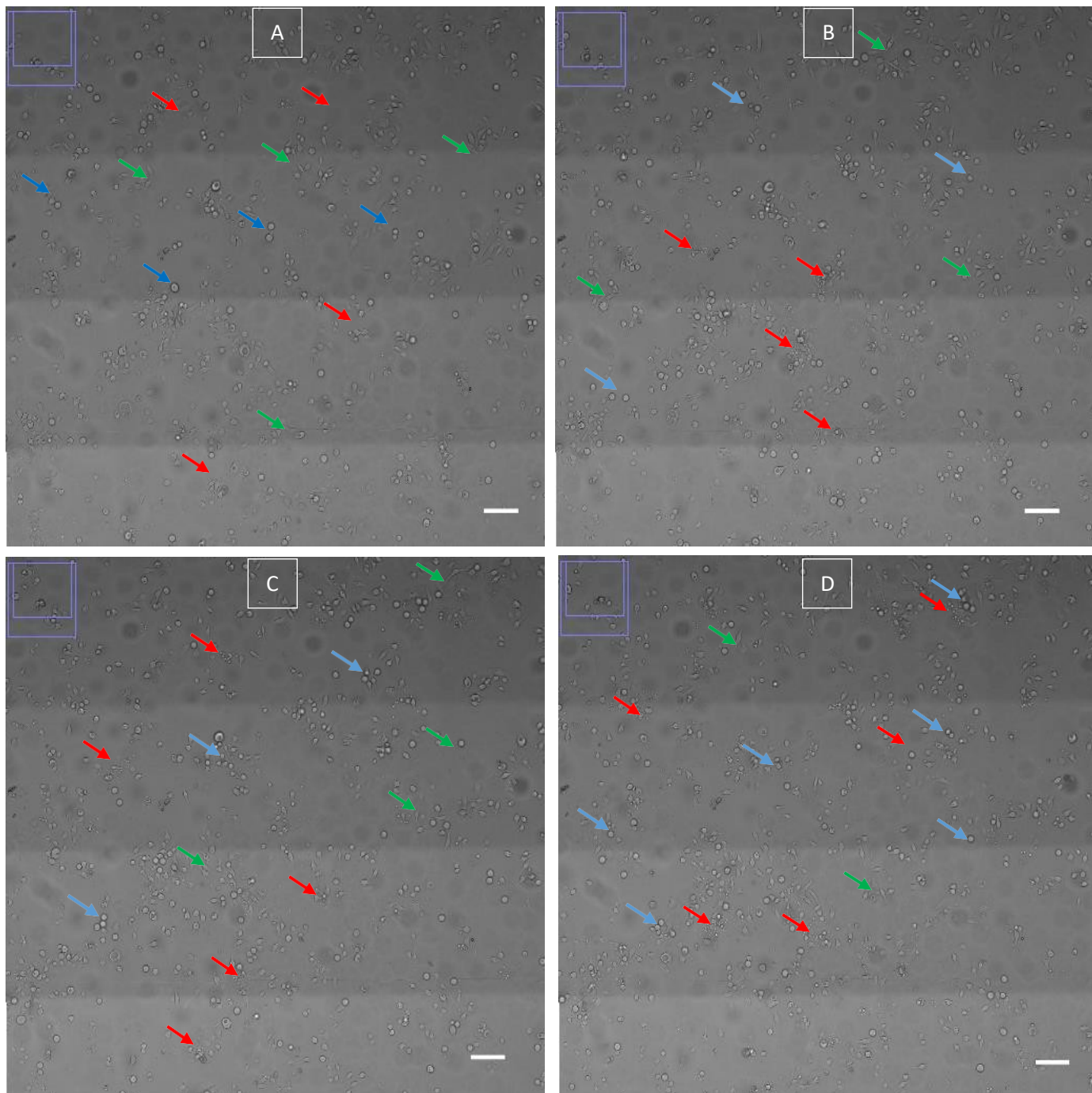
Table 4.7: One-way ANOVA with Bonferroni's multiple comparison test for MDA-MB-231 cells treated with fractionated BT20-CM

One-way analysis of variance				
P value				0.002
P value summary				**
Are means significantly Different? (P<0.05)				Yes
Bonferroni's Multiple comparison test				
Groups	Mean Diff.	t	Significant? P<0.05?	Summary
Serum+ vs Serum-	2.639e+006	6.013	Yes	**
Serum+ vs CM Supernatant	2.039e+006	5.175	Yes	**
Serum+ vs CM Pellet	2.006e+006	5.091	Yes	**
Serum- vs CM Supernatant	-330405	0.9375	No	ns
Serum- vs CM Pellet	-363311	1.031	No	ns
CM Supernatant vs Pellet	-32905	0.09337	No	ns

4.3 The biomolecules transferred from MDA-MB-231 cells to BT20 cells promote cell rounding and apoptosis

The crystal violet data suggests that conditioned medium from MDA-MB-231 cells inhibits proliferation of BT20 cells. To further define the anti-proliferative effect of the MDA-MB-231 conditioned medium, real time light microscopy of BT20 cells treated with MDA-MB-231 conditioned media was utilised to analyse morphological changes over time. Morphology was classified into three categories relating to cell health, namely cell rounding, apoptotic bodies and cells with protrusions. C8 exposure was used as a control to induce cell rounding and apoptosis while serum-free and serum containing media were used as the baseline and positive controls. Quantification of

the three categories was performed via manually counting of categorised cells present in each frame every 3 hrs for a 24-hr period using Image-J analysis software (Figure 4.19). MDA-CM resulted in a gradual decrease in BT20 cellular protrusions from 0.8 to 0.5 ratio of cells with protrusions to the total, while a gradual increase in cell rounding from 0.2 to 0.4 ratio of rounded cells to the total and a gradual increase in the presence of apoptotic bodies from 0 to 0.5 ratio of apoptotic cells to the total was observed over time. Serum treatment resulted in a constant cellular morphology profile where cell rounding, apoptotic bodies and protrusion numbers did not change significantly. Treatment of BT20 cells with BT20-CM also did not cause any changes in any of the categories over time. As expected C8 exposure resulted in an increase in the presence of apoptotic bodies and a decrease in cells with protrusions. Area under the curve analysis was performed to directly compare the effects of the different conditions (Figure 4.20). Importantly, MDA-CM significantly increased the presence of apoptotic bodies of BT20 cells to 1.6 ratio of cells when compared to serum exposed cells (0.6) while C8 induced the presence of apoptotic bodies to a level of 4 ratio of cells. Conversely, no significant difference between serum exposed and MDA-CM exposed cells were observed with regards to cell rounding and the presence of protrusions.






Key:	A – 6 hours	C – 18 hours	 Rounded cells
	B – 12 hours	D – 24 hours	 Apoptotic cells/bodies
			 Cell protrusions

Figure 4.18: MDA-CM increases cell rounding and apoptosis in BT20 cells over time. Image frames of three parameters; rounded, apoptotic and cells with protrusions taken over 24-hrs of BT20 cells treated with MDA-MB-231 conditioned media. There is a decrease in cell protrusions and an increase in cell rounding and apoptosis over time. Scale bar = 100 μ m.

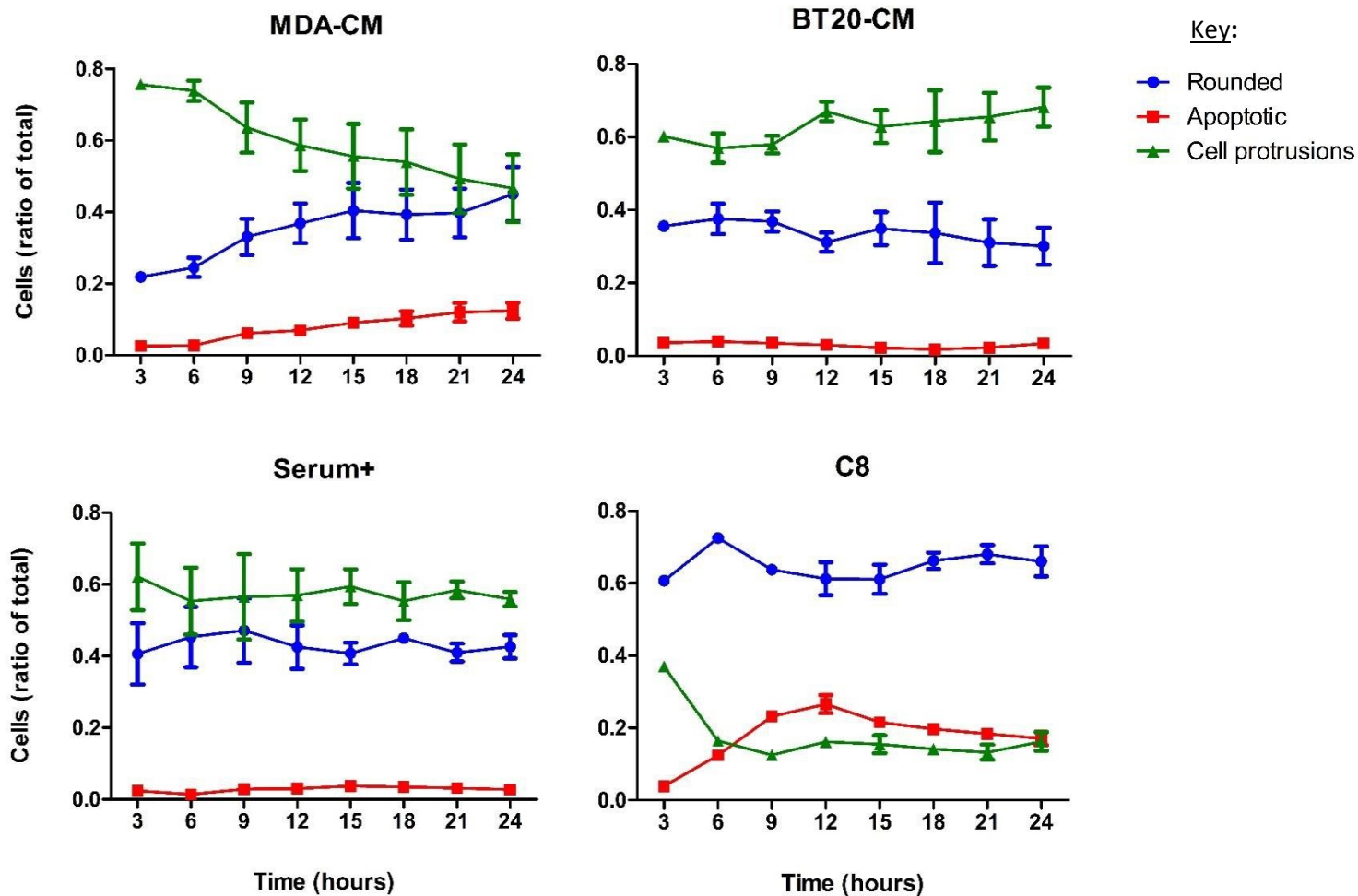


Figure 4.19: MDA-CM decreases cellular protrusions while inducing an increase in cell rounding and apoptosis in BT20 cells. Cell number (ratios of the total) for the three parameters; Rounded, Apoptotic and cells with protrusions taken every three hours from a movie of BT20 cells treated with MDA-MB-231 conditioned media ($n=3$). There is an increase in cell rounding and apoptosis in cells exposed to the conditioned media compared to BT20-CM and serum positive media. C8 is the positive control. Statistical significance determined via a one-way ANOVA followed by a Bonferroni post-test where each cell parameter is compared to one another ($P < 0.05$). ($n=3$)

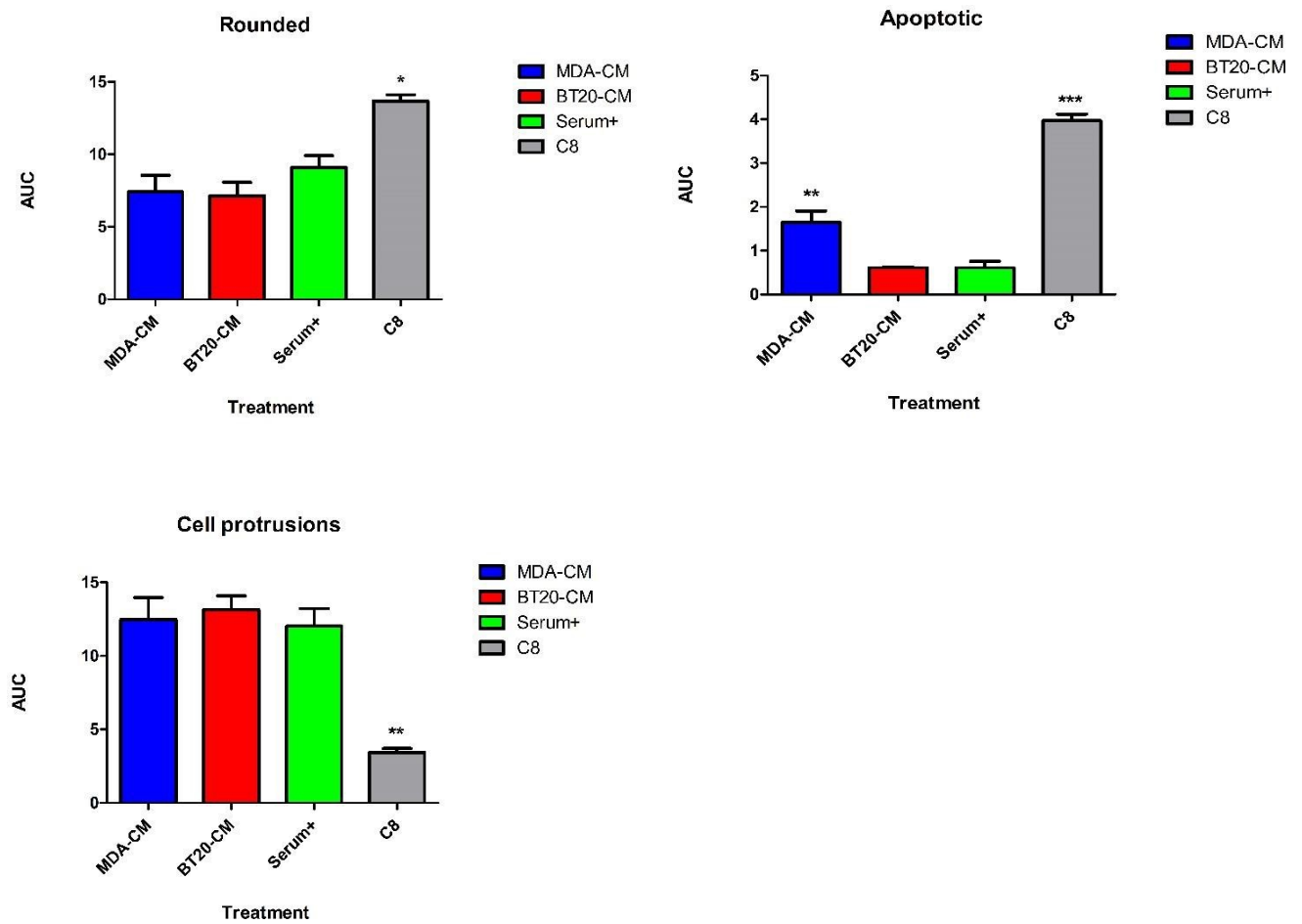


Figure 4.20: MDA-CM significantly increases cellular apoptosis. Bar graphs of the ratios of the total for the three parameters representing area under the curve for BT20 cells treated with MDA-CM, BT20-CM, Serum+ media and C8. Along with C8, MDA-CM resulted in a significant change in cellular morphology. Statistical significance determined via a one-way ANOVA paired with a Dunnett's multiple comparison test with Serum+ treatment as the control group ($P < 0.05$). ($n=3$)

Table 4.8: Dunnett's multiple comparison test results for the three parameters of BT20 cells post MDA-CM treatment

Dunnett's Multiple comparison test				
Groups	Mean Diff.	Q	Significant? P<0.05?	Summary
Parameter: Apoptotic cells				
<i>ANOVA P value <0.0001</i>				
Serum+ vs. MDA-CM	-1.037	4.376	Yes	**
Serum+ vs. BT20-CM	0.0005	0.0021	No	ns
Serum+ vs. C8	-3.359	14.18	Yes	***
Parameter: Rounded cells				
<i>ANOVA P value 0.0023</i>				
Serum+ vs. MDA-CM	1.678	1.374	No	ns
Serum+ vs. BT20-CM	1.960	1.605	No	ns
Serum+ vs. C8	-4.584	3.753	Yes	*
Parameter: Cell protrusions				
<i>ANOVA P value 0.0006</i>				
Serum+ vs. MDA-CM	-0.4503	0.2996	No	ns
Serum+ vs. BT20-CM	-1.122	0.7466	No	ns
Serum+ vs. C8	8.595	5.717	Yes	**

4.4: MDA-MB-231 conditioned medium does not affect the actin cytoskeleton or cell adhesion structures.

A possible explanation for the increased presence of apoptotic bodies and decrease in cell survival could be that the conditioned medium impacts on cell adhesion and the actin cytoskeleton. To assess if this was probable, BT20 cells treated with MDA-CM or serum-free media were fixed and processed to visualise focal adhesions using antibodies targeted against FAK and a stain specifically binding to actin fibres.

Analysis by confocal microscopy of the processed cells showed no discernible differences in the presence or distribution of adhesion structures or in the organisation of the actin cytoskeleton (Figure 4.21). The lack of changes in adhesion structures and

the actin cytoskeleton suggests the conditioned medium does not act by inhibiting cell adhesion.

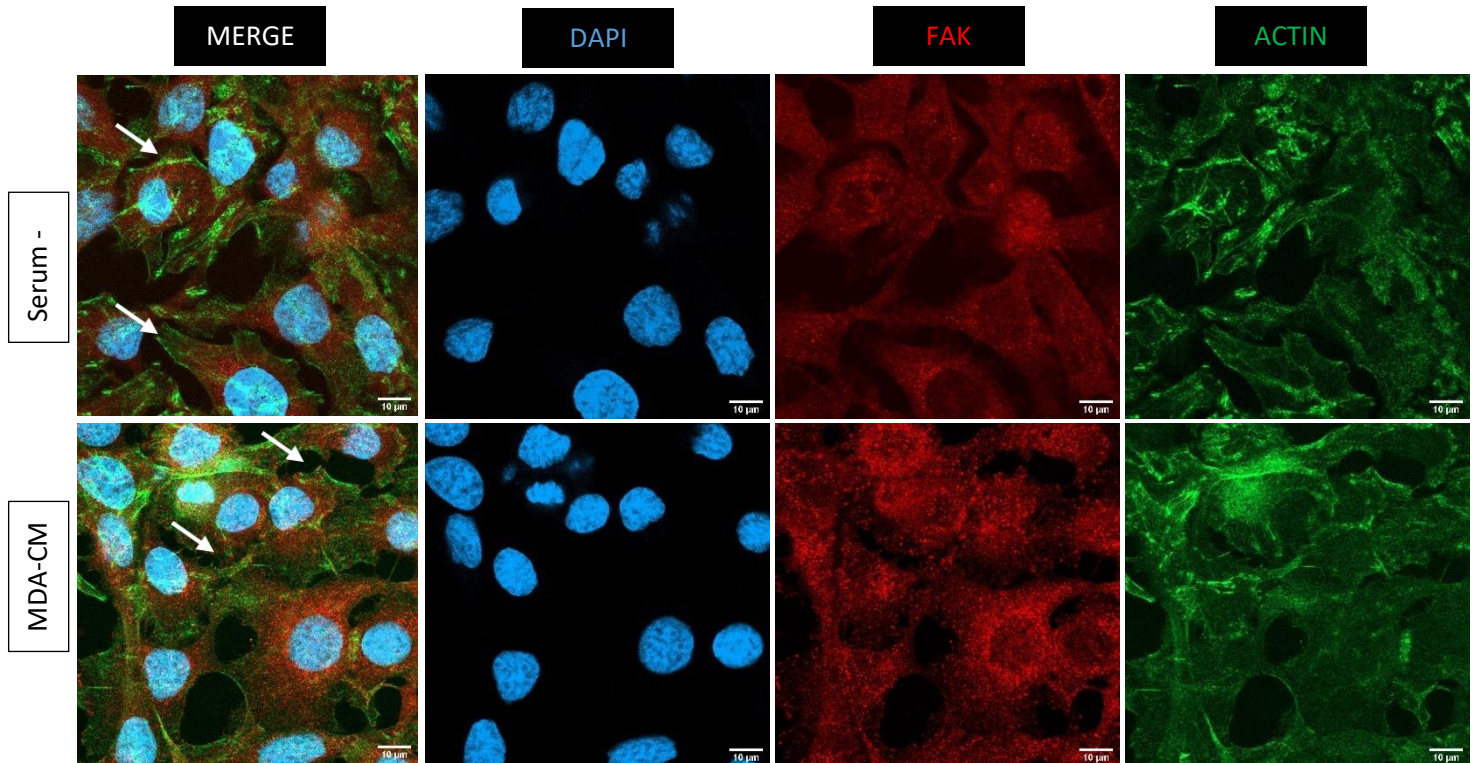


Figure 4.21: MDA-CM does not alter cell adhesion structure architecture in BT20 cells. *Focal adhesions visualised through FAK (red) and actin (green) staining. Co-stained with DAPI (blue) for the nucleus. There are similar focal adhesion profiles for BT20 cells treated with serum-free media (top row) and MDA-MB-231 conditioned media (bottom row). The arrows show regions where actin binds the focal adhesions.*

4.5: Treatment of BT20 cells with MDA-MB-231 conditioned medium induces cell cycle exit.

Since MDA-MB-231 conditioned medium has anti-proliferative effects on BT20 cells, it was hypothesised that it may be inducing cell death directly or indirectly by inducing cells to exit the cell cycle. To analyse the effect on cell cycle, cellular DNA content was assessed by PI staining and subsequent deconvolution of the DNA contents' frequency histograms.

BT20 and MDA-MB-231 cells were seeded, allowed to attach and then treated with conditioned medium and appropriate controls for 72 hrs. Afterwards, cells were stained using PI and fluorescence levels were analysed by flow cytometry using a CytoFLEX® flow cytometer. The histograms were obtained using Kaluza analysis software (Figure 4.22 and 4.24). For comparative analysis, the percentage of cells in each part of the cell cycle was determined and compared between the different treatments (Figures 4.23 and 4.25).

BT20 cells treated with serum-free medium (SFM), serum containing medium (Serum+) or BT20 conditioned medium (BT20-CM) showed quite similar cell cycle profiles with about 1.7% in G₀, ~75% in G₁/S, ~9% in S, and 15% in G₂/M, although there was a small but insignificant increase in G₀ to ~4.5% in cells in SFM. However, there was a significant increase in cells in the S phase (~11%) for cells exposed to serum when compared to cells in serum-free medium (Figures 4.22 and 4.23). In contrast, exposure of the BT20 cells to MDA-CM yielded a significant increase of cells in G₀ to about ~10%, coupled to a significant decrease in cells in G₁/S, to ~65% (Figure 4.23). Thus, MDA-MB-231 conditioned medium increases the proportion of cells in the G₁/S phase, with a proportion of cells also exiting the cell cycle into the G₀ phase. Conversely, exposure of MDA-MB-231 cells to conditioned media did not change the cell cycle profiles except that cells exposed to MDA-MB-231 conditioned medium had a slightly increased number of cells in the S-phase which is in contrast to BT20 cells (Figures 4.24 and 4.25).

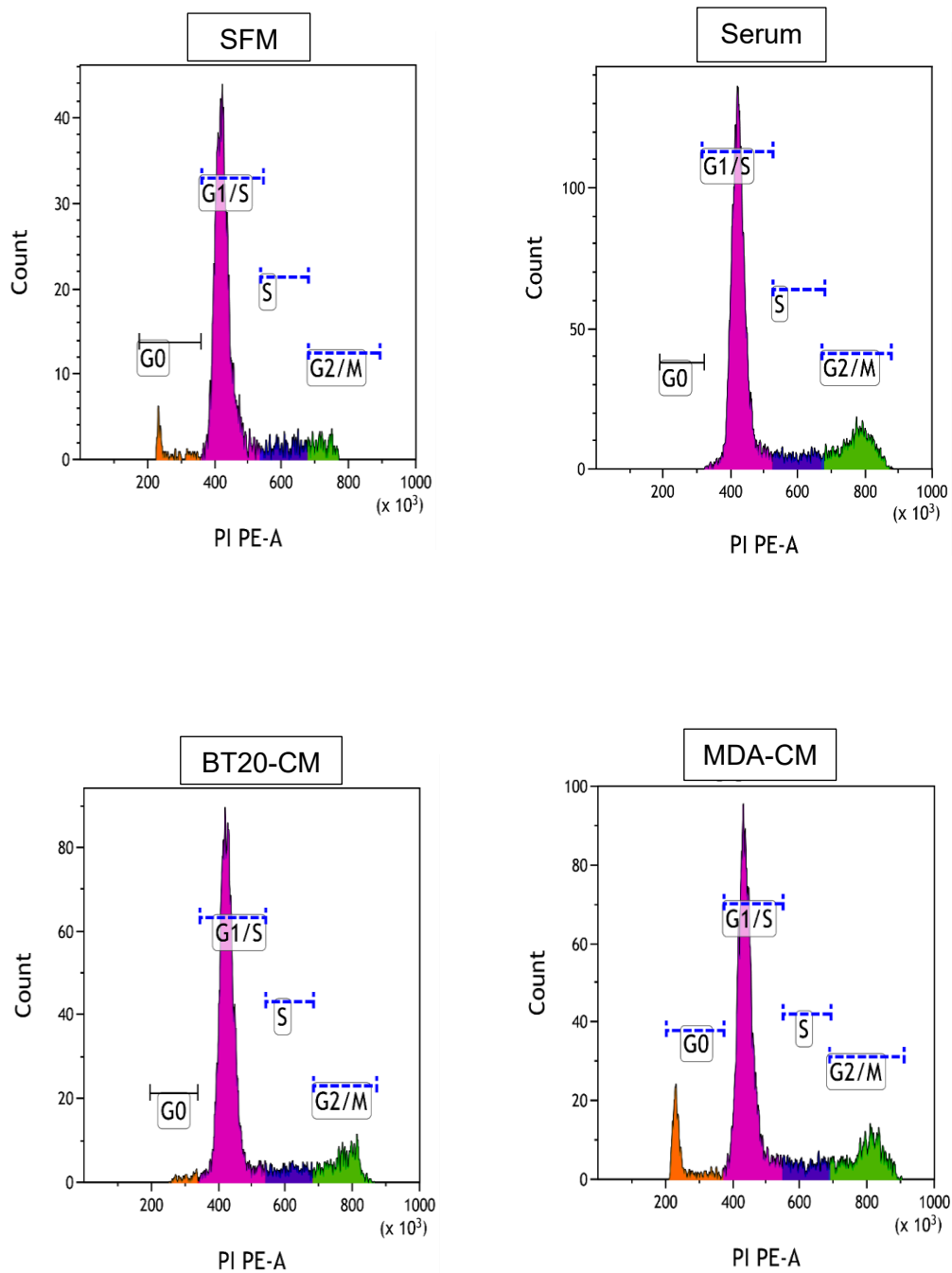


Figure 4.22: MDA-CM results in more cells in G0 phase of cell cycle. Cell cycle analysis of the BT20 cell line, histograms obtained via propidium iodide staining and flow cytometry following treatment with media. MDA-CM blocks G1/S phase of BT20 cell cycle and subsequent cell exit into G0 phase.

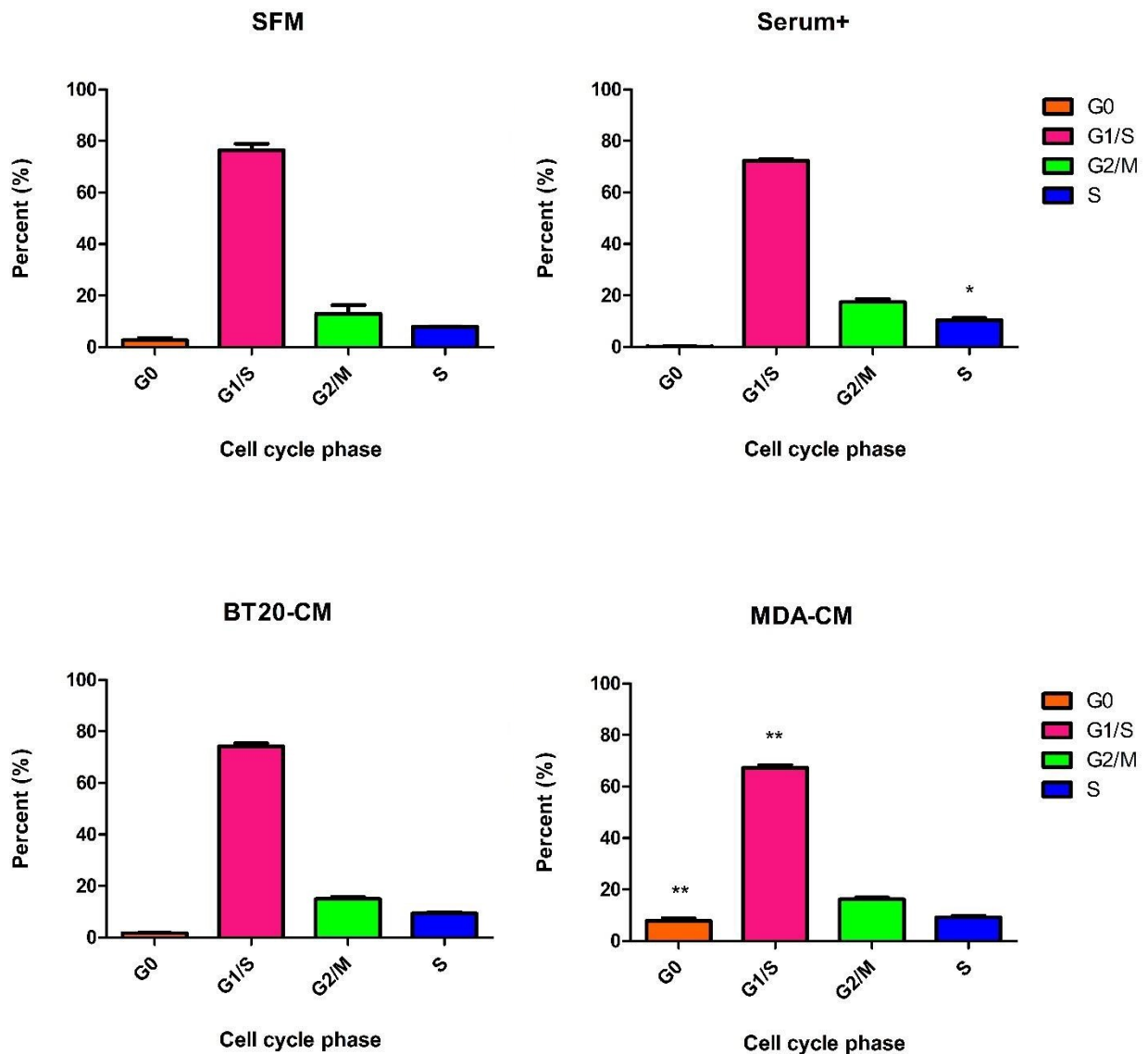


Figure 4.23: Conditioned media from the metastatic MDA-MB-231 cell lines results in more quiescent cells in the BT20 cell cycle. Bar graphs representing the percentage distribution of BT20 cells through the cell cycle post treatment with Serum-free media (SFM), Serum positive media (Serum+), BT20-conditioned media (BT20-CM), MDA-MB-231-conditioned media (BT20-CM). Error bars represent mean + SEM. Statistical significance determined via one-way ANOVA with Dunnett's multiple comparison test comparing all treatments to SFM. (n = 3)

Table 4.9: One-way ANOVA with Dunnett's multiple comparison test for BT20 cells comparing all treatments to the control – serum-free media (SFM)

Dunnett's Multiple comparison test				
Groups	Mean Diff.	q	Significant? P<0.05?	Summary
<i>ANOVA P value 0.0003</i>				
Phase: G0				
SFM vs. Serum +	2.573	2.553	No	ns
SFM vs. BT20-CM	0.9900	0.9822	No	ns
SFM vs. MDA-CM	-5.120	5.080	Yes	**
<i>ANOVA P value 0.0144</i>				
Phase: G1/ S				
SFM vs. Serum +	4.197	1.932	No	ns
SFM vs. BT20-CM	2.340	1.077	No	ns
SFM vs. MDA-CM	9.327	4.293	Yes	**
<i>ANOVA P value 0.4053</i>				
Phase: G2/M				
SFM vs. Serum +	-4.537	1.742	No	ns
SFM vs. BT20-CM	-2.030	0.7795	No	ns
SFM vs. MDA-CM	-3.233	1.242	No	ns
<i>ANOVA P value 0.1009</i>				
Phase: S				
SFM vs. Serum +	-2.410	2.951	Yes	*
SFM vs. BT20-CM	-1.300	1.592	No	ns
SFM vs. MDA-CM	-1.237	1.514	No	ns

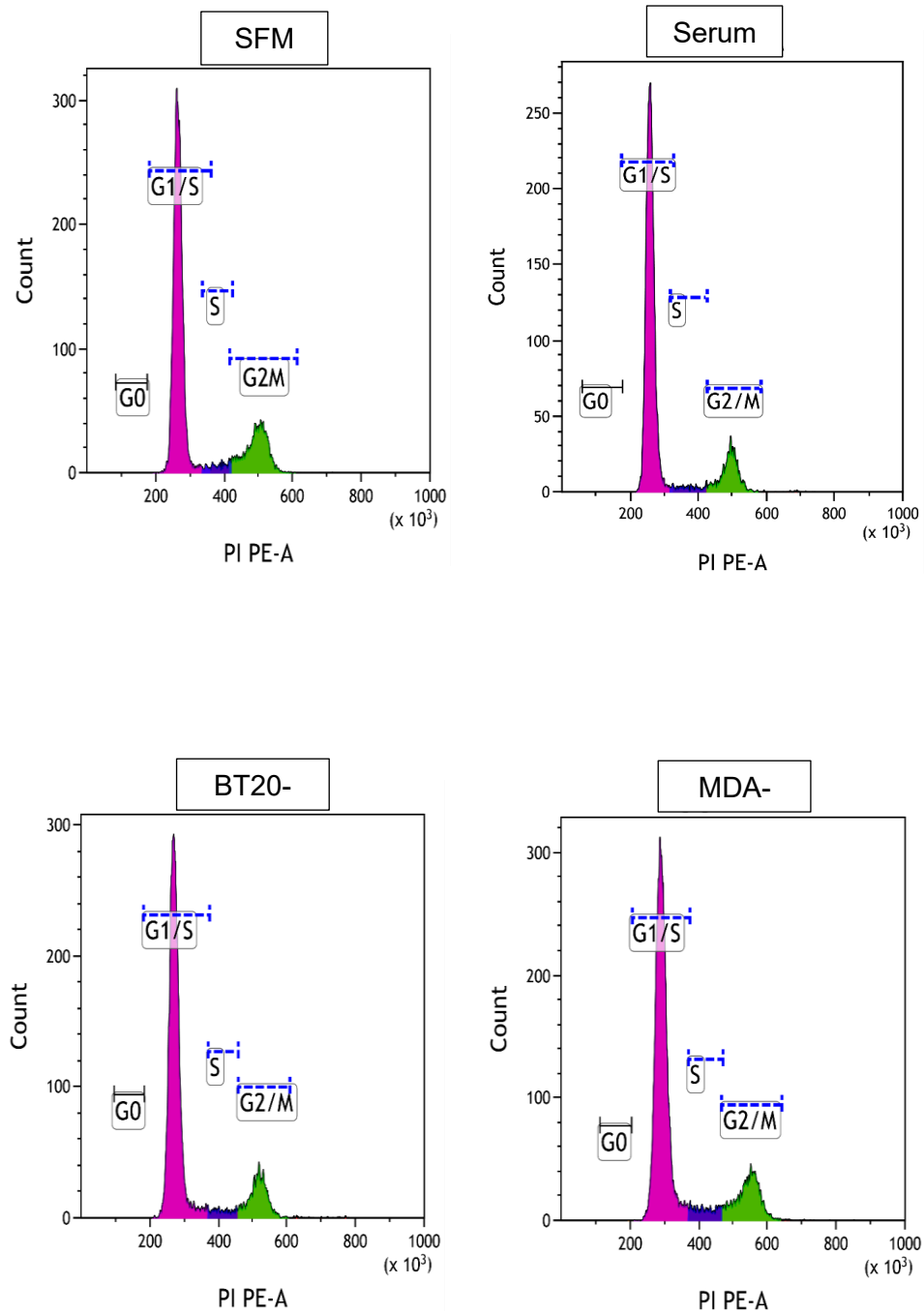


Figure 4.24: MDA-231 cell cycle relatively unaffected by treatment. *Cell cycle analysis of the MDA-231 cell line, histograms obtained via propidium iodide staining and flow cytometry following treatment with media. The metastatic cell line remained relatively unaffected by media treatment.*

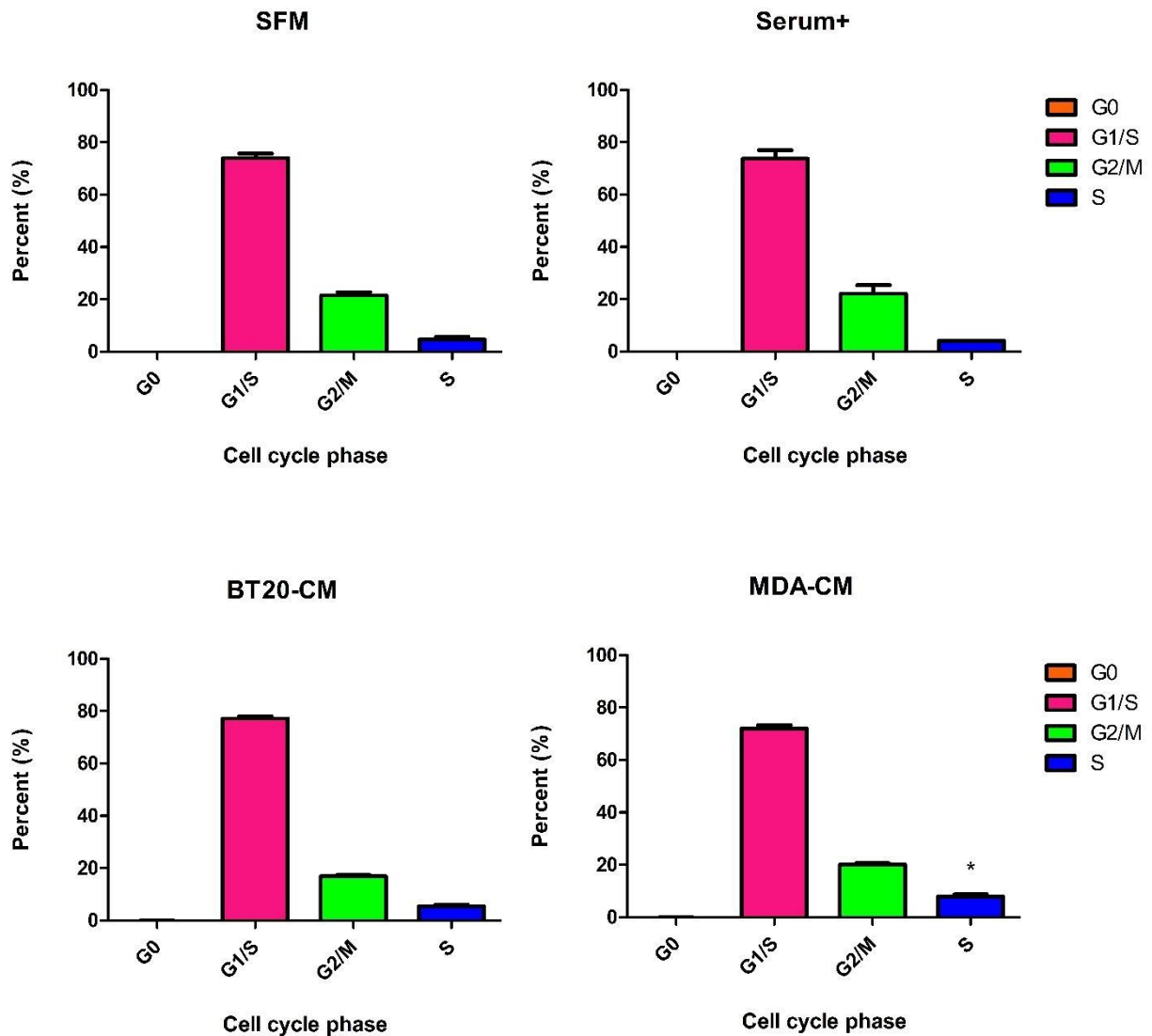


Figure 4.25: Treatment of the metastatic MDA-MB-231 cell line with any of the conditions does not significantly alter the cell lines' progression through the cell cycle. Bar graphs representing the percentage distribution of MDA-MB-231 cells through the cell cycle post treatment with Serum-free media (SFM), Serum positive media (Serum+), BT20-conditioned media (BT20-CM), MDA-MB-231-conditioned media (BT20-CM). Error bars represent mean + SEM. Statistical significance determined via one-way ANOVA with Dunnett's multiple comparison test comparing all treatments to SFM. (n = 3)

Table 4.10: One-way ANOVA with Dunnett's multiple comparison test for MDA-MB-231 cells comparing all treatments to the control – serum-free media (SFM)

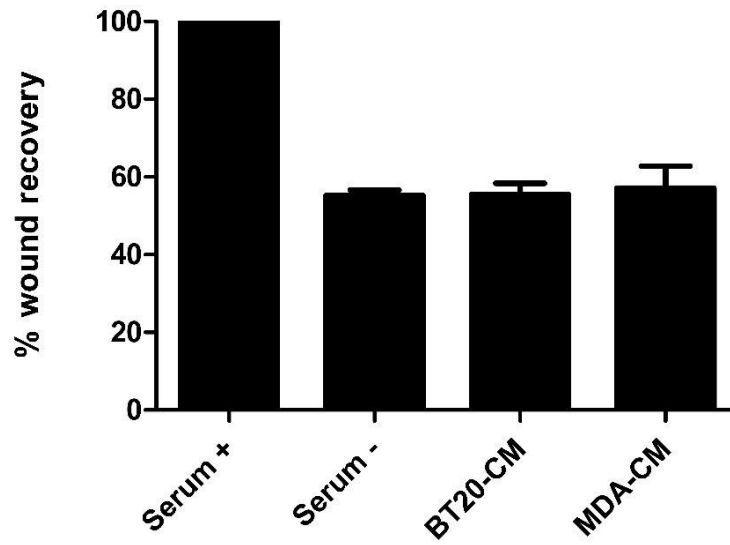
Dunnett's Multiple comparison test				
Groups	Mean Diff.	q	Significant? P<0.05?	Summary
Phase: G0				
<i>ANOVA P value 0.3363</i>				
SFM vs. Serum +	0.0167	1.826	No	ns
SFM vs. BT20-CM	0.0133	1.461	No	ns
SFM vs. MDA-CM	0.0133	1.461	No	ns
Phase: G1/ S				
<i>ANOVA P value 0.3822</i>				
SFM vs. Serum +	0.2533	0.090	No	ns
SFM vs. BT20-CM	-3.133	1.119	No	ns
SFM vs. MDA-CM	2.000	0.714	No	ns
Phase: G2/M				
<i>ANOVA P value 0.2291</i>				
SFM vs. Serum +	-0.637	0.255	No	ns
SFM vs. BT20-CM	4.647	1.860	No	ns
SFM vs. MDA-CM	1.373	0.550	No	ns
Phase: S				
<i>ANOVA P value 0.0268</i>				
SFM vs. Serum +	0.613	0.588	No	ns
SFM vs. BT20-CM	-0.783	0.750	No	ns
SFM vs. MDA-CM	-3.247	3.110	Yes	*

4.6: Conditioned media treatment of the MDA-MB-231 breast cancer cell line does not impact migration rate.

While no proliferative effect of BT20-CM on MDA-MB-231 was observed, it could still be possible that the non-migratory BT20 cells could release factors that inhibit migration. To test this hypothesis, the rate of MDA-MB-231 cell migration was measured using a 'scratch assay' where cell monolayers were exposed to different medias after creation of a cell free zone at time point zero. The cell free zone was photographed using a Zeiss Axiovert inverted microscope at time point zero ($t = 0$) and after 18 hrs ($t = 18$) of incubation (Figure 4.26-B). The difference in area representing the migration of cells into the cell free zone was calculated using Image J analysis software (Figure 4.26-A).

Given the lack of significant changes to the cytoskeleton (see Figure 4.21), and the non-migratory and non-metastatic nature of the BT20 cell line, we investigated the impact of conditioned media on the migration rate of the migratory MDA-MB-231 cell line. MDA-MB-231 cells were seeded and grown to confluency before cell-free zones were generated and cells allowed to migrate in the presence of serum, absence of serum, BT20 conditioned medium, or MDA-MB-231 conditioned medium. The data obtained shows that the cell free zone was completely closed when cells were treated with serum positive media (Serum+). Serum-free medium-exposed cells migrated 50% of distance of the cells under serum exposure. Neither exposure to BT20- nor MDA-MB-231 conditioned medium resulted in a change in migration rate compared to serum-free media (Figure 4.26A+B). Thus, conditioned medium does not appear to affect cell migration.

Migration assay



B

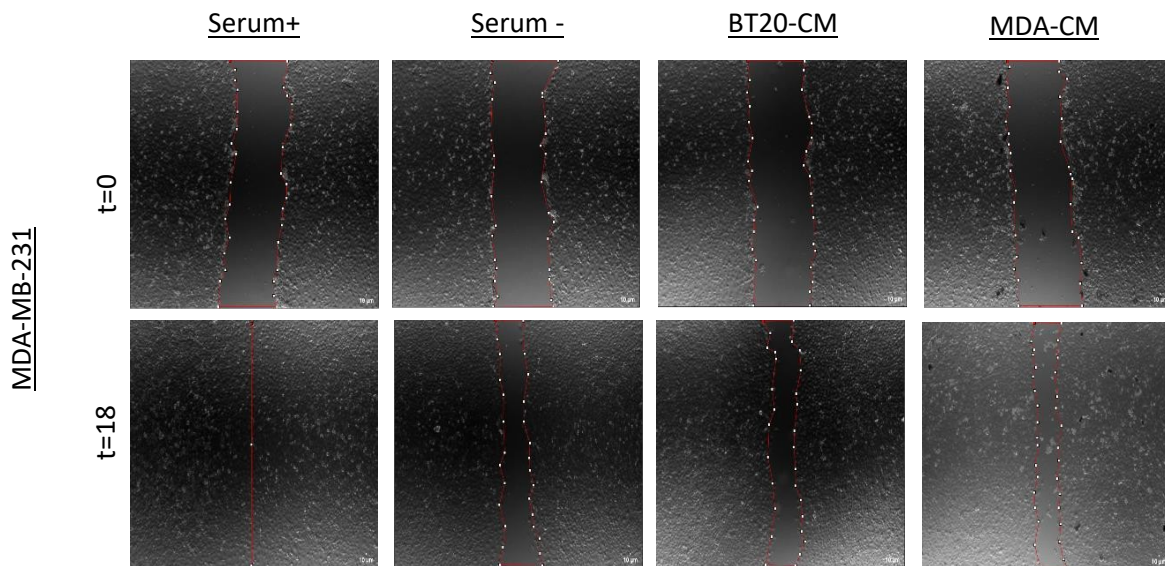


Figure 4.26: Treatment of MDA-MB-231 cells with BT20-CM and MDA-CM does not influence migration. (A) Percentage wound closure was measured after treatment (t=0) and an 18-hr incubation (t=18) with different compounds. (B) Micrographs representing MDA cell migration into a cell free zone over an 18-hr period. 2.5x Magnification (n=3).

4.7: Biomolecules are transferred from MDA-MB-231 cells to BT20 cells

4.8.1 Introduction

Since the data showed that MDA-CM impacts BT20 cell proliferation, we then sought to determine if there is direct transfer of biomolecules from the donor MDA-MB-231 cells to the recipient BT20 cells. To prove that this phenomenon occurs, a fluorescence visualisation method can be employed that offers direct proof of molecule transfer. Previously, Prof. Jacco van Rheenen established such a “colour switch” system that can track the uptake of biomolecules in individual cells.⁸⁰

4.8.2 Establishment of donor and recipient cell lines

The colour switch system developed by Prof. van Rheenen is made up of two parts. Within the construct introduced in the recipient cells, a region encoding a red fluorophore (dsRed) is flanked by loxP sites and precedes a region encoding GFP (Appendix E). This means that if Cre recombinase is present in the cell, it will recognise the loxP sites and excise the DNA sequence between the two sites, thereby removing the red fluorophore gene and its stop codon. As a result, cells will stop expressing the red fluorophore and instead switch to expressing GFP (Figure 4.27). The donor cells are modified to express Cre recombinase under the direction of an estrogen response element such that Cre will only be expressed in the presence of estrogen or the anti-estrogen, 4HT. As a marker for donor cell identity, the donor MDA cells also expressed H2B-CFP which shows up as a blue fluorescence in the nucleus. All plasmids were introduced stably into the target cells via lentiviral transduction.

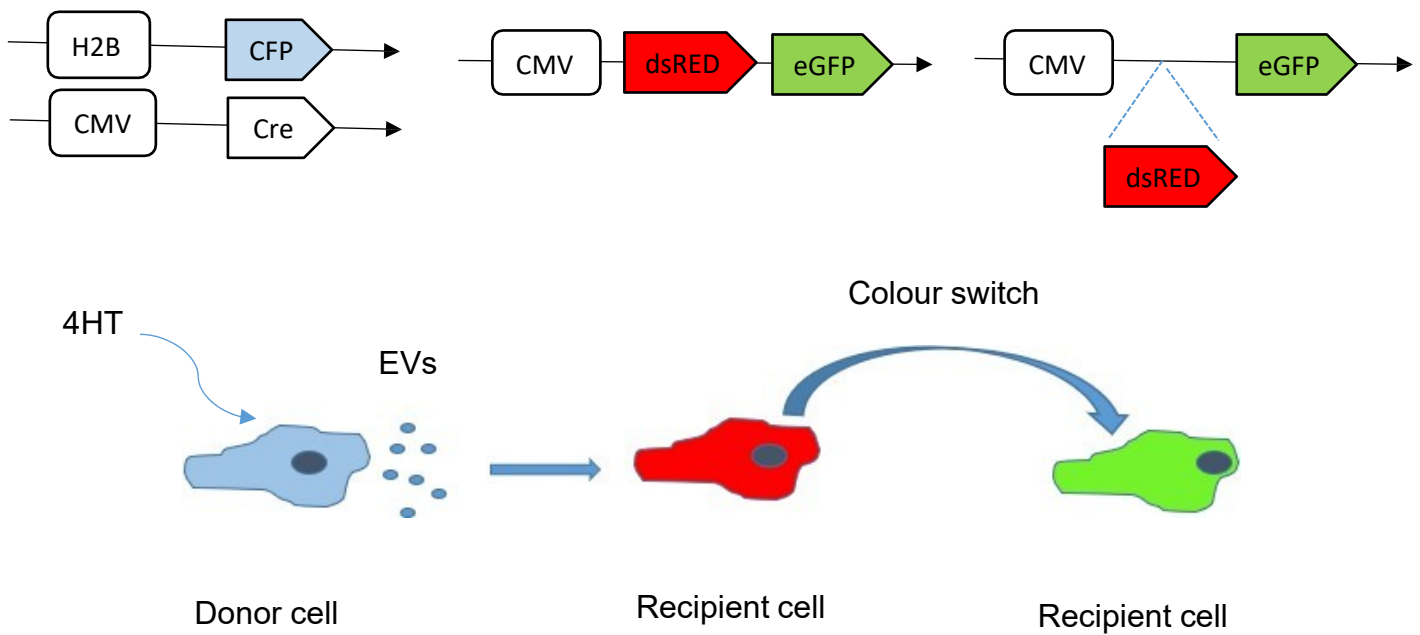
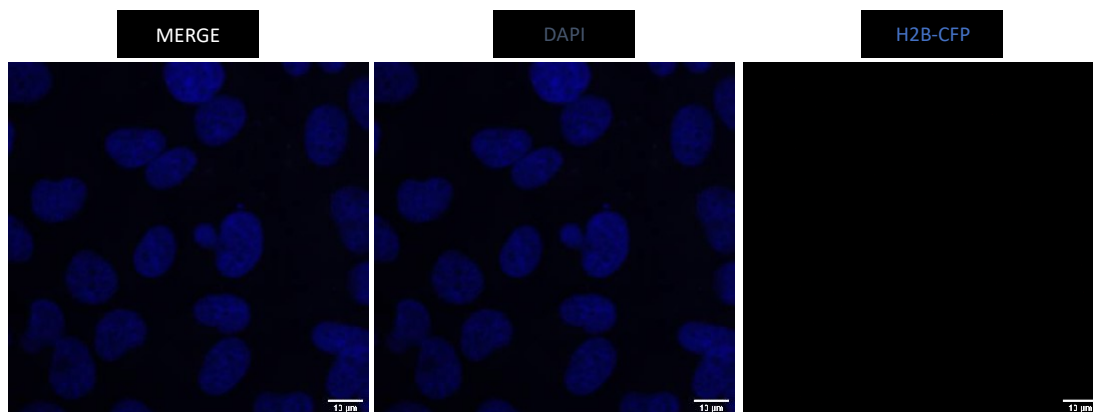


Figure 4.27: The colour switch system is inducible. *The active metabolite of tamoxifen, 4HT, induces the production of the Cre enzyme, which upon endocytosis by the recipient cell line, the enzyme recombines the recipient cell from expressing dsRed to expressing eGFP through excision of dsRED. There is an observed colour switch from red to green in the recipient cell.*

MDA-MB-231 cells were infected with both Cre-ERT and H2B-CFP-carrying lentivirus (Appendix C and D respectively), to create the donor cell line “MDA-CRE-CFP”. Pure cell populations were obtained by FACS sorting for CFP-expressing cells. To show that the Cre-ERT cells express CFP, normal MDA-MB-231 and CRE-CFP MDA-MB-231 cells were mounted and stained with DAPI nuclear stain. Images were taken with settings to detect CFP and DAPI separately (Figure 4.28). Parental MDA-MB-231 breast cancer cells have visible nuclei in the channel for DAPI but no fluorescence is present in the CFP channel. Conversely, the CRE-CFP MDA-MB231 cells fluoresce in both the DAPI channel and the CFP channel with the fluorescence perfectly overlapping indicating that the CFP is located in the nucleus as directed by the H2B histone sequence it is fused to.

The recipient cell line was created by infecting the parental BT20 cell line with the switch module-carrying lentivirus. To ascertain that a pure population was selected, cells were sorted for red fluorescence using FACS and positive cells were isolated and expanded. Switch BT20 and parental BT20 cells were fixed and mounted with DAPI for confocal imaging. As expected, parental BT20 cells fluoresced in the DAPI channel but no fluorescence was observed in the GFP or dsRed channels. (Figure 4.29-A). However, the Switch-BT20 cell line not only fluoresced in the DAPI channel as expected but all cells imaged also showed fluorescence in the dsRed channel (Figure 4.29-B). Importantly, no GFP expression was observed in cells indicating that the switch module successfully terminated expression of the dsRed protein without any read through to the GFP gene. Thus, these data confirmed the successful generation of a stable donor MDA-MB-231 cell line and a recipient BT20 cell line.

A) Cell line: MDA-MB-231



B) Cell line: MDA-CRE-CFP

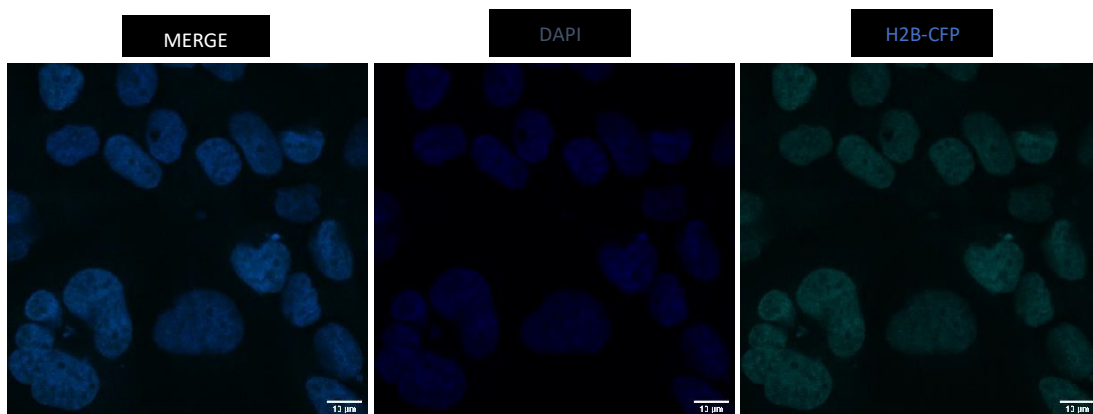
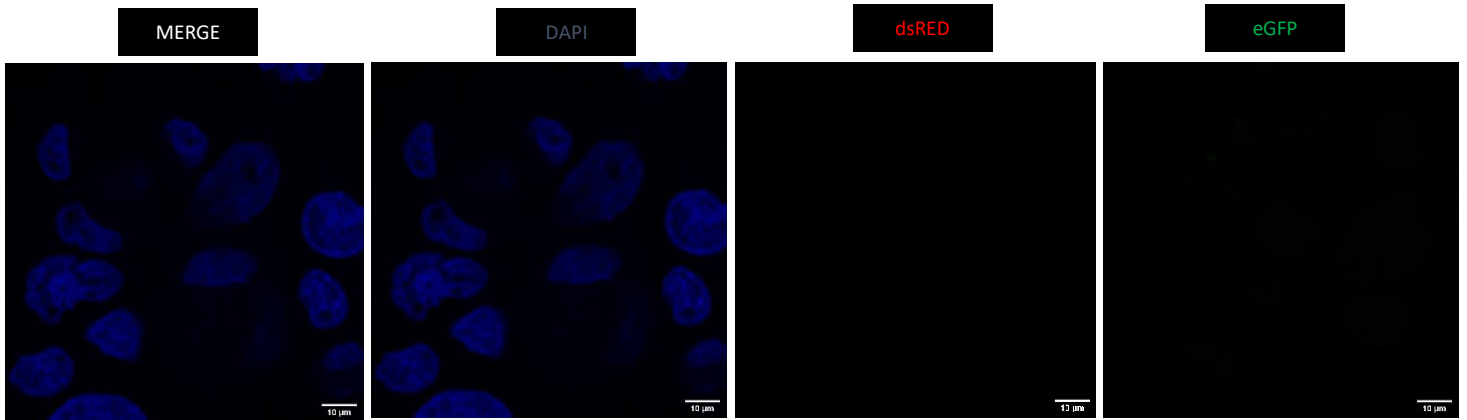


Figure 4.28: The stable (donor) but not parental MDA-MB-231 cells displayed CFP fluorescence. Parental MDA-MB-231 cells (A) and the stable fluorophore expressing MDA-MB-231 cell line (B) were stained with DAPI (dark blue). The presence of CFP fluorescence (light blue) shows the successful plasmid integration in the stable cell line.

A) Cell line: BT20



B) Cell line: BT20 Switch

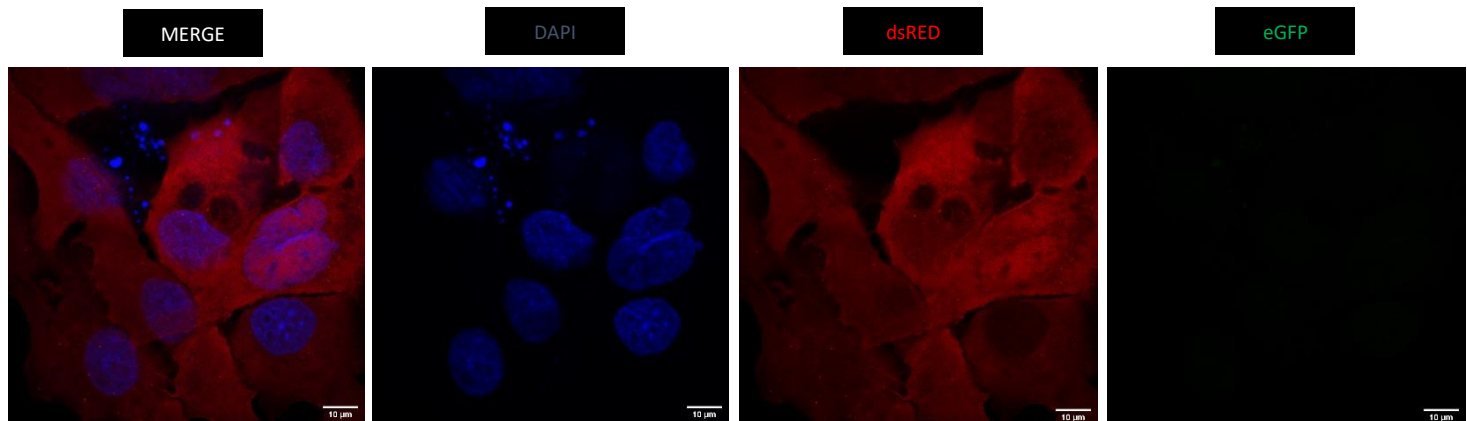


Figure 4.29: The stable (recipient) but not parental BT20 cells displayed dsRED fluorescence. Parental BT20 cells (A) and the stable fluorophore expressing BT20 cell line (B) were stained with DAPI (dark blue). The presence of dsRed fluorescence (red) shows the successful plasmid integration in the stable cell line.

4.8.3 Recipient cells display Cre recombinase dependent colour switch only in the presence of tamoxifen.

To determine if communication occurs between the donor Cre-CFP MDA-MB-231 cell line and the recipient Switch-BT20 cell line, Cre recombinase expression was induced in the Cre-CFP MDA-MB-231 cell line through exposure to 3 μ M 4HT. Subsequently, conditioned media from these cells was collected and the recipient BT20 cells were incubated with this medium. Control conditioned medium from Cre-CFP cells exposed only to vehicle control was also collected and used to expose recipient cells.

Cells incubated with the conditioned medium from cells without tamoxifen were all positive in the red channel with no cells positive in the green channel (Figure 4.30A). In contrast, recipient cells that were exposed to the conditioned medium from tamoxifen-positive cells were all positive in the red channel although some showed lower intensity than others, while a few cells were clearly positive for GFP in the green channel. These GFP positive cells were also the cells with lower red intensity (Figure 4.30B).

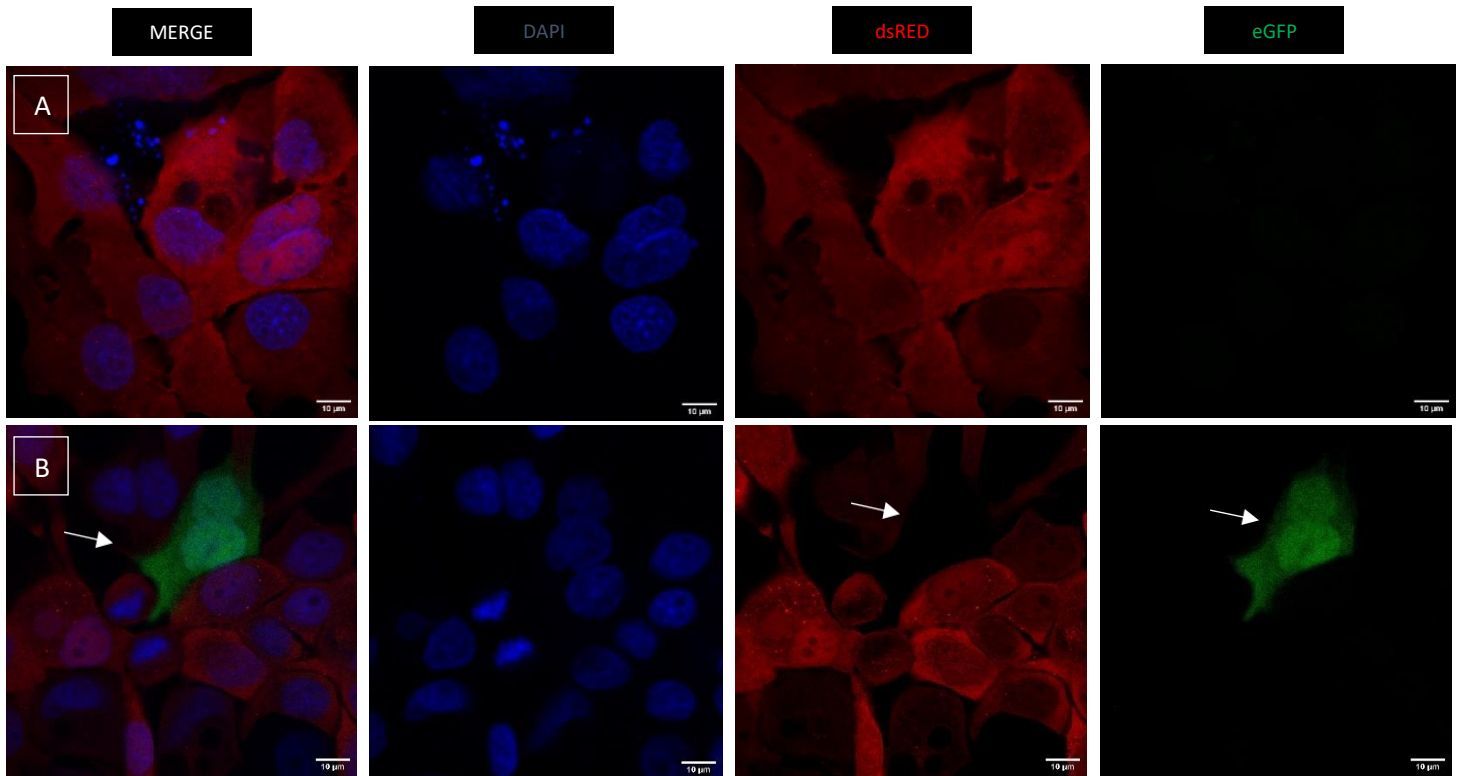


Figure 4.30: Tamoxifen induces the production of Cre recombinase leading to a colour switch in recipient cells. A) When BT20 cells are treated with conditioned media harvested in the absence of tamoxifen, there is no colour switching. B) When BT20 cells are treated with conditioned media harvested in the presence of tamoxifen, the donor cells produce the Cre enzyme, which is then present within the conditioned media resulting in colour switching. White arrows represent colour switched cell.

To determine if cells can directly communicate when in close proximity, co-cultures of the donor and recipient cells were generated. Cells were seeded at a ratio of 1 to 10 'MDA-CRE-CFP' to 'BT20 Switch' to accommodate the difference in growth rate of the cell lines. Parented cell lines were also used as controls. Each cell combination was treated with serum positive media with or without 4HT and incubated for at least 48 hrs at 37 °C.

With the co-culture of the stable cells, in the absence of 4HT, no colour switch was observed, with no cells positive in the GFP channel, while the recipient cells were positive in the red channel and the donor cells were positive in the CFP channel (Figure 4.31). When normal MDA-MB-231 cells were co-cultured with BT20 Switch

cells and treated with tamoxifen, no GFP-positive cells were observed indicating that tamoxifen on its own cannot induce a switch (Figure 4.32). When the BT20 Switch cell line is co-cultured with the MDA-CRE-CFP cell line in the presence of 4HT, there is an observed colour switch in BT20 Switch cells from expressing dsRed (red) to eGFP (green) (Figure 4.33). Thus, these data suggest that the presence of 4HT induces the production of the Cre enzyme in the donor MDA-CRE-CFP cell line, which is packaged, enters the medium and is endocytosed by the recipient BT20 Switch cell line where the Cre enzyme triggers recombination within the recipient cell line inducing an observable change in colour. Interestingly, the cells that have undergone colour switching are in close proximity to one another, suggesting that cells that take up the enzyme containing EVs could be transferring the enzyme between them through direct communication e.g. via intracellular junctions such as gap junctions. For Figure 4.33 and 4.34, the co-cultures slides were mounted using DAPI-containing mounting fluid. Therefore, the non-red but DAPI-positive cells are MDA-MB-231 cells.

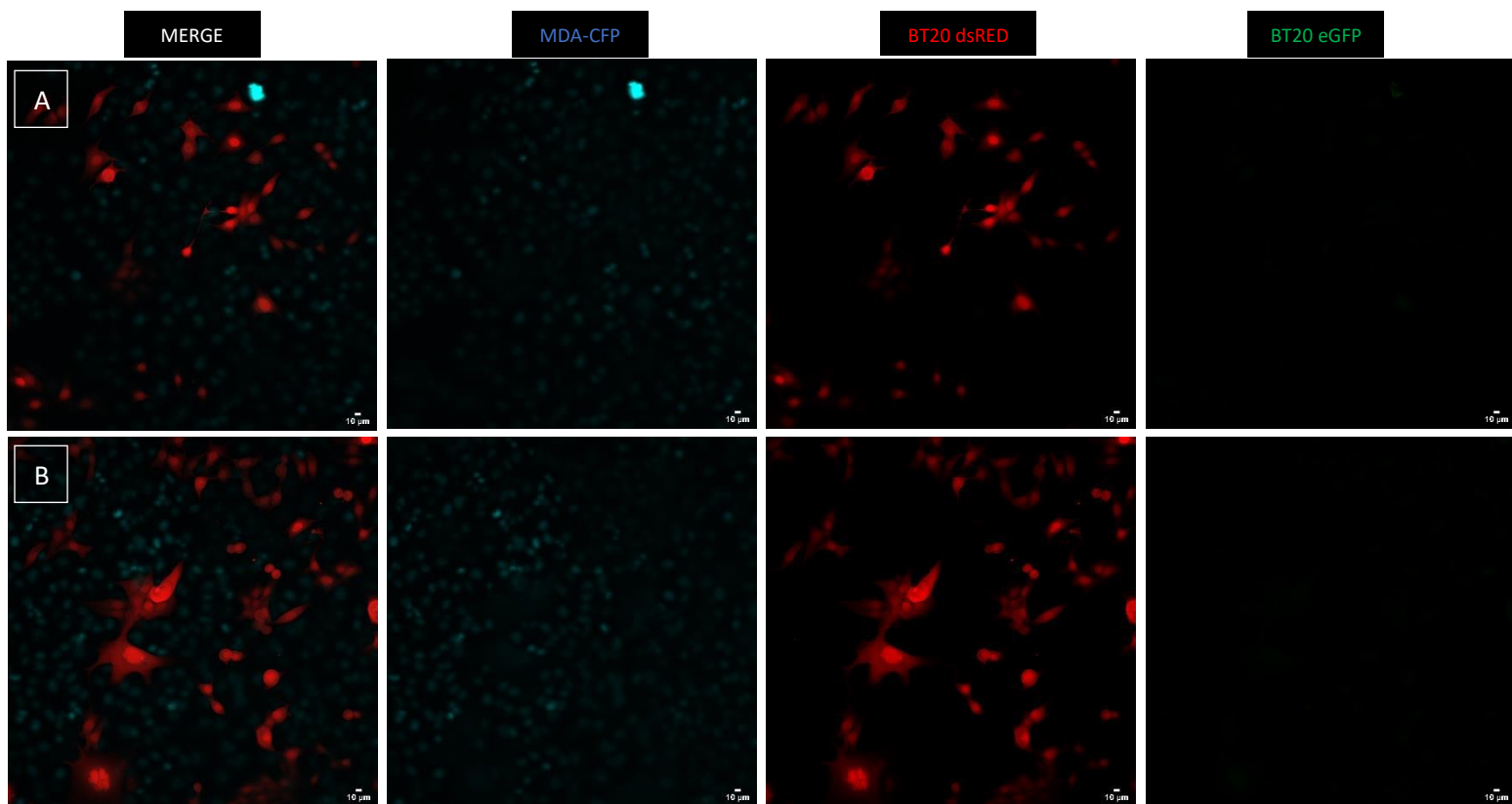


Figure 4.31: There is no colour switching in the absence of tamoxifen for donor and reporter cell co-cultures. *Cre recombinase expressing cells will not produce the enzyme in the absence of the active variant of tamoxifen, 4HT which induces the production of the Cre enzyme within the donor cell. There is no recombination at the switch module and no colour switching occurs. A and B represent repeats.*

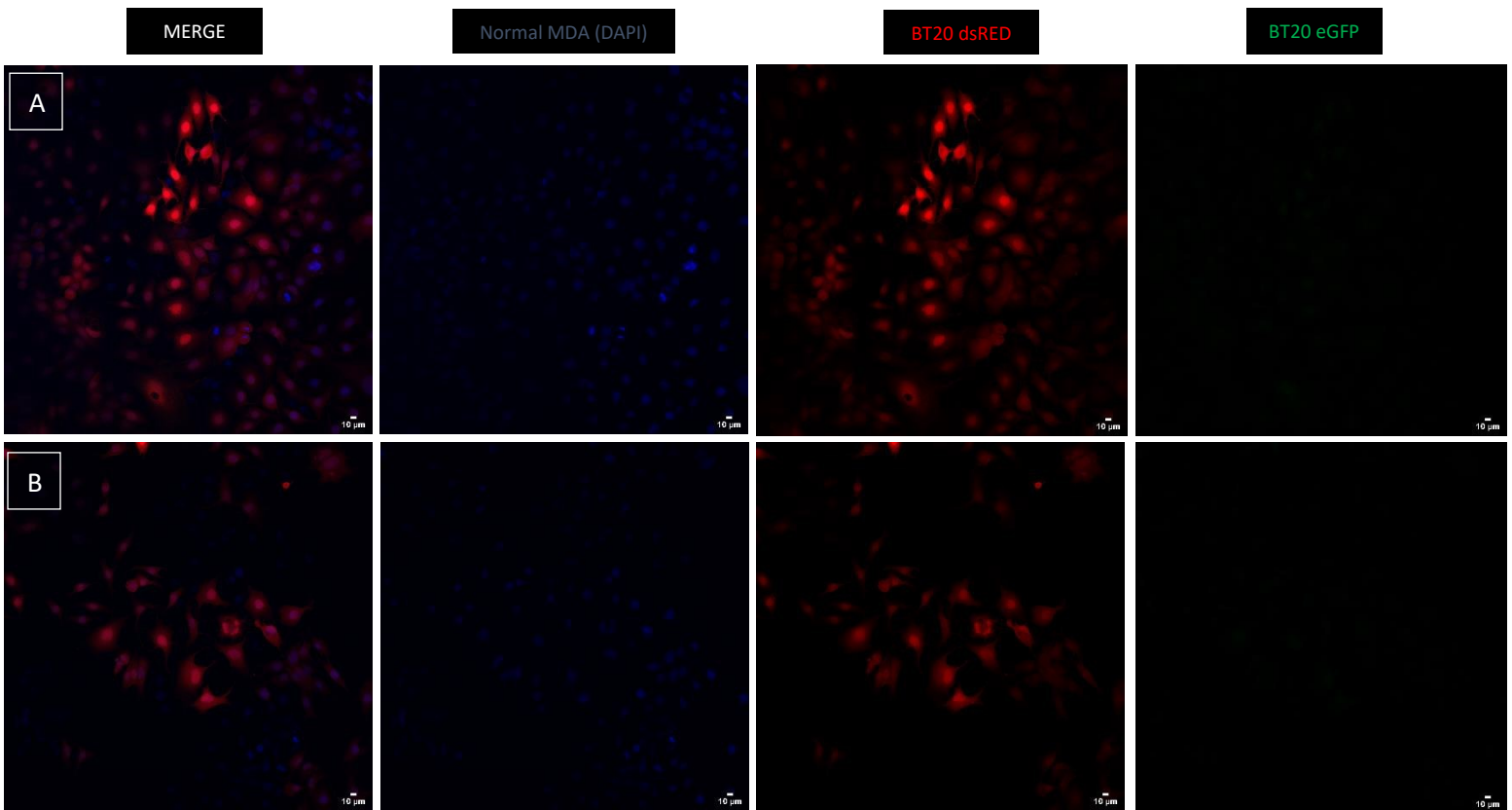


Figure 4.32: The normal MDA-MB-231 variant does not produce Cre recombinase when treated with tamoxifen. The normal MDA-MB-231 cell line variant does not express Cre recombinase. Therefore 4HT (3 μ M) is incapable of inducing the production of the Cre enzyme within the donor cell. There is no colour switching. A and B represent repeats.

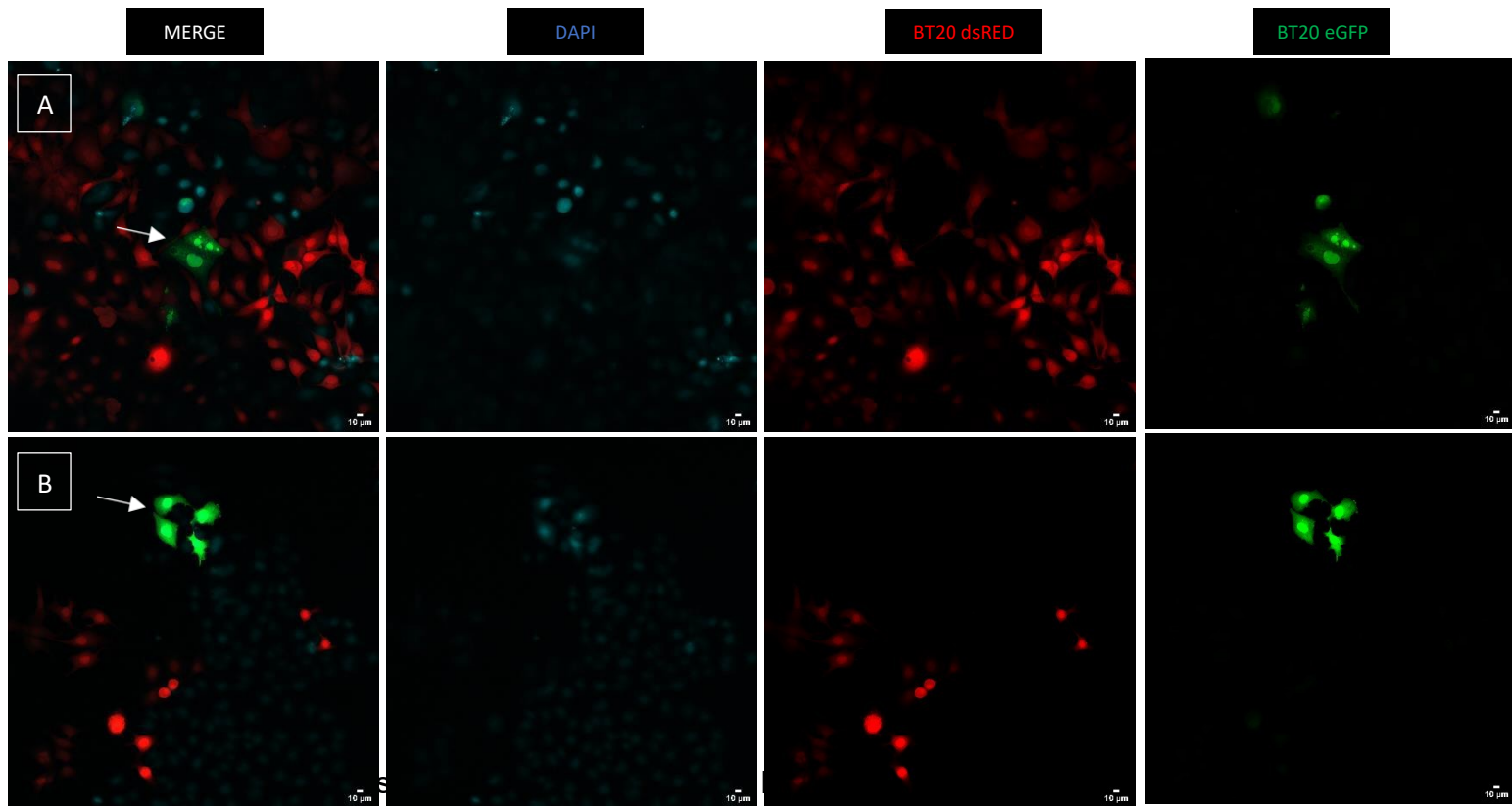


Figure 4.33: The MDA-CRE-CFP variant produces Cre recombinase when treated with tamoxifen resulting in the induction of colour switching. *The MDA-CRE-CFP cell line variant expresses Cre recombinase. Therefore, in the presence of 4HT (3 μ M) there is production of the Cre enzyme within the donor cell. Exchange of extracellular vesicles containing the enzyme resulted in the induction of colour switching. A and B represent repeats.*

4.8.4 There is cell-to-cell transfer of Cre recombinase in co-culture 3D spheroids.

To determine if the transfer of biomolecules could occur in a densely packed epithelial-like tissue (i.e. more closely aligned to a natural tumour environment), we established 3D spheroid co-cultures with the two stable cell lines and treated these with tamoxifen to determine if any dsRed to GFP switch occurs. Previous studies have shown that 3D cultures allow for more efficient biomolecule transfer than corresponding 2D cultures.¹² To generate co-culture spheroids, cells were seeded in 96-well plates coated with 2% agarose and were cultured until spheroids formed. Half of the spheroids were treated with 4HT and were grown for 7 days, with the medium changed every 72 hrs. Spheroid growth images were taken (Appendix F). Data similar to the 2D co-cultures was observed within the 3D co-cultures. When no 4HT is present, despite the presence of the MDA-CRE-CFP cell line, no recombination resulting in green fluorescent cells occurs (Figure 4.34A). Upon treatment with tamoxifen, cells were present that have undergone recombination and have switched from expressing dsRed to expressing eGFP (4.34B). Interestingly, green fluorescent cells are localised within the same area of the spheroid in a similar manner to what was observed in 2D cultures.

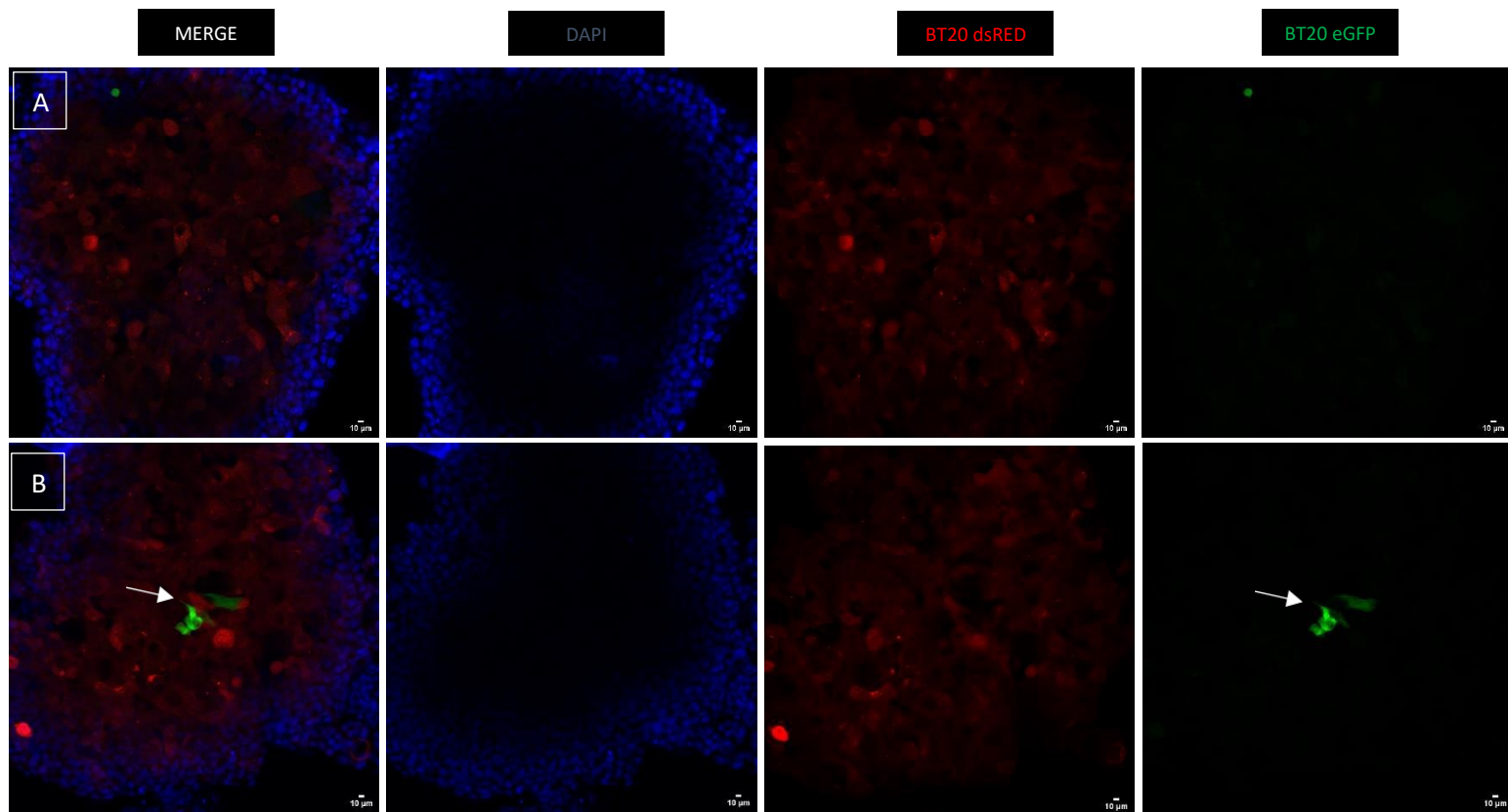


Figure 4.34: Biomolecule transfer occurs in 3D co-culture spheroids after tamoxifen exposure. *[A] Representative image of a BT20/MDA-MB-231 hybrid spheroid in the absence of 4HT. [B] Representative image of a BT20/MDA-MB-231 hybrid spheroid in the presence of tamoxifen. White arrows represent colour switching BT20 cells induced by the Cre enzyme.*

CHAPTER 5 DISCUSSION

5. DISCUSSION

5.1 A metastatic breast cancer cell line secretes biomolecules that decrease the proliferation of the BT20 cell line

Metastasis is dependent on the migration of cells to a secondary site. During this process it is likely that cells do not proliferate.¹²² This lack of proliferation may be aligned with the epithelial-to-mesenchymal transition cells undergo before invading tissue. It is now also clear that metastasis may, at least in part, rely on collective movement of cancer cells with different subpopulations of the tumour represented in such migrating colonies.⁴³ It has been observed that metastatic breast cancer cells have the ability to coax non-metastatic cells into taking on the appearance and abilities of metastatic cells. In an compelling study using fluorophores to prove the presence of biomolecule transfer via extracellular vesicles, it was shown that the transfer of biomolecules from malignant, metastatic MDA-MB-231 cells to the less malignant T47D cells conferred a migratory phenotype on the recipient cells.^{80,123} It is thus likely that MDA-MB-231 cells can transfer molecules that promote a migratory, and thus, anti-proliferative state in recipient cells.

In this report, we tested the hypothesis that MDA-MB-231 cells can transfer molecules that will inhibit cell proliferation. Firstly, we analysed cell proliferation by measuring cell number at different timepoints using crystal violet as a quantifiable cell stain. This method is easy but depends on washing the cells a number of times which may wash away some cells that are weakly attached potentially skewing the results. Also, no distinction can be made between induction of cell death or inhibition of proliferation using this analysis. Neither does it directly measure proliferation itself, to accurately speak to this, assessment of proliferative markers or DNA content is necessary. Nonetheless, the assay gives a good indication of cell survival and/proliferation over time. Conditioned medium was generated by culturing densely growing cells in serum-free medium and harvesting this after 48h. We compared the conditioned medium generated from the highly malignant MDA-MB-231 to the migratory but poorly metastatic MCF7 to the non-metastatic and poorly malignant BT20 breast cancer cell lines as we believe this in some way may mimic the heterogeneity one would encounter within a breast tumour. When BT20 cells were treated with conditioned medium from MDA-MB-231, cell numbers increased at a slower rate

than those cells grown in serum-free medium only, or those treated with BT20-CM. In fact, BT20-CM increased the proliferation rate somewhat.

Thus, MDA-MB-231 cells seem to produce anti-proliferative factors that affect BT20 cell survival or proliferation. The anti-proliferative effect was specific to the highly malignant MDA-MB-231 cell line as treatment of BT20 cells with conditioned medium from the migratory, but poorly metastatic MCF7 cell line did not significantly alter BT20 proliferation or survival. To test if the anti-proliferative effect of the MDA-CM was specific to the non-metastatic epithelial-like cancer cells or more general, MCF7 cells were also exposed to this conditioned medium. No significant result was observed. Moreover, BT20-CM also did not affect MDA-MB-231 cell proliferation. Thus, our data suggests malignant metastatic breast cancer cells can reduce cell proliferation of cancer cells that are in an epithelial state. By doing so they may be removing one of the hurdles for the epithelial cancer cells to become more migratory. Notably, the T47D cell line is an epithelial one, and when Donnarumma *et al* looked at proliferation, migration and invasion effects, they found that the epithelial cell type is most likely affected, similar to what we observed and hypothesized.¹²³ Future works could examine the proliferation, migration and invasion effects on a wider range of different breast cancer lines or primary cell lines to further interrogate this theory, attempting to tease out which cell types or lines are most responsive and why, in turn, establishing the possible mechanism.

An important caveat when assessing effects of conditioned medium is the potential effect of nutrition depletion on cell growth. Different cell lines will display different metabolic rates with highly metabolic cell lines diminishing the nutrient load of medium faster than slower growing cell lines.^{18,124-125} Others have generated conditioned medium by allowing cells to reach confluence and subsequently the medium was changed to serum-free media and cells were then grown in hypoxic conditions (2% O₂, 5% CO₂) for 72 hrs.¹²⁴ In contrast, Takeuchi *et al* generated conditioned medium in a more similar way than we did here by allowing cells to reach 80% confluence before conditioning serum-free media for 48hrs. Moreover, the authors also explore media depletion as a possible confounding variable.¹²⁶ While they found that the presence of mesenchymal stem cell (MSC) derived exosomes promoted cellular migration within human bone marrow derived mesenchymal stem cell (hMSC), they

found a negligible effect of media depletion.¹²⁴⁻¹²⁶ Our studies always include conditioned medium generated from the target cell. For instance, when assessing BT20 cell growth, a control of BT20 cells exposed to BT20 conditioned medium is included to account for possible medium depletion effects. Our data suggests that medium depletion is not a significant factor since BT20 conditioned medium did not inhibit cell proliferation when compared to cells grown in serum-free medium. Thus, any effect observed can reliably be relayed to factors or vesicles secreted by the donor cells into the medium.

While crystal violet-based analysis can indicate effects of proliferation or survival, it is a limited analysis and can be easily misinterpreted. We therefore performed further analyses to understand exactly how the MDA-CM affected BT20 cell proliferation or survival. Cell health was assessed by measuring cellular metabolism through the quantification of resazurin reduction. Unlike with the crystal violet assay, BT20 cellular metabolism, as quantified by resazurin reduction, did not change when cells were exposed to MDA-CM. Cells exposed to serum did however have a higher metabolism compared to the serum-free exposed cells indicating that cells do respond to the growth factors in the serum by increasing their metabolism and confirming the validity of the assay for measuring cellular metabolism. The data suggests that there may be a combination of soluble factors and extracellular vesicles are responsible for the anti-proliferative effect of MDA-MB-231 conditioned medium on BT20 cells. However, it is also possible that the processing of the conditioned medium negatively impacts on this ability. Another possibility, especially when interrogating the differences between the crystal violet and resazurin data is that MDA-CM only triggers cellular detachment leading to apoptosis within the BT20 cell line, which is then interpreted as a decrease in cellular proliferation via the crystal violet assay although not necessarily due to proliferation or cell number, the resazurin assay consists of less washing steps so the detached cells acted upon by MDA-CM are not lost in the assay, with the microscopy data possibly supporting this via the observed increase in cell rounding and apoptosis (see section 4.4). Unfortunately, crystal violet assays with the fractionated medium were not carried out prohibiting us from determining if soluble factors or extracellular vesicles are responsible for the effect on BT20 proliferation or survival.

5.2 MDA-CM induces cellular rounding and the appearance of apoptotic bodies

To further investigate the effect of the conditioned medium on BT20 cells, cell morphology was classified over time to identify if there is a specific change in morphology. An inverted light microscope with climate control was used to generate images over time for this experiment and ImageJ software was used for the analysis. Morphology of individual cells were classified as (i) having cellular protrusions - meaning the cells are well attached, spread and form protrusions indicating activity. This is most common in healthy cells growing in sub-confluent density. (ii) Being rounded - cells in this class would be highly refractive or bright with a small cell body and no protrusions. This state indicates that a cell is dividing or is retained in mitosis or is in the early process of dying through apoptosis. (iii) Having apoptotic bodies - while not always easy to observe, the presence of multiple small amoeboid bodies around the larger cell body is suggestive of a cell in late apoptosis. Our data showed that conditioned medium from BT20 cells had no effect on the prevalence of the three classes when compared to cells grown in serum conditions. This was expected as it has been previously reported in literature that cells exposed to conditioned medium from the same cell line do not suffer adverse effects.¹²⁴ In contrast, MDA-MB-231 conditioned medium exposure induced a gradual decrease in the prevalence of cells with cellular protrusions while both rounded cells and cells with apoptotic bodies increased. Since there is an increase in rounded and apoptotic cells rather than no increase, we can conclude that the conditioned medium does not merely inhibit proliferation but may in fact be inducing apoptosis. Thus, the crystal violet results together with this data point to a pro-apoptotic effect of the medium on BT20 cells.

5.3 MDA-MB-231 conditioned medium induces BT20 cells to exit the cell cycle

Cells, including cancer cells, progress through the cell cycle to proliferate through division.¹²⁷ Inherent control mechanisms in healthy cells will induce cell cycle exit or senescence when signalled to do so. In contrast, cancer cells override these controls to become immortalised which results in continuous proliferation. This process can be influenced by external signals such as growth factors. This may result in increased proliferation or it could induce cell cycle exit or apoptosis.¹²⁸ As we have seen that BT20 cells become rounded and display apoptotic bodies in increasing numbers when

they are exposed to MDA-CM. We hypothesised that this phenomenon is related to an increase in cell death and a reduction in cells actively progressing through the cell cycle. Indeed, cell cycle analysis indicates that when BT20 cells were treated with MDA-CM more cells were present in the sub-G1 phase when compared to cells exposed to serum-free medium. Additionally, the percentage of cells in G1/S are reduced. Together, these data suggest that cells are blocked at the G1 phase leading to their exit into G0. Exit into G0 and blockage of G0/1 does eventually lead to apoptosis which correlates with the cell morphology analysis. We therefore suggest that components present in the MDA-CM induce cell cycle exit and apoptosis. However, additional analysis needs to be done to definitively prove that apoptosis is indeed activated. Having ruminated on the data, if the time constraint created by the pandemic was absent, doing fractionation experiments on all the assays in which differences were observed, crystal violet or cell cycle analysis via flow cytometry for example, would be the next step, a result such as only the pellet fraction triggering a physiological change would not only direct the future studies on isolating the causative agent but it would also shed more light on media depletion.

Exposure of BT20 cells to BT20-CM resulted in an increase of cells in S phase. As we saw a small but significant increase in cell number under these conditions using crystal violet analysis, we propose that BT20-CM increases cell proliferation marginally. Interestingly, we did not observe a difference in cell cycle progression of MDA-MB-231 cells when in serum-free medium vs. serum containing medium. While we cannot point to a specific reason it may be that MDA-MB-231 cells are so adept at survival that the loss of serum does not alter the cell cycle at least in the timeframe measured here.

How could MDA-MB-231 cells induce apoptosis in BT20 cells? It has previously been shown that proneurotrophins such as pro-bone derived neurotrophic factor (pro-BDNF) can induce cell death, whilst cleaved mature neurotrophins such as BDNF promote cell survival.¹²⁹⁻¹³⁰ Dorandish *et al* and Alhusban *et al* showed that MDA-MB-231 cells secrete both the precursor neurotrophin pro-brain derived neurotrophic factor (pro-BDNF) and BDNF into medium. Furthermore, they showed that the secreted pro-BDNF, but not BDNF, inhibited migration and tube formation of endothelial cells. Similarly, proBDNF or other neurotrophins secreted by MDA-MB-231 cells could affect

cell survival. We could not assess whether there was also an effect of conditioned media on BT20 cell migration since these cells are epithelial-like and do not migrate to any significant extent. Conversely, MDA-MB-231 cells do migrate well. We analysed whether the non-migratory BT20 cells could affect MDA-MB-231 cell migration but the movement into the cell free zone with the scratch assay was not significantly altered when compared to cells in serum-free medium. While effects on cell migration were difficult to study using the wound healing assay, we did investigate if conditioned medium exposure could lead to altered actin cytoskeleton organisation and focal adhesion distribution as potential precursors for migratory effects. Confocal microscopy using a stain for actin and fluorophore conjugated antibodies directed against focal adhesion kinase showed no clear changes with small focal adhesions present throughout the cells connected to actin fibers. Thus, our data suggests an effect directed to induce cell cycle exit and possibly apoptosis but not at migration. Earlier, (see Section 5.1), we hypothesized that the MDA-CM could possibly be transferring biomolecules that promote a migratory, and thus anti-proliferative state in recipient cells as seen for the T47D cell line, but interestingly, the data showing the promotion of cell cycle exit and possibly apoptosis suggests otherwise.^{80,123} Therefore, the MDA-CM conveying an anti-proliferative message on epithelial cell types developing to it impacting different cell lines differently is an interesting and possible route of investigation for future studies.

5.4 Extracellular vesicles transfer biomolecules from MDA-MB-231 to BT20 cells

While the preceding experiments show that contents of the conditioned medium affect cell survival, they lack the resolution to directly show transfer of biomolecules (whether soluble or in vesicles) from the donor cells to the recipient cells. Furthermore, it is of use to have proof of transfer to cells to allow researchers to be able to link transfer and physiological output in individual cells. A system to detect biomolecule transfer to specific cells was established by Jacco van Rheenen and has been used to show that biomolecules are transferred between tumour and non-tumour cells. Moreover, transfer can also occur between different tumour cells with subsequent phenocopying of the donor cell by the recipient cell.^{80,131} This is possible due to the transfer of molecules such as miRNA, mRNA and proteins in extracellular vesicles that can exercise a function once taken up by the recipient cell. The detection system depends

on a switchable fluorophore in the recipient cell and a Cre recombinase expressed in the donor cell that will act as the switch once it enters the recipient cell.⁸⁰

In this study we generated an inducible MDA-MB-231 cell line for Cre recombinase expression and a BT20 recipient fluorophore switch cell line to allow us to visualise transfer of Cre recombinase from the MDA-MB-231 cells to the BT20 cells. We hypothesised that, since we see that MDA-MB-231 cells produce factors that induce BT20 cell apoptosis, this should be dependent on transfer of biomolecules. Indeed, exposure of monolayers of BT20 cells to conditioned medium of induced MDA-MB-231 Cre cells, resulted in the appearance of cells with GFP expression while the conditioned medium from uninduced MDA-MB-231 Cre cells did not result in the appearance of GFP positive BT20 cells. Thus, the conditioned medium of MDA-MB-231 cells carries biomolecules that are taken up by BT20 cells. This points to a potential pathway for entry of factors that can induce apoptosis in these cells. We confirmed that transfer takes place by co-culturing the donor and recipient cells in the presence of 4HT. This resulted in the appearance of a small number of GFP-positive cells indicating transfer of Cre recombinase took place. It is clear that transfer is not very efficient since only a small number of cells are positive. Moreover, in the co-culture model the positive cells are not uniformly spread but are mostly located close to each other. Several factors could be playing a role in these observations. Firstly, it could be that the induction of Cre recombinase is inefficient. This may be due to heterogeneity in the MDA-MB-231 Cre cell line which could be caused by less-than-optimal selection. Alternatively, expression levels of Cre in this cell line could be too low to efficiently produce extracellular vesicles containing Cre recombinase. Alternatively, it could be that Cre recombinase transfer happens soon after induction of expression and the recipient BT20 cell divides after the dsRed gene has been excised giving rise to daughter cells expressing GFP. Lastly, it is possible that once one cell absorbs Cre recombinase containing vesicles, the enzyme is distributed to neighbouring cells via gap junctions.

In vitro co-cultures of different cancer cellular types are vital to the investigation of numerous scientific questions.¹³² Two-dimensional cell monolayers provide simplicity and convenience during cancer and drug research but there is a need for extrapolation when analysing the data in relation to the solid tumour.¹³²⁻¹³⁴ Most of the limitations are rooted in a lack of reproducibility, for example, in the organisation of the

cytoskeleton or the inadequate portrayal of the complex cell-to-substrate interactions, resulting in failure to predict clinical efficacy.¹³⁴⁻¹³⁶ Literature shows that 3D cultures (spheroids) better recapitulate the complex *in vivo* microenvironment of the solid tumour.¹³¹⁻¹³⁶ They more accurately depict signalling pathways, gene expression patterns and the effect of drug testing/evaluation.^{132,137} For example, the presence of the extracellular matrix not only offers mechanical support but additionally directs cellular behaviour.^{133,135} We hypothesized that the colour switch system would be reproducible within 3D cultures and, in accordance with previous literature, there would be an increased efficiency within the system in comparison to the 2D cultures. Our data shows that the colour switch can indeed be reproduced within spheroids, including its' inducible nature with the presence and absence of tamoxifen. The degree to which colour switching occurs seems more prevalent in comparison to the 2D samples but more quantitative data is needed to reach a conclusion in this regard. Interestingly, the cells that have undergone colour switching were in close proximity to one another as was observed within 2D co-cultures.

CHAPTER 6 CONCLUSION

6. CONCLUSION

It is clear that tumours are heterogeneous collections of subpopulations that wax and wane according to their adaptation to the current environment. However, the understanding of the interaction between these groups is still unclear. Previous studies show that cancer cells can induce phenocopying in adjacent cells through the process of extravesicular transfer of biomolecules.¹³⁸⁻¹³⁹

In this study we sought to show that communication does take place between similar, but not identical, breast cancer cell lines and that this communication can have physiological effects on the recipient cell. Indeed, we achieved our aim through showing that a metastatic cell line (MDA-MB-231) can exclusively induce apoptosis or cell cycle exit in a non-metastatic breast cancer cell line (BT20), as shown by the lack of anti-proliferative effects in the metastatic MCF7 cell line. Moreover, we show that extracellular vesicle mediated biomolecule transfer does take place between the donor MDA-MB-231 cell line and the recipient BT20 cell line. These data therefore demonstrate that cell-to-cell communication between different types of breast cancer cells can alter their cellular physiology. Important questions remain however:

1. What molecules produced by the MDA-MB-231 cell line initiate cell cycle exit and apoptosis in BT20 cells?
2. How are these molecules transferred between the two cell lines?
3. Why does the MDA-MB-231 cell line produce pro-apoptotic molecules?
4. What other molecules are transferred between the two cell lines?
5. Most importantly, is this system present in in vivo tumours and can it have an effect on tumour progression?

This study has provided a first glimpse at a potentially interesting phenomenon and it has established tools with which further research can be carried out. Initially, the communication of neoplastic cells affecting one another's' metastatic aptitude as possible therapeutic targets was a possible avenue of progression for this study, but interestingly, the induction of cell cycle exit along with the raising of the above questions provide another possible avenue, one where we can expand on how different breast cancer cell lines can affect other breast cancer cell lines and types. If it proves fruitful, maybe how neoplastic prostate cancer cell lines, for example, can

impact or be impacted by breast cancer cell lines. That and the isolation of the biomolecules inducing cell cycle exit. With these as possible future studies, the above mentioned questions could be answered through mass spectroscopy to determine the type of molecules produced, contrasting possible modes of communication (direct contact versus nanotubules versus vesicles i.e.) and shifting to investigating communication in 3D cultures for they better recapitulate the tumour microenvironment.

CHAPTER 7 REFERENCES

7. REFERENCES

1. Lukong KE. Understanding breast cancer - the long and winding road. *BBA Clin.* 2017; 7:64-77.
2. Bray F, Ferlay J, Soerjomataram I, Siegel RL, Torre LA, Jemal A. Global cancer statistics 2018: Globocan estimates of incidence and mortality worldwide for 36 cancers in 185 countries. *CA Cancer J Clin.* 2018; 68(6):394-424.
3. Sudhakar A. History of cancer, ancient and modern treatment methods. *J Cancer Sci Ther.* 2009; 1(2):1-4.
4. Hanahan D, Weinberg RA. Hallmarks of cancer: The next generation. *Cell.* 2011; 144(5):646-74.
5. Bogenrieder T, Herlyn M. Axis of evil: Molecular mechanisms of cancer metastasis. *Oncogene.* 2003; 22(42):6524-36.
6. Hanahan D, Weinberg RA. The hallmarks of cancer. *Cell.* 2000; 100, 57-70
7. Pan Z, Xing X. Brca mutations in the manifestation and treatment of ovarian cancer. *Oncotarget.* 2017; 8(57).
8. Theodoratou E, Timofeeva M, Li X, Meng X, Ioannidis JPA. Nature, nurture, and cancer risks: Genetic and nutritional contributions to cancer. *Annu Rev Nutr.* 2017; 37:293-320.
9. Plaks V, Kong N, Werb Z. The cancer stem cell niche: How essential is the niche in regulating stemness of tumor cells? *Cell Stem Cell.* 2015; 16(3):225-38.
10. Ren Z, Li Y, Hameed O, Siegal GP, Wei S. Prognostic factors in patients with metastatic breast cancer at the time of diagnosis. *Pathol Res Pract.* 2014; 210(5):301-6.
11. Caon I, Bartolini B, Parnigoni A, Carava E, Moretto P, Viola M, et al. Revisiting the hallmarks of cancer: The role of hyaluronan. *Semin Cancer Biol.* 2020; 62:9-19.
12. Chiodoni C, Di Martino MT, Zazzeroni F, Caraglia M, Donadelli M, Meschini S, et al. Cell communication and signaling: How to turn bad language into positive one. *J Exp Clin Cancer Res.* 2019; 38(1):128.
13. C; FYA. Revisiting the hallmarks of cancer *American journal of cancer research.* 2017; 7(5):1016-36.
14. Gilmore A, King L. Emerging approaches to target mitochondrial apoptosis in cancer cells. *F1000Res.* 2019; 8.
15. Jan R, Chaudhry GE. Understanding apoptosis and apoptotic pathways targeted cancer therapeutics. *Adv Pharm Bull.* 2019; 9(2):205-18.
16. E AAA. Apoptosis insight into stages extrinsic and intrinsic pathways. *Open Science Journal of Clinical Medicine.* 2019; 7(3):80-2.
17. Sharma A, Boise LH, Shanmugam M. Cancer metabolism and the evasion of apoptotic cell death. *Cancers (Basel).* 2019; 11(8).
18. Nenclares P, Harrington KJ. The biology of cancer. *Medicine.* 2020; 48(2):67-72.
19. Jayatilleke KM, Hulett MD. Heparanase and the hallmarks of cancer. *J Transl Med.* 2020; 18(1):453.
20. Shen Z. Genomic instability and cancer: An introduction. *J Mol Cell Biol.* 2011; 3(1):1-3.

21. Pikor L, Thu K, Vucic E, Lam W. The detection and implication of genome instability in cancer. *Cancer Metastasis Rev.* 2013; 32(3-4):341-52.
22. Abbas T, Keaton MA, Dutta A. Genomic instability in cancer. *Cold Spring Harb Perspect Biol.* 2013; 5(3):a012914.
23. Mehrotra S, Mitra I. Origin of genome instability and determinants of mutational landscape in cancer cells. *Genes (Basel).* 2020; 11(9).
24. Labi V, Erlacher M. How cell death shapes cancer. *Cell Death Dis.* 2015; 6:e1675.
25. Letai A. Apoptosis and cancer. *Annual Review of Cancer Biology.* 2017; 1(1):275-94.
26. Stahler A, Stintzing S, von Einem JC, Westphalen CB, Heinrich K, Kramer N, et al. Single-nucleotide variants, tumour mutational burden and microsatellite instability in patients with metastatic colorectal cancer: Next-generation sequencing results of the FIRE-3 trial. *Eur J Cancer.* 2020; 137:250-9.
27. Nakamura K, Smyth M, Martinet L. Cancer immunoediting and immune dysregulation in multiple myeloma. *American society of Haematology.* 2020; 136(24):2731-40.
28. Garg AD, Agostinis P. Cell death and immunity in cancer: From danger signals to mimicry of pathogen defense responses. *Immunol Rev.* 2017; 280(1):126-48.
29. Yaswen P, MacKenzie KL, Keith WN, Hentosh P, Rodier F, Zhu J, et al. Therapeutic targeting of replicative immortality. *Semin Cancer Biol.* 2015; 35 Suppl:S104-S28.
30. Nishida N, Yano H, Nishida T, Kamura T, Kojiro M. Angiogenesis in cancer. *Vascular health and risk management.* 2006; 2(3):213-9.
31. Rajabi M, Mousa SA. The role of angiogenesis in cancer treatment. *Biomedicines.* 2017; 5(2).
32. Lugano R, Ramachandran M, Dimberg A. Tumor angiogenesis: Causes, consequences, challenges and opportunities. *Cell Mol Life Sci.* 2020; 77(9):1745-70.
33. Piotrowski I, Kulcenty K, Suchorska W. Interplay between inflammation and cancer. *Rep Pract Oncol Radiother.* 2020; 25(3):422-7.
34. Siriwarin B WB. Roles of reactive oxygen species (ros) in inflammation and cancer. *Rangsit Journal of Arts and Sciences.* 2014; 4(2).
35. Mantovani A, Allavena P, Sica A, Balkwill F. Cancer-related inflammation. *Nature.* 2008; 454(7203):436-44.
36. Thiery JP, Acloque H, Huang RY, Nieto MA. Epithelial-mesenchymal transitions in development and disease. *Cell.* 2009; 139(5):871-90.
37. Ananthakrishnan RE, A;. Ananthakrishnan2007 the forces behind cell movement. *International Journal of Biological Sciences.* 2007.
38. Eslami-S Z, Cortés-Hernández LE, Alix-Panabières C. The metastatic cascade as the basis for liquid biopsy development. *Frontiers in Oncology.* 2020; 10.
39. Ocana OH, Corcoles R, Fabra A, Moreno-Bueno G, Acloque H, Vega S, et al. Metastatic colonization requires the repression of the epithelial-mesenchymal transition inducer prrx1. *Cancer Cell.* 2012; 22(6):709-24.
40. Du B, Shim JS. Targeting epithelial-mesenchymal transition (emt) to overcome drug resistance in cancer. *Molecules.* 2016; 21(7).
41. Neelakantan D, Zhou H, Oliphant MUJ, Zhang X, Simon LM, Henke DM, et al. Emt cells increase breast cancer metastasis via paracrine gli activation in neighbouring tumour cells. *Nat Commun.* 2017; 8:15773.
42. van Zijl F, Krupitza G, Mikulits W. Initial steps of metastasis: Cell invasion and endothelial transmigration. *Mutat Res.* 2011; 728(1-2):23-34.

43. Fares J, Fares MY, Khachfe HH, Salhab HA, Fares Y. Molecular principles of metastasis: A hallmark of cancer revisited. *Signal Transduct Target Ther.* 2020; 5(1):28.
44. Lambert AW, Pattabiraman DR, Weinberg RA. Emerging biological principles of metastasis. *Cell.* 2017; 168(4):670-91.
45. Angadi P, Kale A. Epithelial-mesenchymal transition - a fundamental mechanism in cancer progression: An overview. *Indian Journal of Health Sciences.* 2015; 8(2).
46. Moustakas A, Heldin CH. Mechanisms of tgfbeta-induced epithelial-mesenchymal transition. *J Clin Med.* 2016; 5(7).
47. Wang L, Saci A, Szabo PM, Chasalow SD, Castillo-Martin M, Domingo-Domenech J, et al. Emt- and stroma-related gene expression and resistance to pd-1 blockade in urothelial cancer. *Nat Commun.* 2018; 9(1):3503.
48. Tsubakihara Y, Moustakas A. Epithelial-mesenchymal transition and metastasis under the control of transforming growth factor beta. *Int J Mol Sci.* 2018; 19(11).
49. Jolly MK, Ware KE, Gilja S, Somarelli JA, Levine H. Emt and met: Necessary or permissive for metastasis? *Mol Oncol.* 2017; 11(7):755-69.
50. Battle E, Sancho E, Franci C, Dominguez D, Monfar M, Baulida J, Garcia de Herreros A. The transcription factor snail is a repressor of e-cadherin gene expression in epithelial tumour cells. *Nature Cell Biology.* 2000; 2(2).
51. Yang J, Mani SA, Donaher JL, Ramaswamy S, Itzykson RA, Come C, et al. Twist, a master regulator of morphogenesis, plays an essential role in tumor metastasis. *Cell.* 2004; 117(7):927-39.
52. Yoshihara M, Yamakita Y, Kajiyama H, Senga T, Koya Y, Yamashita M, et al. Filopodia play an important role in the trans-mesothelial migration of ovarian cancer cells. *Exp Cell Res.* 2020; 392(2):112011.
53. Yan X, Cao N, Chen Y, Lan HY, Cha JH, Yang WH, et al. Mt4-mmp promotes invadopodia formation and cell motility in fadu head and neck cancer cells. *Biochem Biophys Res Commun.* 2020; 522(4):1009-14.
54. Mondal S, Adhikari N, Banerjee S, Amin SA, Jha T. Matrix metalloproteinase-9 (mmp-9) and its inhibitors in cancer: A minireview. *Eur J Med Chem.* 2020; 194:112260.
55. Franchi M, Piperigkou Z, Riti E, Masola V, Onisto M, Karamanos NK. Long filopodia and tunneling nanotubes define new phenotypes of breast cancer cells in 3d cultures. *Matrix Biol Plus.* 2020; 6-7:100026.
56. Arjonen A, Kaukonen R, Ivaska J. Filopodia and adhesion in cancer cell motility. *Cell Adh Migr.* 2011; 5(5):421-30.
57. Pagès D-L, Dornier E, De Seze J, Wang L, Luan R, Cartry J, et al. Cell clusters adopt a collective amoeboid mode of migration in confined non-adhesive environments. *Oncotarget.* 2020
58. Holle AW, Govindan Kutty Devi N, Clar K, Fan A, Saif T, Kemkemer R, et al. Cancer cells invade confined microchannels via a self-directed mesenchymal-to-amoeboid transition. *Nano Lett.* 2019; 19(4):2280-90.
59. Heerboth S, Housman G, Leary M, Longacre M, Byler S, Lapinska K, et al. Emt and tumor metastasis. *Clin Transl Med.* 2015; 4:6.
60. Paoli P, Giannoni E, Chiarugi P. Anoikis molecular pathways and its role in cancer progression. *Biochim Biophys Acta.* 2013; 1833(12):3481-98.

61. Fofaria NM, Srivastava SK. Stat3 induces anoikis resistance, promotes cell invasion and metastatic potential in pancreatic cancer cells. *Carcinogenesis*. 2015; 36(1):142-50.
62. Luey BC, May FE. Insulin-like growth factors are essential to prevent anoikis in oestrogen-responsive breast cancer cells: Importance of the type I igf receptor and pi3-kinase/akt pathway. *Mol Cancer*. 2016; 15:8.
63. Alvarado-Estrada K, Marenco-Hillebrand L, Maharjan S, Mainardi VL, Zhang YS, Zarco N, et al. Circulatory shear stress induces molecular changes and side population enrichment in primary tumor-derived lung cancer cells with higher metastatic potential. *Sci Rep*. 2021; 11(1):2800.
64. Cai WL, Huang WD, Li B, Chen TR, Li ZX, Zhao CL, et al. MicroRNA-124 inhibits bone metastasis of breast cancer by repressing interleukin-11. *Mol Cancer*. 2018; 17(1):9.
65. Al-Mahmood S, Sapiezynski J, Garbuzenko OB, Minko T. Metastatic and triple-negative breast cancer: Challenges and treatment options. *Drug Deliv Transl Res*. 2018; 8(5):1483-507.
66. Dittmer J. Mechanisms governing metastatic dormancy in breast cancer. *Semin Cancer Biol*. 2017; 44:72-82.
67. Mack GS, Marshall A. Lost in migration. *Nat Biotechnol*. 2010; 28(3):214-29.
68. Budczies J vWM, Klauschen F, Bockmayr M LJ, Denkert C, Wolf T, Warth A DM, Anagnostopoulos I, Weichert W, A WDaS. The landscape of metastatic progression patterns across major human cancers. *Oncotarget*. 2015; 6(1).
69. Holch JW, Demmer M, Lamersdorf C, Michl M, Schulz C, von Einem JC, et al. Pattern and dynamics of distant metastases in metastatic colorectal cancer. *Visc Med*. 2017; 33(1):70-5.
70. Chen MT, Sun HF, Zhao Y, Fu WY, Yang LP, Gao SP, et al. Comparison of patterns and prognosis among distant metastatic breast cancer patients by age groups: A seer population-based analysis. *Sci Rep*. 2017; 7(1):9254.
71. Reiter JG, Makohon-Moore AP, Gerold JM, Bozic I, Chatterjee K, Iacobuzio-Donahue CA, et al. Reconstructing metastatic seeding patterns of human cancers. *Nature Communications*. 2017; 8(1).
72. Goubran HA, Kotb RR, Stakiw J, Emara ME, Burnouf T. Regulation of tumor growth and metastasis: The role of tumor microenvironment. *Cancer Growth Metastasis*. 2014; 7:9-18.
73. Fidler IJ. The pathogenesis of cancer metastasis; the seed and soil hypothesis revisited. *Nature Reviews*. 2003; 3.
74. Fidler IJ, Kim SJ, Langley RR. The role of the organ microenvironment in the biology and therapy of cancer metastasis. *J Cell Biochem*. 2007; 101(4):927-36.
75. Fidler IJ, Kripke ML. The challenge of targeting metastasis. *Cancer Metastasis Rev*. 2015; 34(4):635-41.
76. Owusu-Akyaw A, Krishnamoorthy K, Goldsmith LT, Morelli SS. The role of mesenchymal-epithelial transition in endometrial function. *Hum Reprod Update*. 2019; 25(1):114-33.
77. Hamilton G, Rath B. Mesenchymal-epithelial transition and circulating tumor cells in small cell lung cancer. *Adv Exp Med Biol*. 2017; 994:229-45.
78. Sun J, Li Q, Lian X, Zhu Z, Chen X, Pei W, et al. MicroRNA-29b mediates lung mesenchymal-epithelial transition and prevents lung fibrosis in the silicosis model. *Mol Ther Nucleic Acids*. 2019; 14:20-31.

79. Mason KL, Jonathan; Singer, S;. Biology tenth edition. McGraw-Hill, editor: McGraw-Hill; 2014.
80. Steenbeek SC, Pham TV, de Ligt J, Zomer A, Knol JC, Piersma SR, et al. Cancer cells copy migratory behavior and exchange signaling networks via extracellular vesicles. *EMBO J.* 2018; 37(15).
81. Mattes B, Scholpp S. Emerging role of contact-mediated cell communication in tissue development and diseases. *Histochem Cell Biol.* 2018; 150(5):431-42.
82. Dong A, Liu S, Li Y. Gap junctions in the nervous system: Probing functional connections using new imaging approaches. *Frontiers in Cellular Neuroscience.* 2018; 12:320.
83. Liu W CY, Wei J, Sun J, Zheng L & Xie J. Gap junction-mediated cell-to-cell communication in oral development and oral diseases_ a concise review of research progress. *international journal of oral science* 2020; 12(17).
84. Capaldo CT, Farkas AE, Nusrat A. Epithelial adhesive junctions. *F1000Prime Rep.* 2014; 6:1.
85. Nielsen MS, Axelsen LN, Sorgen PL, Verma V, Delmar M, Holstein-Rathlou NH. Gap junctions. *Compr Physiol.* 2012; 2(3):1981-2035.
86. Campbell HK, Maiers JL, DeMali KA. Interplay between tight junctions & adherens junctions. *Experimental Cell Research.* 2017; 358(1):39-44.
87. Gerdes H PR. Cell to cell communication. Current views and future perspectives. *Cell and Tissue Research* 2013 352:1–3.
88. Nawaz M, Fatima F. Extracellular vesicles, tunneling nanotubes, and cellular interplay: Synergies and missing links. *Front Mol Biosci.* 2017; 4:50.
89. Rustom A SR, Markovic I,. Nanotubular highways for intercellular organelle transport. *Science.* 2004; 303(5660):1007-10.
90. Onfelt B, Purbhoo, M. A., Nedvetzki, S., Sowinski, S., & Davis, D. M. . Long-distance calls between cells connected by tunnelling nanotubules. *Science signaling,* 2005; (313) : 55-9
91. Lou E, Fujisawa S, Morozov A, Barlas A, Romin Y, Dogan Y, et al. Tunneling nanotubes provide a unique conduit for intercellular transfer of cellular contents in human malignant pleural mesothelioma. *PLoS One.* 2012; 7(3):e33093.
92. Gousset K, Marzo L, Commere PH, Zurzolo C. Myo10 is a key regulator of tnt formation in neuronal cells. *J Cell Sci.* 2013; 126(Pt 19):4424-35.
93. Rustom A SR, Markovic I,, Walther P GH. Nanotubular highways for intercellular organelle transport. *Science* 2004; 303(5660):1007-10.
94. Delage E, Cervantes DC, Penard E, Schmitt C, Syan S, Disanza A, et al. Differential identity of filopodia and tunneling nanotubes revealed by the opposite functions of actin regulatory complexes. *Sci Rep.* 2016; 6:39632.
95. Bayraktar R RK, Calin G. Cell-to-cell communication_ micrnas as hormones. *Molecular Oncology.* 2017.
96. Ghoshal P, Singla B, Lin H, Cherian-Shaw M, Tritz R, Padgett CA, et al. Loss of gtpase activating protein neurofibromin stimulates paracrine cell communication via macropinocytosis. *Redox Biol.* 2019; 27:101224.
97. Byrne MB, Trump L, Desai AV, Schook LB, Gaskins HR, Kenis PJ. Microfluidic platform for the study of intercellular communication via soluble factor-cell and cell-cell paracrine signaling. *Biomicrofluidics.* 2014; 8(4):044104.
98. Ansorge M, Pompe T. Systems for localized release to mimic paracrine cell communication in vitro. *J Control Release.* 2018; 278:24-36.

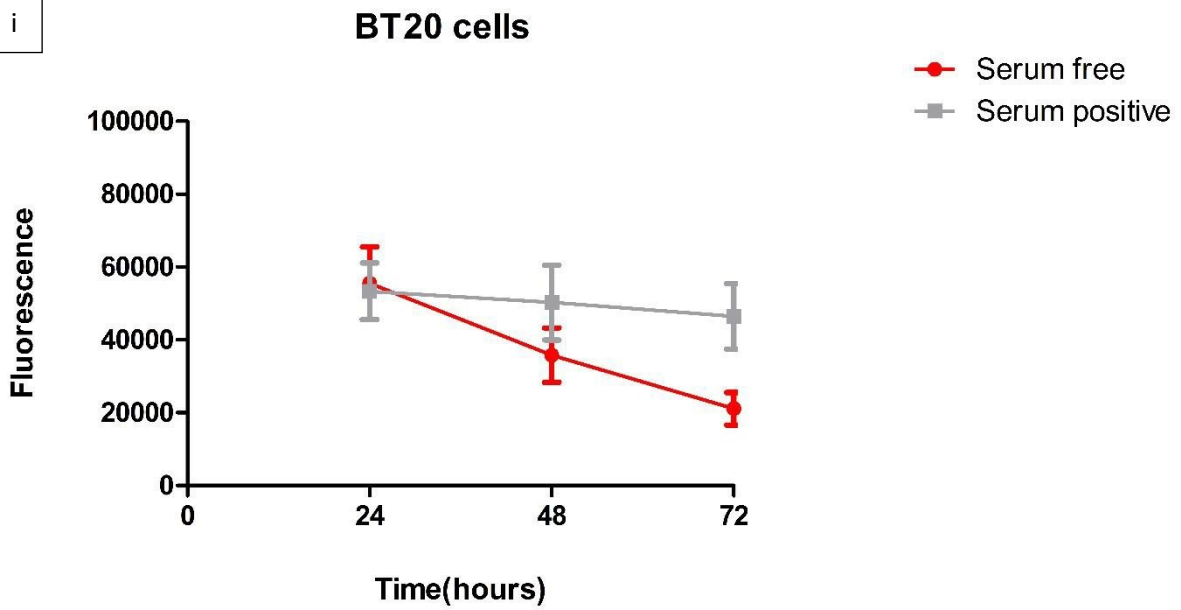
99. Tetta C, Ghigo E, Silengo L, Deregibus MC, Camussi G. Extracellular vesicles as an emerging mechanism of cell-to-cell communication. *Endocrine*. 2013; 44(1):11-9.
100. Cocucci E, Meldolesi J. Ectosomes and exosomes: Shedding the confusion between extracellular vesicles. *Trends Cell Biol*. 2015; 25(6):364-72.
101. Raposo G, Nijman HW, Stoorvogel W, Liejendekker R, Harding CV, Melief CJ, et al. B lymphocytes secrete antigen-presenting vesicles. *J Exp Med*. 1996; 183(3):1161-72.
102. Zaborowski MP, Balaj L, Breakefield XO, Lai CP. Extracellular vesicles: Composition, biological relevance, and methods of study. *Bioscience*. 2015; 65(8):783-97.
103. Dong Gao¹, Lingling Jiang^{2,3*}. Exosomes in cancer therapy: A novel experimental strategy. *American journal of cancer research*. 2018; 8(11):2165-75.
104. Poon IKH, Gregory CD, Kaparakis-Liaskos M. Editorial: The immunomodulatory properties of extracellular vesicles from pathogens, immune cells, and non-immune cells. *Front Immunol*. 2018; 9:3024.
105. Kuipers ME, Hokke CH, Smits HH, Nolte-'t Hoen ENM. Pathogen-derived extracellular vesicle-associated molecules that affect the host immune system: An overview. *Front Microbiol*. 2018; 9:2182.
106. Lapitz A, Arbelaiz A, Olaizola P, Aranburu A, Bujanda L, Perugorria MJ, et al. Extracellular vesicles in hepatobiliary malignancies. *Front Immunol*. 2018; 9:2270.
107. Li P, Kaslan M, Lee SH, Yao J, Gao Z. Progress in exosome isolation techniques. *Theranostics*. 2017; 7(3):789-804.
108. Colombo M, Raposo G, Thery C. Biogenesis, secretion, and intercellular interactions of exosomes and other extracellular vesicles. *Annu Rev Cell Dev Biol*. 2014; 30:255-89.
109. Elia I, Haigis MC. Metabolites and the tumour microenvironment: From cellular mechanisms to systemic metabolism. *Nat Metab*. 2021; 3(1):21-32.
110. Singleton DC, Macann A, Wilson WR. Therapeutic targeting of the hypoxic tumour microenvironment. *Nat Rev Clin Oncol*. 2021; 18(12):751-72.
111. Cummings MC, Simpson PT, Reid LE, Jayanthan J, Skerman J, Song S, et al. Metastatic progression of breast cancer: Insights from 50 years of autopsies. *J Pathol*. 2014; 232(1):23-31.
112. Vuong D, Simpson PT, Green B, Cummings MC, Lakhani SR. Molecular classification of breast cancer. *Virchows Arch*. 2014; 465(1):1-14.
113. Hussein IA, Ahmed ST, Hameedi AD, Naji RZ, Alharbawi L, Alkhaytt M, et al. Immunohistochemical expression of brca1 protein, er, pr and her2/neu in breast cancer: A clinicopathological study. *Asian Pac J Cancer Prev*. 2020; 21(4):1025-9.
114. Lin YC, Boone M, Meuris L, Lemmens I, Van Roy N, Soete A, et al. Genome dynamics of the human embryonic kidney 293 lineage in response to cell biology manipulations. *Nat Commun*. 2014; 5:4767.
115. Chin CL, Goh JB, Srinivasan H, Liu KI, Gowher A, Shanmugam R, et al. A human expression system based on hek293 for the stable production of recombinant erythropoietin. *Scientific Reports*. 2019; 9(1).
116. Mori Y, Yoshida Y, Satoh A, Moriya H. Development of an experimental method of systematically estimating protein expression limits in hek293 cells. *Sci Rep*. 2020; 10(1):4798.
117. Lasfargues E OL. Cultivation of human breast carcinoma. National cancer institute. 1958.

118. Kim KC, Lee EJ. Studies on conditioned media in human cells: Evaluation using various cell and culture conditions, animal disease models. *Journal of Animal Reproduction and Biotechnology*. 2018; 33(1):41-8.
119. Liu X, Li YP, Zhong ZM, Tan HQ, Lin HP, Chen SJ, et al. Incorporation of viral glycoprotein vsv-g improves the delivery of DNA by erythrocyte ghost into cells refractory to conventional transfection. *Appl Biochem Biotechnol*. 2017; 181(2):748-61.
120. Jia H, Fang R, Lin J, Tian X, Zhao Y, Chen L, et al. Evaluation of resazurin-based assay for rapid detection of polymyxin-resistant gram-negative bacteria. *BMC Microbiology*. 2020; 20(1).
121. Montero-Vilchez T, Sierra-Sanchez A, Sanchez-Diaz M, Quinones-Vico MI, Sanabria-de-la-Torre R, Martinez-Lopez A, et al. Mesenchymal stromal cell-conditioned medium for skin diseases: A systematic review. *Front Cell Dev Biol*. 2021; 9:654210.
122. Matus D LL, Kelley L, Schindler A, Kohrman A, Barkoulas M, Zhang W, Chi Q, and Sherwood D. Invasive cell fate requires G1 cell-cycle arrest and histone deacetylase-mediated changes in gene expression. *Developmental Cell*. 2015; 35(2):162-74.
123. Donnarumma E FD, Nappa M, Roscigno G, Adamo A IM, Russo V, Affinito A,, Puoti I QC, Rienzo A, Piscuoglio S, Thomas R CG. Cancer associated fibroblasts release exosomal mirnas that dictate an aggressive phenotype in breast cancer. *Oncotarget*. 2017; 8(12):19592-608.
124. Zhou BR, Xu Y, Guo SL, Xu Y, Wang Y, Zhu F. The effect of conditioned media of adipose-derived stem cells on wound healing after ablative fractional carbon dioxide laser resurfacing. *Biomed Res Int*. 2013; 2013:519126.
125. Takeuchi R KW, Endo S, Kobayashi T. Exosomes from conditioned media of bone marrow-derived mesenchymal stem cells promote bone regeneration by enhancing angiogenesis *PLoS One*. 2019; 14(11).
126. Takeuchi R KW, Endo S, Kobayashi T. Exosomes from conditioned media of bone marrow-derived mesenchymal stem cells promote bone regeneration by enhancing angiogenesis. *PLoS One*. 2019; 14(11).
127. Oshi M TH, ToKumar Y, Yan L, Rashid O. G2m cell cycle pathway score as a prognostic biomarker of metastasis in estrogen receptor (er)-positive breast cancer. *Int J Mol Sci*. 2020; 21:2921.
128. Gookin S MM, Phadke H, Chung M, Moser J, Miller I, Carter, Spencer S. A map of protein dynamics during cell-cycle progression and cell-cycle exit. *PLOS Biology*. 2017; 15(9).
129. Dorandish S AS, Ray R, Al Khashali H, Coleman K, Guthrie J, Heyl D, Evans H. Differences in the relative abundance of probdnf and mature bdnf in a549 and h1299 human lung cancer cell media. *Int J Mol Sci*. 2021; 22:7059.
130. Alhusban L aMAN, Alhusban A. Probdnf is a novel mediator of the interaction between MDA-MB-231 breast cancer cells and brain microvascular endothelial cells. *Current molecular medicine*. 2021; 21(10):914-21.
131. Tkach M, Thery C. Communication by extracellular vesicles: Where we are and where we need to go. *Cell*. 2016; 164(6):1226-32.
132. Nunes AS, Barros AS, Costa EC, Moreira AF, Correia IJ. 3D tumor spheroids as in vitro models to mimic in vivo human solid tumors resistance to therapeutic drugs. *Biotechnol Bioeng*. 2019; 116(1):206-26.

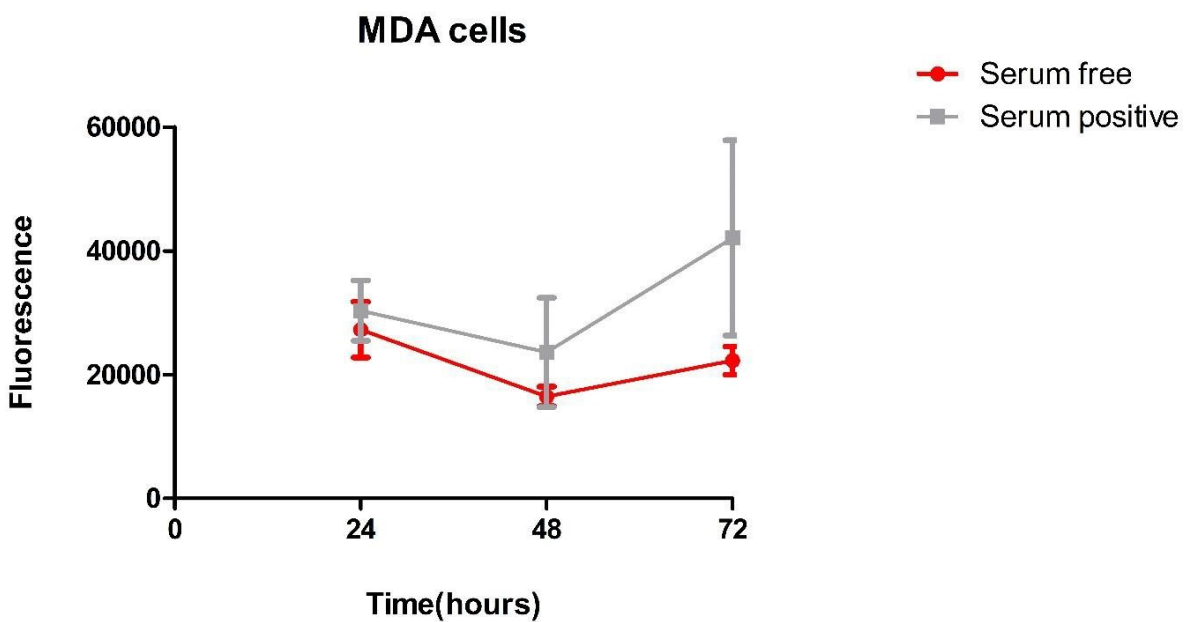
133. Park Y FC, Ryu H, Luan H, Cotton K. Three-dimensional, multifunctional neural interfaces for cortical spheroids and engineered assembloids. *Science advances*. 2021; 7.
134. Dorst N, Oberringer M, Grasser U, Pohlemann T, Metzger W. Analysis of cellular composition of co-culture spheroids. *Ann Anat*. 2014; 196(5):303-11.
135. Cavo M, Fato M, Penuela L, Beltrame F, Raiteri R, Scaglione S. Microenvironment complexity and matrix stiffness regulate breast cancer cell activity in a 3d in vitro model. *Sci Rep*. 2016; 6:35367.
136. Benton G, DeGray G, Kleinman HK, George J, Arnaoutova I. *In vitro* microtumors provide a physiologically predictive tool for breast cancer therapeutic screening. *PLoS One*. 2015; 10(4):e0123312.
137. Tylek T, Schilling T, Schlegelmilch K, Ries M, Rudert M, Jakob F, et al. Platelet lysate outperforms FCS and human serum for co-culture of primary human macrophages and hmscs. *Sci Rep*. 2019; 9(1):3533.
138. Gasser S, Lim LHK, Cheung FSG. The role of the tumour microenvironment in immunotherapy. *Endocr Relat Cancer*. 2017; 24(12):T283-T95.
139. Ho WJ, Jaffee EM, Zheng L. The tumour microenvironment in pancreatic cancer - clinical challenges and opportunities. *Nat Rev Clin Oncol*. 2020; 17(9):527-40.

APPENDIX

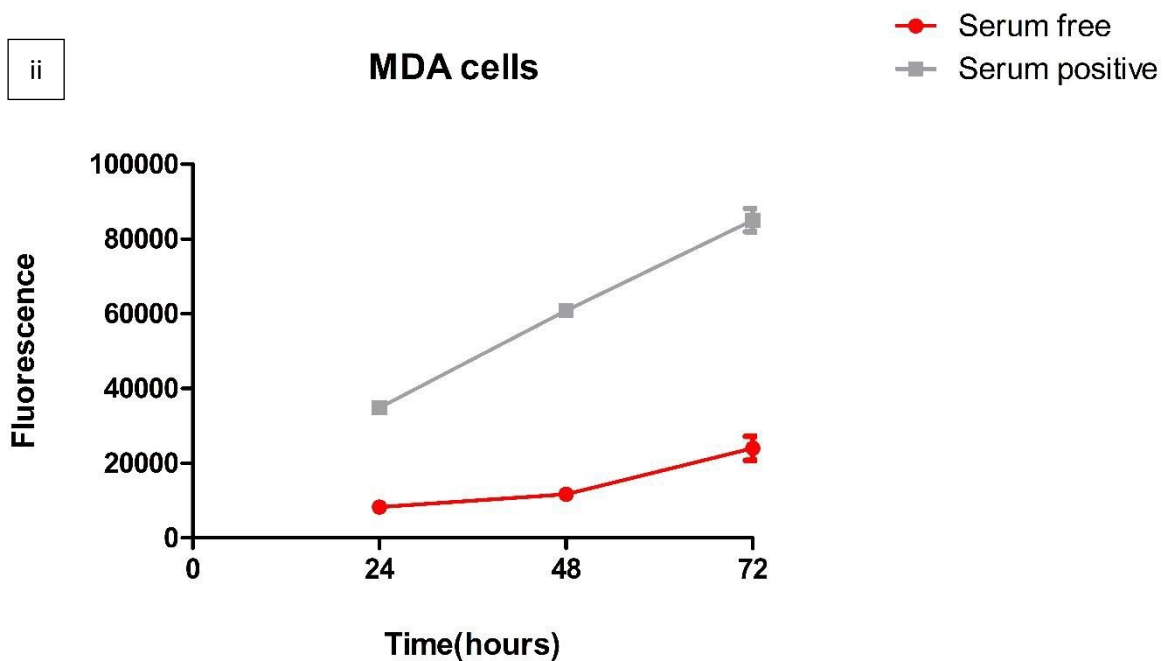
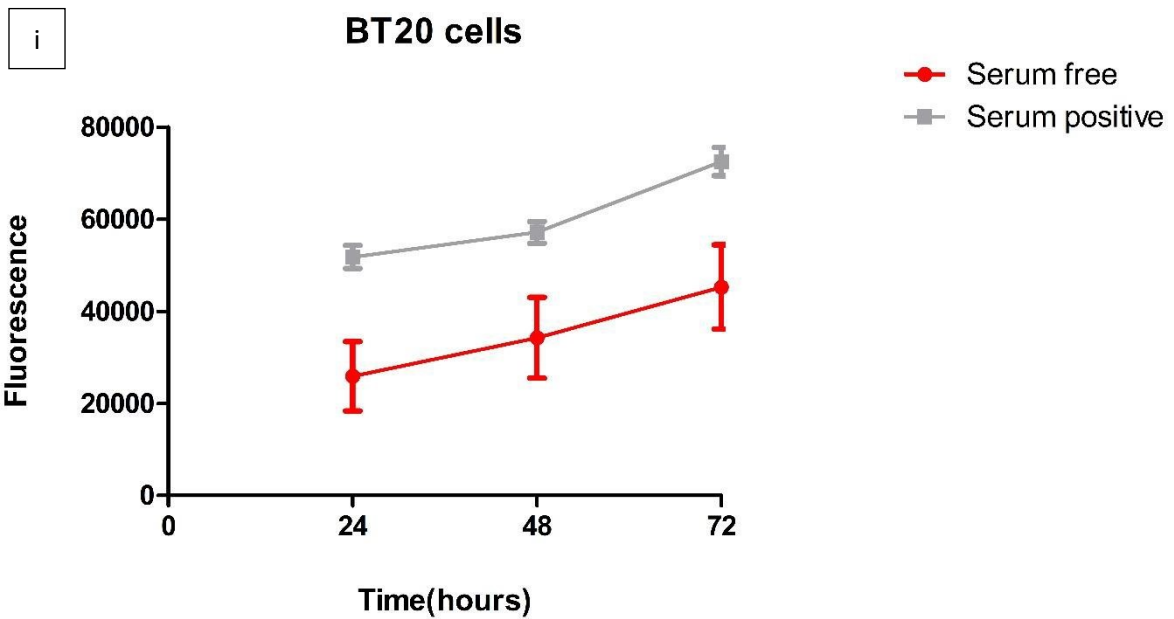
i



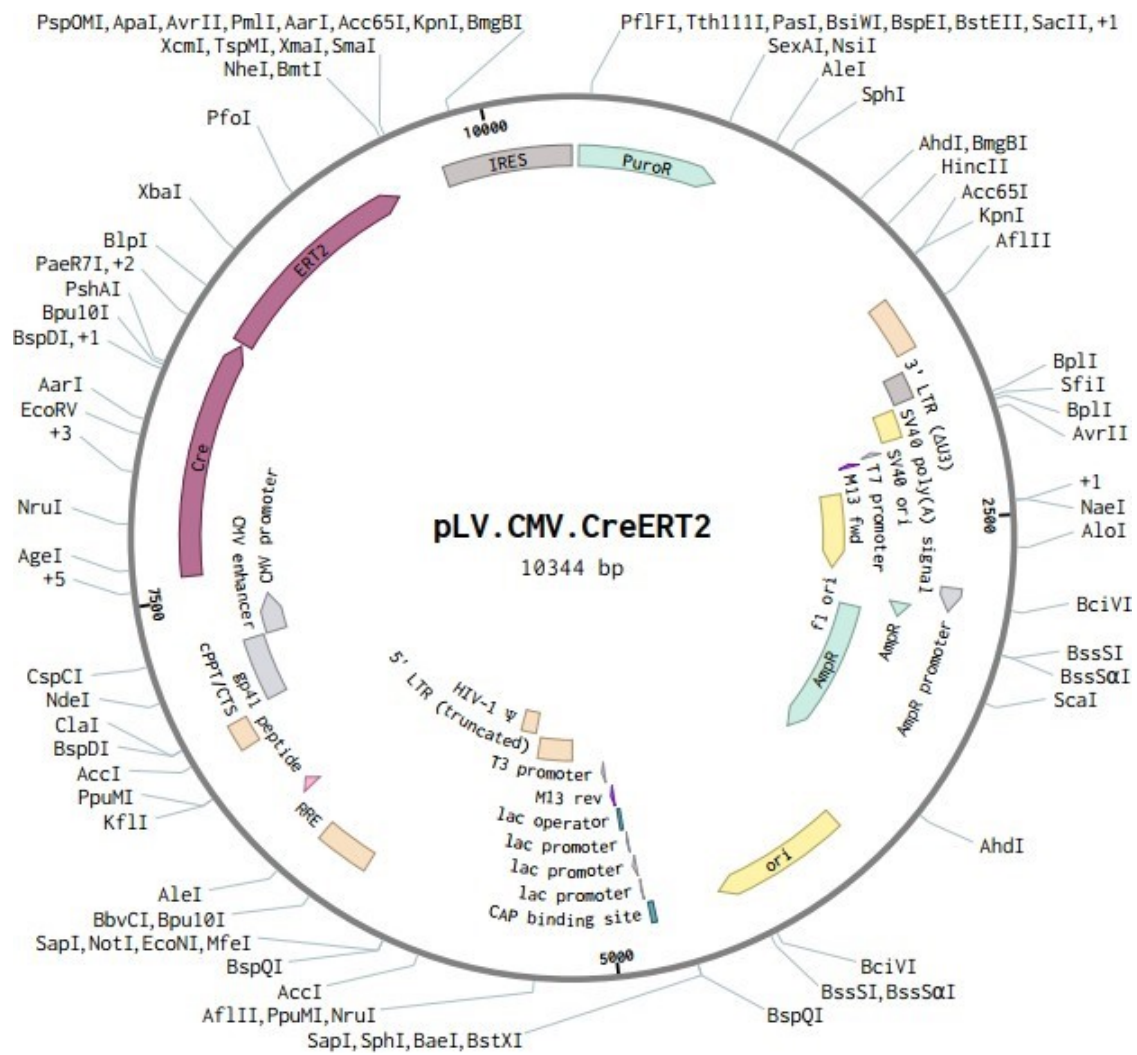
ii



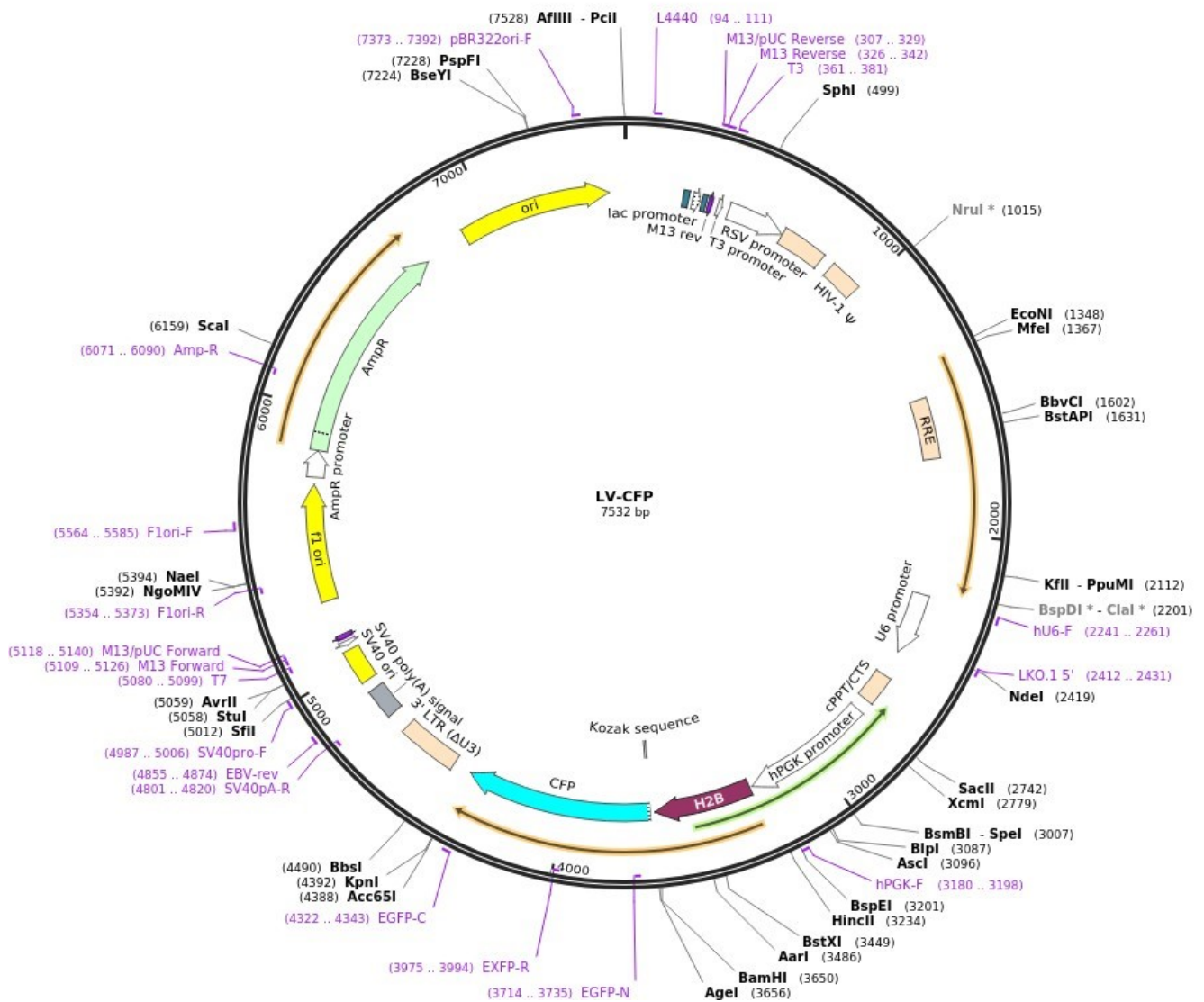
Appendix A: Serum interferes with fluorescence during measurement. *The presence of serum in the media when measuring resazurin fluorescence interferes with the signal. The difference between cells measured in the presence (serum positive) and absence of serum (serum-free) is expected to be higher for BT20 cells (i) and MDA-MB-231 cells (ii).*



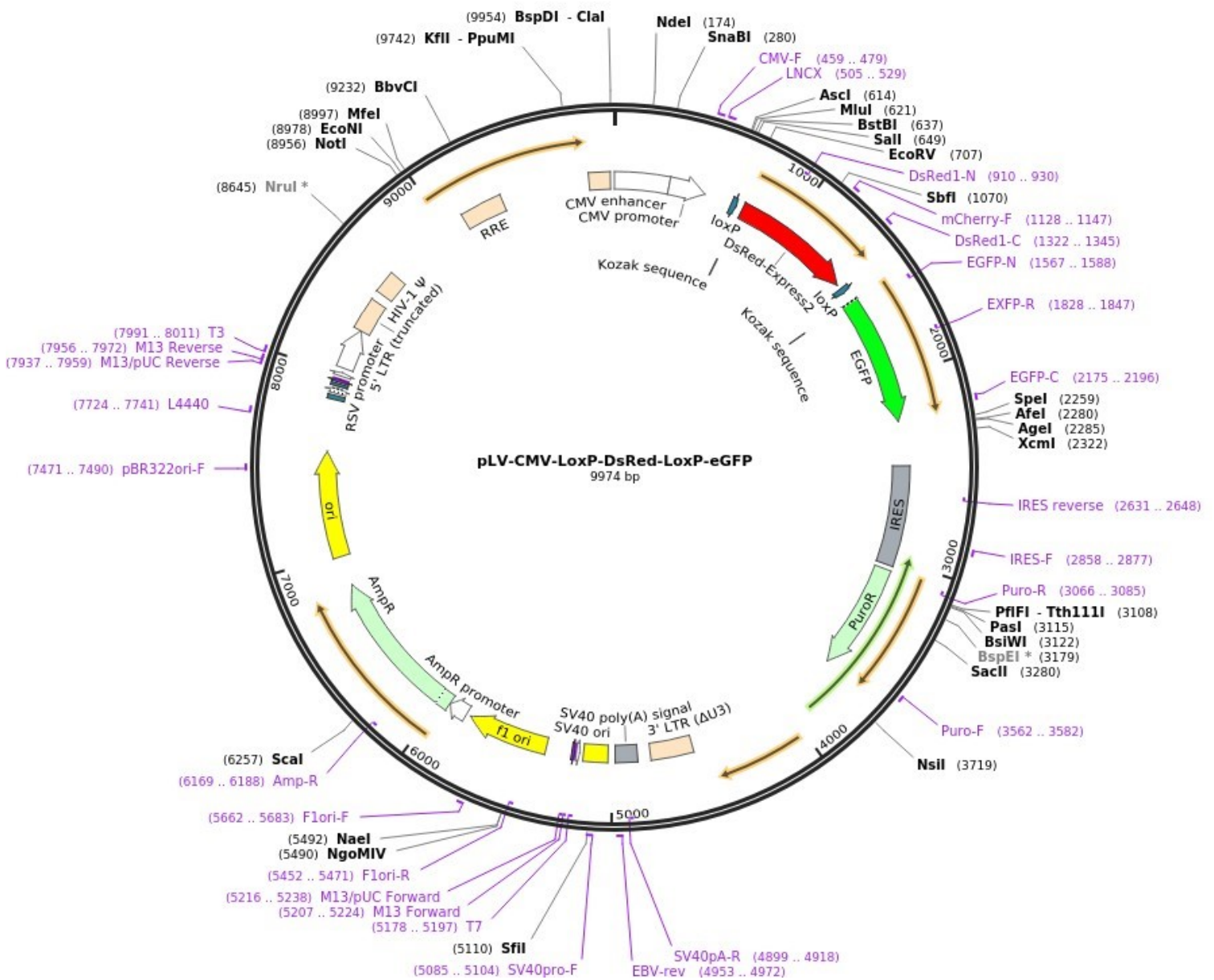
Appendix B: Serum-free media does not affect fluorescence during measurement. *The presence of serum in the media when measuring resazurin fluorescence interferes with the signal. The difference between cells measured in the presence (serum positive) and absence of serum (serum-free) grew for both BT20 (i) and MDA-MB-231 (ii) cells when cells were incubated and metabolism measured.*



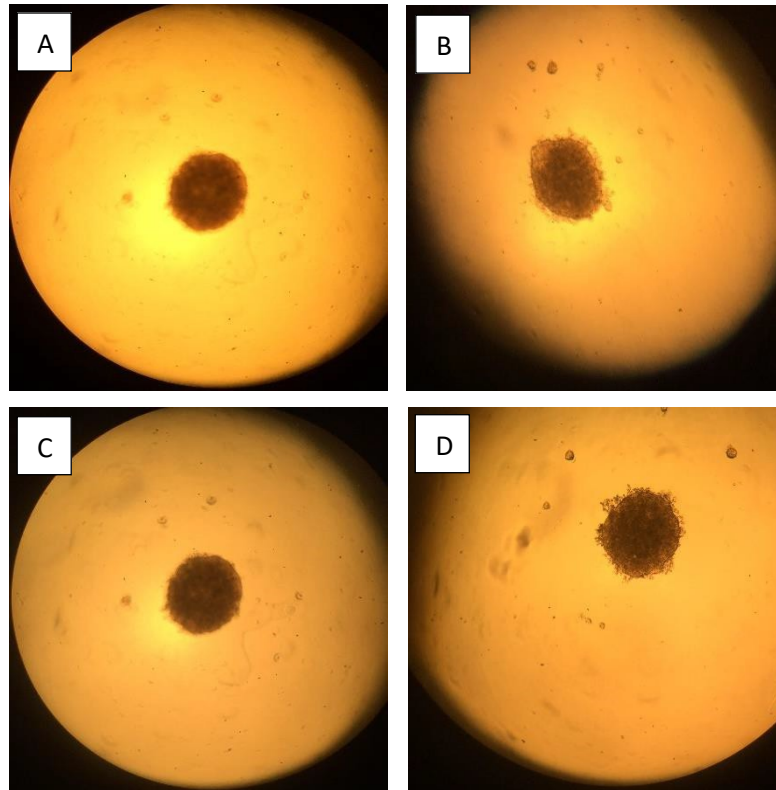
Appendix C: Plasmid map; CreERT2. The plasmid allows for the production of the Cre recombinase enzyme by the donor cell; responsible for the colour switching observed in the recipient cell line. Plasmid inserted into MDA-MB-231 cell line.



Appendix D: Plasmid map; LV-CFP. The plasmid allows for the expression of the Cyan fluorescent protein (CFP) within the donor cell. Plasmid inserted into MDA-MB-231 cell line.



Appendix E: Plasmid map; The switch module. *The plasmid acts as a genetic Cre reporter, switching from expressing DsRed to eGFP upon recombination by the Cre recombinase enzyme. Presenting as the observed cellular colour switching from fluorescing red to green. Plasmid inserted in the BT20 cell line.*



Appendix F: Three dimensional co-cultures. *[A-D] MDA-MB-231:BT20 cell co-culture spheroids at a ratio of 1 to 4 and 10x magnification. Images show different spheroids after a week of growth. The presence of agarose deprives the cells of attachment to the plate and promotes attachment to other cells, resulting in the spherical shape observed.*



UNIVERSITEIT VAN PRETORIA
UNIVERSITY OF PRETORIA
YUNIBESITHI YA PRETORIA

Faculty of Health Sciences

SUBMISSION FORM / RESUBMISSION FORM: MINI-DISSERTATION, DISSERTATION, THESIS
(This form must be submitted together with the copies of the mini-dissertation, dissertation or thesis to the Student Administration office of the faculty)

STUDENT NUMBER: 14218594

Mr LB Pedzisayi
Unit 24
Elwood flats
199 Uys Street
Rynfield, Benoni
Rynfield AH Ext 2
1501
South Africa

(Please print)

Tel:	068 264 3780	Mobile tel: 078 687 9018
Work address:	N/A	
Postal code:	Tel:	

Details of mini-dissertation/dissertation/thesis:

Programme: MSc	Plan: Human Physiology
Department:	CENTRE FOR NEUROENDOCRINOLOGY
Supervisor:	DR J.I. VAN DEN BOUT
Co-supervisor(s):	DR C. NEWTON

Title of the mini-dissertation/dissertation/thesis:

(Exactly as approved by the postgraduate committee including upper case, lower case and punctuation)
The role of cell-to-cell communication in guiding breast cancer cell physiology

Statement by candidate:

1. I am aware that, should the mini-dissertation, dissertation or thesis be accepted, I must submit the additional copies as well as a copy of the draft article (Doctoral students: proof that it has been accepted for publication or published by an accredited journal) before 15 February for the Autumn graduation or before 15 July for the Spring Graduation as required by the relevant regulations and that the degree will not be conferred if this requirement has not been fulfilled.
2. I declare that the mini-dissertation, dissertation or thesis, which I hereby submit for the degree programme at the University of Pretoria, is my own work and has not previously been submitted by me for a degree at another university. Where secondary material is used, it has been carefully acknowledged and referenced in accordance with University requirements. I am aware of the University's policy and implications regarding plagiarism.

Signature: 	Date: 06/04/2022
---	-------------------------

Statement by the Supervisor:

I hereby declare that I approve that Mr LB Pedzisayi may submit his/her mini-dissertation/dissertation/thesis for examination. The co-supervisor has agreed to the submission.

Signature (Supervisor):	Date:
Signature (Co-supervisor(s)):	Date:
FOR OFFICE USE	
Received by:	Date:

Appendix G: Title change approval within intent to submit



MSc Committee
School of Medicine
Faculty of Health Sciences

MSc Committee
27 June 2019

Dr van den Bout
Department of Physiology
Faculty of Health Sciences

Dear Dr,

Mr L Pedzisayi, Student no 14218594

Please receive the following comments with reference to the MSc Committee submission of the abovementioned student:

Student name	Mr Leslie Pedzisayi	Student number	14218594
Name of study leader	Dr I van den Bout		
Department	Physiology		
Title of MSc	Role of cell-to-cell communication in determining metastatic behaviour of breast cancer cells		
Date of first submission	March 2019		
April 2019	<ul style="list-style-type: none"> • Thank you for the submitting the revised protocol and MSc form. • Thank you for submitting a clarification of reasons to not include a non-cancerous control group. • Please remember to include number of repeats to be done as well as how data will be analysed. 		
June 2019	<ul style="list-style-type: none"> • Thank you for submitting the ethics approval letter. 		
Decision	<p>This protocol has been approved. Ethics approval has been obtained.</p> <p>The internal and external examiners can be nominated and submitted to the MSc Committee six months prior to submission of the dissertation. Please ensure that the CV of the examiners includes: supervision, examination and publication records.</p>		

Yours sincerely



Prof Marleen Kock
Chair: MSc Committee

MSc Committee, School of Medicine
Faculty of Health Sciences
University of Pretoria,
Private Bag X323
Pretoria 0001, South Africa
Tel +27 (0)12 319 2325
Fax +27 (0)12 323 0732

Fakulteit Gesondheidswetenskappe
Lefapha la Disaense tša Maphelo

Appendix H: MSc committee approval



Faculty of Health Sciences
Department of Immunology

Letter of Statistical Clearance

Thursday, March 14, 2019

This letter is to confirm that the student with the Name; Leslie Pedzisayi, Student No: 14218594 studying at the University of Pretoria, discussed the project with the title; Investigating the role of cell-to-cell communication in determining metastatic behaviour of breast cancer cells with me.

I hereby confirm that I am aware of the project and the statistical analysis of the data generated from the project.

The statistics and analytical tools (Graphpad Prism) that will be used will suffice to achieve the objective(s) of the study.

Yours sincerely

Prof Pieter WA Meyer
Ass. Professor and HoD



Room 5-40, Level 5, Pathology Building
University of Pretoria, Private Bag X320
Pretoria 0001, South Africa
Tel +27 (0)12 319 2877
Fax +27 (0)12 323 0732
Email name: pieter.meyer@up.ac.za
www.up.ac.za

Fakulteit Gesondheidswetenskappe
Departement Immunologie
Lefapha la Disaense tsa Maphelo
Kgoro ya Immunolotši

Appendix I: Letter of statistical clearance



Faculty of Health Sciences

The Research Ethics Committee, Faculty Health Sciences, University of Pretoria complies with ICH-GCP guidelines and has US Federal wide Assurance.

- FWA 00002567, Approved dd 22 May 2002 and Expires 03/20/2022.
- IRB 0000 2235 IORG0001762 Approved dd 22/04/2014 and Expires 03/14/2020.

18 June 2019

**Approval Certificate
New Application**

Ethics Reference No.: 290/2019

Title: Role of cell-to-cell communication in determining metastatic behaviour of breast cancer cells

Dear Mr LB Pedzisayi

The **New Application** as supported by documents received between 2019-05-02 and 2019-06-12 for your research, was approved by the Faculty of Health Sciences Research Ethics Committee on its quorate meeting of 2019-06-12.

Please note the following about your ethics approval:

- Ethics Approval is valid for 1 year and needs to be renewed annually by 2020-06-18.
- Please remember to use your protocol number (290/2019) on any documents or correspondence with the Research Ethics Committee regarding your research.
- Please note that the Research Ethics Committee may ask further questions, seek additional information, require further modification, monitor the conduct of your research, or suspend or withdraw ethics approval.

Ethics approval is subject to the following:

- The ethics approval is conditional on the research being conducted as stipulated by the details of all documents submitted to the Committee. In the event that a further need arises to change who the investigators are, the methods or any other aspect, such changes must be submitted as an Amendment for approval by the Committee.

We wish you the best with your research.

Yours sincerely



Dr R Sommers

MBChB MMed (Int) MPharmMed PhD

Deputy Chairperson of the Faculty of Health Sciences Research Ethics Committee, University of Pretoria

The Faculty of Health Sciences Research Ethics Committee complies with the SA National Act 61 of 2003 as it pertains to health research and the United States Code of Federal Regulations Title 45 and 46. This committee abides by the ethical norms and principles for research, established by the Declaration of Helsinki, the South African Medical Research Council Guidelines as well as the Guidelines for Ethical Research: Principles Structures and Processes, Second Edition 2015 (Department of Health)

Research Ethics Committee
Room 4-60, Level 4, Tswelopele Building
University of Pretoria, Private Bag X323
Arcadia 0007, South Africa
Tel +27 (0)12 356 3084
Email deepeka.behari@up.ac.za
www.up.ac.za

Fakulteit Gesondheidswetenskappe
Lefapha la Disaense tša Maphelo

Appendix J: Ethics approval 2019



Faculty of Health Sciences

Institution: The Research Ethics Committee, Faculty Health Sciences, University of Pretoria complies with ICH-GCP guidelines and has US Federal wide Assurance.

- FWA 00002567, Approved dd 22 May 2002 and Expires 03/20/2022.
- IORG #: IORG0001762 OMB No. 0990-0279 Approved for use through February 28, 2022 and Expires: 03/04/2023.

20 July 2020

**Approval Certificate
Annual Renewal**

Ethics Reference No.: 290/2019

Title: Role of cell-to-cell communication in determining metastatic behaviour of breast cancer cells.

Dear Mr LB Pedzisayi

The **Annual Renewal** as supported by documents received between 2020-06-19 and 2020-07-15 for your research, was approved by the Faculty of Health Sciences Research Ethics Committee on its quorate meeting of 2020-07-15.

Please note the following about your ethics approval:

- Renewal of ethics approval is valid for 1 year, subsequent annual renewal will become due on 2021-07-20.
- Please remember to use your protocol number (290/2019) on any documents or correspondence with the Research Ethics Committee regarding your research.
- Please note that the Research Ethics Committee may ask further questions, seek additional information, require further modification, monitor the conduct of your research, or suspend or withdraw ethics approval.

Ethics approval is subject to the following:

- The ethics approval is conditional on the research being conducted as stipulated by the details of all documents submitted to the Committee. In the event that a further need arises to change who the investigators are, the methods or any other aspect, such changes must be submitted as an Amendment for approval by the Committee.

We wish you the best with your research.

Yours sincerely

Dr R Sommers

MBChB MMed (Int) MPharmMed PhD

Deputy Chairperson of the Faculty of Health Sciences Research Ethics Committee, University of Pretoria

The Faculty of Health Sciences Research Ethics Committee complies with the SA National Act 61 of 2003 as it pertains to health research and the United States Code of Federal Regulations Title 45 and 46. This committee abides by the ethical norms and principles for research, established by the Declaration of Helsinki, the South African Medical Research Council Guidelines as well as the Guidelines for Ethical Research: Principles Structures and Processes, Second Edition 2015 (Department of Health)

Research Ethics Committee
Room 4-60, Level 4, Tswelopele Building
University of Pretoria, Private Bag x323
Gezina 0031, South Africa
Tel +27 (0)12 350 3084
Email: deepika.behari@up.ac.za
www.up.ac.za

Fakulteit Gesondheidswetenskappe
Lefapha la Ditsaense Sa Maphelo

Appendix K: Ethics approval 2020



Faculty of Health Sciences

Institution: The Research Ethics Committee, Faculty Health Sciences, University of Pretoria complies with ICH-GCP guidelines and has US Federal wide Assurance.

- FWA 00002567, Approved dd 22 May 2002 and Expires 03/20/2022.
- IORG #: IORG0001762 OMB No. 0990-0279 Approved for use through February 28, 2022 and Expires: 03/04/2023.

15 April 2021

**Approval Certificate
Annual Renewal**

Ethics Reference No.: 290/2019

Title: Role of cell-to-cell communication in determining metastatic behaviour of breast cancer cells.

Dear Mr LB Pedzisay

The **Annual Renewal** as supported by documents received between 2021-03-17 and 2021-04-14 for your research, was approved by the Faculty of Health Sciences Research Ethics Committee on 2021-04-14 as resolved by its quorate meeting.

Please note the following about your ethics approval:

- Renewal of ethics approval is valid for 1 year, subsequent annual renewal will become due on 2022-04-15.
- Please remember to use your protocol number (290/2019) on any documents or correspondence with the Research Ethics Committee regarding your research.
- Please note that the Research Ethics Committee may ask further questions, seek additional information, require further modification, monitor the conduct of your research, or suspend or withdraw ethics approval.

Ethics approval is subject to the following:

- The ethics approval is conditional on the research being conducted as stipulated by the details of all documents submitted to the Committee. In the event that a further need arises to change who the investigators are, the methods or any other aspect, such changes must be submitted as an Amendment for approval by the Committee.

We wish you the best with your research.

Yours sincerely

Professor Werdie (CW) Van Staden
MBChB MMed(Psych) MD FCPsych(SA) FTCL UPLM
Chairperson: Faculty of Health Sciences Research Ethics Committee

The Faculty of Health Sciences Research Ethics Committee complies with the SA National Act 61 of 2003 as it pertains to health research and the United States Code of Federal Regulations Title 45 and 46. This committee abides by the ethical norms and principles for research, established by the Declaration of Helsinki, the South African Medical Research Council Guidelines as well as the Guidelines for Ethical Research: Principles Structures and Processes, Second Edition 2015 (Department of Health)

Research Ethics Committee
Room 4-60, Level 4, Tswelopele Building
University of Pretoria, Private Bag x323
Gezina 0031, South Africa
Tel 427 (0)12 350 3084
Email: deepika.behari@up.ac.za
www.up.ac.za

Fakulteit Gesondheidswetenskappe
Lefapha la Disaense Sa Maphele

Appendix L: Ethics approval 2021